

Testing and Recommended Practices to Improve Nurse Tank Safety, Phase I



U.S. Department of Transportation
Federal Motor Carrier Safety Administration

October 2013

FOREWORD

This report presents findings of causes for stress corrosion cracks (SCC) and possible inspection strategies for non-destructively identifying such flaws in nurse tanks, which are used to transport anhydrous ammonia (NH₃) over both public roadways and farm fields. Historically the tanks were 1,000 or 1,500 gallons. Recently, dual, and even tri-mounted 3,000-gallon tanks are being used by some large farms. On the road, these tanks can be pulled by pickup trucks or tractors. Many of the reportedly 200,000 nurse tanks in use in the United States are 3 to 5 decades old. Several failures caused extensive property damage, serious injuries, and death. This research further confirms that SCC is the greatest threat to nurse tank integrity.

NH₃ is a hazardous material that can cause chemical burns, frostbite, and suffocation. Nurse tanks hold the NH₃ at multiple times the atmospheric pressure. Tank failures can release this pressure with catastrophic force, posing the additional risk of impact injury to workers and bystanders. This research study addressed this problem in several ways, including:

- Purchase and examination of 20 used nurse tanks by metallography, glow discharge spectroscopy, neutron diffraction analysis of residual stresses, as well as ultrasound and fluorescent dye penetrant examinations for indications of possible cracks.
- Exposure of 56 test sample specimens of commonly used steel to NH₃. Steel samples were tension-stressed while immersed in liquid NH₃ or exposed to pure NH₃ vapor for 7 months to study initiation and growth of stress corrosion cracks.
- Preparation of a survey of the technical literature on nurse tank properties and case studies of tank failures.

This document reports the findings and recommendations for best inspection practices to reduce risks associated with nurse tank failures. This report may interest nurse tank owners, manufacturers, repair businesses, and farmers using nurse tanks to fertilize their crops, as well as all other parties concerned about public roadway safety. This document is the first report resulting from this ongoing research.

NOTICE

This document is disseminated under the sponsorship of the U.S. Department of Transportation in the interest of information exchange. The United States Government assumes no liability for its contents or the use thereof.

The contents of this report reflect the views of the contractor, who is responsible for the accuracy of the data presented herein. The contents do not necessarily reflect the official policy of the U.S. Department of Transportation.

This report does not constitute a standard, specification, or regulation.

The United States Government does not endorse products or manufacturers named herein. Trade or manufacturers' names appear herein solely because they are considered essential to the objective of this report.

Technical Report Documentation Page

1. Report No. FMCSA-RRR-13-032	2. Government Accession No.	3. Recipient's Catalog No.	
4. Title and Subtitle Testing and Recommended Practices to Improve Nurse Tank Safety, Phase I		5. Report Date October 2013	
		6. Performing Organization Code	
7. Author(s) Russell, Alan M., Chumbley, L. Scott, Becker, Andrew, Vennerberg, Daniel, and White, Emma.		8. Performing Organization Report No.	
9. Performing Organization Name and Address Iowa State University Ames, Iowa		10. Work Unit No. (TRAVIS)	
		11. Contract or Grant No. DTMC75-07-D-00006 Task order DTMC75-08-J-00017	
12. Sponsoring Agency Name and Address U.S. Department of Transportation Federal Motor Carrier Safety Administration Office of Analysis, Research, and Technology 1200 New Jersey Ave., SE Washington, DC 20590		13. Type of Report Final Report	
		14. Sponsoring Agency Code FMCSA	
15. Supplementary Notes Contracting Officer's Representative: David Goettee			
16. Abstract This research project studied causes and possible remediation inspection strategies to prevent failures for anhydrous ammonia (NH₃) nurse tanks. Nurse tanks are steel tanks used to transport NH₃ locally over public roadways and farm fields. Many of the reportedly 200,000 nurse tanks in use in the United States are 3 to 5 decades old. Several tank failures have occurred in recent years. Nurse tank failures can injure workers and bystanders by way of chemical burns, frostbite, suffocation, and physical injuries caused by the catastrophic force of rupture. This research study addressed this problem by: surveying the technical literature on nurse tank properties and case studies of tank failures; examination of 20 used nurse tanks by metallography, glow discharge spectroscopy, neutron diffraction analysis of residual stresses, ultrasound, and fluorescent dye penetrant examination for cracks. It exposed 56 specimens of the commonly used tank steel, stressed in tension, while either immersed in liquid NH₃ or exposed to pure NH₃ vapor, for 7 months to study the initiation and growth of stress corrosion cracks. This research further confirms that stress corrosion cracking is the greatest threat to nurse tank integrity. Recommendations for best inspection practices are presented on how to reduce the risks associated with nurse tank failures.			
17. Key Words Ammonia, anhydrous ammonia, nurse tanks, pressurized steel tank, safety, tanks		18. Distribution Statement No restrictions	
19. Security Classif. (of this report) Unclassified	20. Security Classif. (of this page) Unclassified	21. No. of Pages 128	22. Price

SI* (MODERN METRIC) CONVERSION FACTORS

TABLE OF APPROXIMATE CONVERSIONS TO SI UNITS

Symbol	When You Know	Multiply By	To Find	Symbol
LENGTH				
in	inches	25.4	millimeters	mm
ft	feet	0.305	meters	m
yd	yards	0.914	meters	m
mi	miles	1.61	kilometers	km
AREA				
in ²	square inches	645.2	square millimeters	mm ²
ft ²	square feet	0.093	square meters	m ²
yd ²	square yards	0.836	square meters	m ²
ac	acres	0.405	hectares	ha
mi ²	square miles	2.59	square kilometers	km ²
VOLUME				
fl oz	fluid ounces	29.57	1,000 L shall be shown in m ³ milliliters	ml
gal	gallons	3.785	Liters	L
ft ³	cubic feet	0.028	cubic meters	m ³
yd ³	cubic yards	0.765	cubic meters	m ³
MASS				
oz	ounces	28.35	grams	g
lb	pounds	0.454	kilograms	kg
t	short tons (2,000 lb)	0.907	megagrams (or "metric ton")	mg (or "t")
TEMPERATURE				
°F	Fahrenheit	$5 \times (F-32) \div 9$ or $(F-32) \div 1.8$	Temperature is in exact degrees Celsius	°C
ILLUMINATION				
fc	foot-candles	10.76	lux	lx
fl	foot-Lamberts	3.426	candela/m ²	cd/m ²
Force and Pressure or Stress				
lbf	poundforce	4.45	newtons	N
lbf/in ²	poundforce per square inch	6.89	kilopascals	kPa

TABLE OF APPROXIMATE CONVERSIONS FROM SI UNITS

Symbol	When You Know	Multiply By	To Find	Symbol
LENGTH				
mm	millimeters	0.039	inches	in
m	meters	3.28	feet	ft
m	meters	1.09	yards	yd
km	kilometers	0.621	miles	mi
AREA				
mm ²	square millimeters	0.0016	square inches	in ²
m ²	square meters	10.764	square feet	ft ²
m ²	square meters	1.195	square yards	yd ²
ha	hectares	2.47	acres	ac
km ²	square kilometers	0.386	square miles	mi ²
VOLUME				
ml	milliliters	0.034	fluid ounces	fl oz
L	liters	0.264	gallons	gal
m ³	cubic meters	35.314	cubic feet	ft ³
m ³	cubic meters	1.307	cubic yards	yd ³
MASS				
g	grams	0.035	ounces	oz
kg	kilograms	2.202	pounds	lb
mg (or "t")	megagrams (or "metric ton")	1.103	short tons (2,000 lb)	T
TEMPERATURE				
°C	Celsius	$1.8C + 32$	Temperature is in exact degrees Fahrenheit	°F
ILLUMINATION				
lx	lux	0.0929	foot-candles	fc
cd/m ²	candela/m ²	0.2919	foot-lamberts	fl
Force & Pressure Or Stress				
n	newtons	0.225	poundforce	lbf
kPa	kilopascals	0.145	poundforce per square inch	lbf/in ²

* SI is the symbol for the International System of Units. Appropriate rounding should be made to comply with Section 4 of ASTM E380. (Revised March 2003, Section 508-accessible version September 2009.)

TABLE OF CONTENTS

EXECUTIVE SUMMARY	xv
1. INTRODUCTION.....	1
1.1 PRIOR STUDIES OF STRESS CORROSION CRACKING IN NURSE TANKS	4
1.1.1 Stress Corrosion Cracking (SCC).....	4
1.1.2 Mechanisms of Anhydrous Ammonia Stress Corrosion Cracking in Steel	5
1.2 EXAMPLES OF CATASTROPHIC FAILURE CAUSED BY STRESS CORROSION CRACKING	6
1.2.1 Calamus, Iowa Incident	7
1.2.2 Morris, Minnesota Incident.....	7
1.2.3 Silver Lake, Minnesota Explosion.....	7
1.2.4 Middleton, Ohio Tanker Accident	8
2. TANK ACQUISITION AND METALLURGICAL EVALUATIONS	11
2.1 TANK ACQUISITIONS	11
2.2 TANK EVALUATION BY THE ANGLE-BEAM ULTRASOUND TECHNIQUE.....	11
2.3 TANK EVALUATION BY METALLOGRAPHY	11
2.4 TANK EVALUATION BY GLOW DISCHARGE SPECTROSCOPY	12
2.5 TANK EVALUATION BY TENSILE TESTING.....	13
2.6 TANK EVALUATION BY MAGNETIC PARTICLE-FLUORESCENT DYE PENETRANT TESTING	14
2.7 TANK EVALUATION BY SCANNING ELECTRON MICROSCOPY (SEM) OF FRACTURE SURFACES	15
3. TANK EVALUATION BY NEUTRON DIFFRACTION ANALYSIS.....	17
3.1 RESIDUAL STRESS IN WELDMENTS	17
3.2 RESIDUAL STRESS MEASUREMENTS.....	17
3.3 IMPLICATIONS OF THE RESIDUAL STRESS FINDINGS FOR STRESS CORROSION CRACKING IN NURSE TANKS.....	20
4. STRESS CORROSION CRACKING EXPERIMENTS	23
4.1 THE STRESS CORROSION CRACKING EXPERIMENTAL PLAN	23
4.2 THE STRESS CORROSION CRACKING EXPERIMENTAL RESULTS.....	23
5. CONCLUSIONS	27
6. RECOMMENDATIONS.....	29

ACKNOWLEDGEMENTS103
REFERENCES.....105

LIST OF APPENDICES

APPENDIX A—STRESS INTENSITY FACTOR ANALYSIS AND APPLICATION OF THIS ANALYSIS TO PREDICT CRACK PROPAGATION RATES IN NURSE TANKS.....33
APPENDIX B—TENSILE TESTS47
APPENDIX C—INVESTIGATION OF A STRESS CORROSION CRACK IN A 1,450-GALLON NURSE TANK MANUFACTURED BY CHEMI-TROL IN 1977.....51
APPENDIX D—LATTICE PARAMETER AND STRAIN CALCULATIONS USED TO DEVELOP NEUTRON DIFFRACTION RESIDUAL STRESS DETERMINATIONS59
APPENDIX E—LITERATURE REVIEW: ANHYDROUS AMMONIA NURSE TANK STRESS CORROSION CRACKING.....71

LIST OF FIGURES AND FORMULAS

Figure 1. Photograph. Metallographic cross-section of tank wall steel containing a crack.	12
Figure 2. Graph. Glow discharge spectroscopy results from first 6 microns of steel at the inner tank wall.	13
Figure 3. Graph. Tensile test results from a 1,000-gallon nurse tank manufactured in 1966.	14
Figure 4. Photograph. One of several cracks made visible by ultraviolet-light-induced fluorescence of magnetic particles poised at the crack edges.....	15
Figure 5. Image. Photographs of a typical fracture surface in one of the tanks examined.	16
Figure 6. Diagram. Location of hoop weld sections cut from tanks.....	18
Figure 7. Photograph. Nurse tank hoop section in the neutron beam line at LANSCE.	18
Figure 8. Graph. Residual hoop stress distributions measured by neutron diffraction at LANSCE.....	19
Figure 9. Graph. Superimposition of the maximum residual tensile stress measured at LANSCE (lower horizontal line) with the stress-strain plot for the steel coupons measured from that tank in tensile testing.	20
Figure 10. Graph. Crack size as a function of stress intensity factor after 4 months of exposure to NH ₃	24
Figure 11. Image. Two cracks that initiated and grew during the stress corrosion cracking test.....	25
Figure 12. Flowchart. Preliminary recommended nurse tank inspection, repair, and retirement precepts based on the findings from this study.	29
Figure 13. Formula. Formula for stress intensity caused by an axial through-crack in a thin-walled cylindrical pressure vessel.....	33
Figure 14. Formula. Formula for hoop stress in a thin-walled cylindrical pressure vessel.	33
Figure 15. Formula for chi, a fitting parameter for stress intensity of axial through-cracks in thin-walled cylindrical pressure vessels.....	33
Figure 16. Diagram. Axial flaw in a cylinder subjected to internal pressure.	34
Figure 17. Formula. Example calculation of hoop stress for a specific nurse tank.	34
Figure 18. Graph. K ₁ versus crack length in a 1,000-gallon nurse tank.....	35
Figure 19. Formula. The crack length after y years is equal to the initial crack length plus 3e-7 times the stress intensity squared times the square root of y years.....	36
Figure 20. Formula. This is the derivative with respect to y, time in years, of Figure 19.	36
Figure 21. Formula. The change in length of the crack with respect to the time in years.....	36
Figure 22. Graph. In this representative 1,000-gallon tank, cracks less than 2.75 inches long will not grow to the critical crack length at -94° F for at least 10 years.....	37

Figure 23. Graph. In this representative 1,450-gallon tank, cracks less than 3 inches long will not grow to the critical crack length at -94° F for at least 10 years.....	38
Figure 24. Formula. The crack growth rate in millimeters per year is equal to 3e-4 times the stress intensity squared.	39
Figure 25. Formula. The crack growth rate as a function of thickness, internal pressure, and crack length.	39
Figure 26. Graph. In this representative 1,000-gallon nurse tank with the revised prediction of crack growth rate, cracks less than 2.25 inches long will not reach critical length at -94° F for at least 10 years.....	39
Figure 27. Graph. In this representative 1,450-gallon nurse tank with the revised prediction of crack growth rate, cracks less than 2.5 inches long will not reach critical length at -94° F for at least 10 years.....	40
Figure 28. Formula. The highest crack growth rate in meters per year was 9.41e-7 times the stress intensity squared.	40
Figure 29. Formula. This equation describes the change in length of the crack with respect to the time in years.	41
Figure 30. Graph. In this representative 1,000-gallon nurse tank with crack growth based on the highest measured crack growth rate, cracks less than 1.25 inches long will not reach critical length at -94° F for at least 10 years.	41
Figure 31. Graph. In this representative 1,450-gallon nurse tank with crack growth based on the highest measured crack growth rate, cracks less than 1.25 inches long will not reach critical length at -94° F for at least 10 years.	42
Figure 32. Graph. Hoop stress across the circumferential weld in a 1,000-gallon nurse tank manufactured in 1966. The region of high residual stress extends only 1 inch from the weld.....	44
Figure 33. Graph. Axial stress across a circumferential weld in a 1,000-gallon nurse tank manufactured in 1996.....	45
Figure 34. Diagram. Stresses on a pressure tank. Axial-oriented cracks are opened by hoop stress, and circumferential cracks are opened by axial stress.....	45
Figure 35. Image. Y-shaped cracks highlighted with florescent magnetic particles found on two tanks.	46
Figure 36. Photograph. Fluorescent wet magnetic particle testing of a segment of a crack in the head of the tank. The scale bar is in cm.....	51
Figure 37. Image. The arrow indicates initiation of a crack on the interior of the tank head.	52
Figure 38. Image. Positioning the light source at a different angle revealed several horizontal lines visible in the cracked region of the sample, two of which are indicated by arrows.....	52
Figure 39. Image. Shadow image of surface before cleaning. The right side has no oxide and is clearly faceted due to cleavage fracture when the sample was subjected to an impact loading after cooling to liquid nitrogen temperatures.	53
Figure 40. Image. Vertical cracks produced by backscattered electrons.	53
Figure 41. Image. Secondary electron image of vertical cracks.	54

Figure 42. Image. Vertical cracks produced by backscattered electrons.....	54
Figure 43. Image. After cleaning, the stress corrosion cracking region shows faceted regions indicating intergranular cracking.....	55
Figure 44. Photograph. Cross-section of a penny-sized crack located in a 1,450-gallon nurse tank head manufactured in 1977. The crack originated near the circumferential weld on the interior.	55
Figure 45. Image. Optical microscopy of the cracks indicates intergranular cracking as the crack path swings around grains.....	56
Figure 46. Image. At this point, the crack is larger than the surrounding grains, obscuring whether intergranular or transgranular cracking is occurring.	56
Figure 47. Image. The crack branching is clearly seen in these micrographs.	57
Figure 48. Formula. Lattice strain is calculated by comparing the lattice parameter of a strained region to the lattice parameter of an unstrained region.....	59
Figure 49. Equations. Stress is dependent on strain in three orthogonal directions (hoop, axial, and radial).....	59
Figure 50. Equation. e is the vector sum of the three strains.	59
Figure 51. Equation. λ is related to Poisson's ratio and the elastic modulus.	59
Figure 52. Equation. Modulus of rigidity is proportional to the elastic modulus and inversely related to Poisson's ratio.....	60
Figure 53. Formula. The error in strain is related to the errors in the strains.	60
Figure 54. This portion of the error is dependent on the square root of the sum of the squares of the three orthogonal strain errors.	60
Figure 55. Graph. Hoop lattice parameter across the circumferential weld in a nurse tank manufactured in 1966.....	61
Figure 56. Graph. Hoop strain across the circumferential weld in a 1,000-gallon nurse tank manufactured in 1966.....	61
Figure 57. Graph. Axial strain across the circumferential weld in a 1,000-gallon nurse tank manufactured in 1966. The highest strain is on the inner surface of the tank next to the weld.	62
Figure 58. Graph. Radial strain across the circumferential weld in a 1,000-gallon nurse tank manufactured in 1966. The strain is lower for radial than for axial and hoop.	62
Figure 59. Graph. Hoop strain across the circumferential weld in a 1986 nurse tank.....	63
Figure 60. Graph. Axial strain across the circumferential weld in a 1986 nurse tank.....	63
Figure 61. Graph. Radial strain across the circumferential weld in a 1986 nurse tank.	64
Figure 62. Graph. Hoop strain in the heat-affected zone of the axial weld crossing the circumferential weld in a 1986 nurse tank.	64
Figure 63. Graph. Radial strain in the heat-affected zone of the axial weld crossing the circumferential weld in a 1986 nurse tank.	65
Figure 64. Graph. Radial strain in the heat-affected zone of the axial weld crossing the circumferential weld in a 1986 nurse tank.	65
Figure 65. Graph. Hoop stress across the circumferential weld in a 1,000-gallon nurse tank manufactured in 1986.....	66

Figure 66. Graph. Axial stress across the circumferential weld in a 1,000-gallon nurse tank manufactured in 1986.	66
Figure 67. Graph. Radial stress across the circumferential weld in a 1,000-gallon nurse tank manufactured in 1986.	67
Figure 68. Graph. Hoop stress across the circumferential weld in a 1,000-gallon nurse tank manufactured in 1966.	67
Figure 69. Graph. Radial stress across the circumferential weld in a 1,000-gallon nurse tank manufactured in 1966.	68
Figure 70. Graph. Axial stress across the circumferential weld in a 1,000-gallon nurse tank manufactured in 1966.	68
Figure 71. Graph. Hoop stress in the heat-affected zone of the axial weld crossing the circumferential weld in a 1986 nurse tank.	69
Figure 72. Graph. Axial stress across the circumferential weld in a 1966 nurse tank.	69
Figure 73. Graph. Radial stress across the circumferential weld in a 1986 nurse tank.	70
Figure 74. Diagram. Illustration of film-rupture model in which “competitive” adsorption takes place between oxygen and nitrogen molecules.	75
Figure 75. Diagram. Crack propagation according to the general film-rupture model. Continuous deformation causes the crack tip to stay exposed (a), and when a passivating film does form, it is ruptured again (b) ⁽⁹⁾	75
Figure 76. Equations. Three equations for the chemical mechanism for anhydrous ammonia—oxygen stress corrosion cracking (4e = four free electrons).....	75
Figure 77. Graph. Corrosion potential of carbon steel as a function of time in different environments.	76
Figure 78. Graph. SSC susceptibility as a function of water and oxygen concentrations in anhydrous ammonia at 18° C (64.4° F). No liquid SSC has been observed above and to the left of the line drawn on the graph.....	77
Figure 79. Formula. Model for the maximum crack depth as a function of time and stress intensity factor.	77
Figure 80. Growth rates predicted by the model above for three possible situations:.....	78
Figure 81. Diagram. Compact tension specimen geometry used for crack growth rate studies. This diagram shows specimens with notches in the weld (left) and in the heat-affected zones (right).	79
Figure 82. Graph. Crack depth divided by square root of exposure time plotted against stress intensity factor for carbon steel in different oxygen-water environments.	79
Figure 83. Image. A comparative difference in fracture surface contours between transgranular cracking in the weld metal (top portion of photo) and intergranular cracking in the heat-affected zones (bottom) 125 x magnification.	80
Figure 84. Diagram. Schematic of FSM principles. The top image shows the ideal electric field pattern of an unflawed vessel and the bottom depicts the distorted electric field lines of a flawed vessel.....	83
Figure 85. Photograph. Calamus nurse tank post-accident. The white oval indicates the location of the ruptured seam.	84

Figure 86. Photograph. Close-up picture of the ruptured seam circled in Figure 128.....	85
Figure 87. Photograph. Front end of Cenex vessel showing impact damage.	86
Figure 88. Photograph. Severed tractor and automobile damage caused by the propelled nurse tank.	87
Figure 89. Photograph. Blown-out rear end of nurse tank.....	87
Figure 90. Photograph. Point of vessel where the fracture meets the circumferential weld.	88
Figure 91. Photograph. Silver Lake nurse tank post-accident.	89
Figure 92. Photograph. Ruptured tank head.	89
Figure 93. Photograph. Inside view of the ruptured tank head.	89
Figure 94. Photograph. Crack initiation site.	90
Figure 95. Image. Ferrite/pearlite microstructure at crack initiation site, 200 x magnification. Both transgranular and intergranular fractures are observed.	90
Figure 96. Image. SEM image of fracture surface showing transgranular and intergranular fractures.	91
Figure 97. Diagram. Schematic of observed crack locations. The letter “a” denotes the location of a through-wall crack. Lines represent weld seams.....	92
Figure 98. Photograph. Through-wall crack in head.	92
Figure 99. Photograph. Pieces of LAG cylinder post-explosion.	93
Figure 100. Photograph. Rupture initiation site showing severe cracking.	94
Figure 101. Photograph. Grain boundary microcracks at the crack initiation site.	94
Figure 102. Grouped Image. SEM of fracture site showing grain boundary microcracks (left) and SEM showing the dimpled morphology of the fracture region (right).	94

LIST OF TABLES

Table 1.	Maximum hoop, axial, and radial stresses in a nurse tank resulting from internal pressure and from residual stress in the heat-affected zones near welds.....	20
Table 2.	Data from coupons extracted from used nurse tanks of various ages.	48
Table 3.	Corrosion of A517 grade F steel exposed to different components of air.	73
Table 4.	Summary of SCC test results for A5176 grade F steel in anhydrous ammonia containing various contaminants.	73
Table 5.	Morris nurse tank manufacturing data.....	86
Table 6.	Required chemical composition of steels used for anhydrous ammonia containment (percent maximum unless otherwise noted).	97
Table 7.	ISO-V-notch impact energy requirements for carbon steels.	97

ABBREVIATIONS AND ACRONYMS

Acronym	Definition
ASME	American Society of Mechanical Engineers
ASTM	formerly known as the American Society for Testing and Materials
ADG	Australian dangerous goods
CFR	Code of Federal Regulations
CSA	Canadian Standards Association
FMCSA	Federal Motor Carrier Safety Administration
FSM	Field Signature Method
HAZ	Heat-affected zone
HV	Hardness, Vickers
IACS	International Association of Classification Societies
IRC	Industrial Refrigeration Consortium
ISO	International Organization for Standardization
KI	Stress intensity factor
LAG	liquefied ammonia gas
LANSCE	Los Alamos Neutron Science Center
lb	pounds
LPG	liquid petroleum gas
m	meter
MC	motor carrier
mm	Millimeter
MPa	MegaPascal
NIOSH	National Institute for Occupational Safety and Health
NTSB	National Transportation Safety Board
PSIG	pounds per square inch gauge

PHMSA	Pipeline and Hazardous Materials Safety Administration
ppm	parts per million
SEM	scanning electron microscope
SCC	stress corrosion cracks
TFI	The Fertilizer Institute
USDOT	U.S. Department of Transportation
WFMT	wet fluorescent magnetic particle testing

CHEMICAL ABBREVIATIONS

Al	Aluminum
B	Boron
C	Carbon
CH ₄	Methane
CO	Carbon Monoxide
Co	Cobalt
CO ₂	Carbon Dioxide
Cr	Chromium
Cu	Copper
Fe	Iron
Fe ₃ C	Iron carbide
LN ₂	Liquid Nitrogen
Mg	Magnesium
Mo	Molybdenum
Mn	Manganese
N	Nitrogen (atom)
N ₂	Nitrogen (molecule)
NH ₄ ⁺	Ammonium ion
NH ₄ Cl	Ammonium chloride
(NH ₄) ₂ CO ₃	Ammonium carbonate
NH ₄ HCO ₃	Ammonium bicarbonate
NH ₄ NO ₃	Ammonium nitrate
NO	Nitric oxide
NO ₂	Nitrogen dioxide
N ₂ O	Nitrous oxide

NaNH ₂	Sodium amide
NaNO ₂	Sodium nitrite
NaNO ₃	Sodium nitrate
NaCl	Sodium chloride
Nb	Niobium
NH ₃	Anhydrous Ammonia
Ni	Nickel
O ₂	Oxygen (molecule)
P	Phosphorus
Pb	Lead
S	Sulfur
Si	Silicon
Sn	Tin
SO ₂	Sulfur dioxide
Ti	Titanium
V	Vanadium
W	Tungsten
Z	Zirconium
Zn	Zinc

EXECUTIVE SUMMARY

PURPOSE

This study focuses on determining causes and possible inspection remediation strategies to reduce the occurrence of anhydrous ammonia (NH₃) tank failures. A variety of metallurgical tests were performed on 20 used nurse tanks and on laboratory specimens cut from the tanks and/or created from the steel most commonly used to construct nurse tanks. Testing corroborated the conclusion from other studies that stress corrosion cracking (SCC) is the principal threat to nurse tank integrity. Manufacturing defects are also a possible issue, but many quality control practices have improved. They now include 100-percent radiographic testing of longitudinal welds on the tank shell. A more detailed look at manufacturing defects in nurse tanks is part of a follow-on study that is extending findings from this study. Other possible testing methods that could reduce future occurrences of nurse tank failures are presented in this report.

PROCESS

This study represents a comprehensive initial examination of causes for failures of NH₃ nurse tanks. The study process included the following steps:

- Acquiring 20 used nurse tanks of various ages fabricated by various manufacturers and collecting them at the tank holding worksite in Jordan, Iowa, for study.
- Inspecting these tanks externally using visual and angle-beam ultrasound methods.
- Cutting the tanks into smaller sections to permit internal surface examination by fluorescent dye penetrant, glow discharge spectroscopy, neutron diffraction analysis of residual stresses, tensile testing of sample test steel coupons, and metallographic analysis of the steel's microstructure.
- Acquiring a smaller, custom-built nurse tank with a manway to use as a testbed for SCC studies of the A455 low-carbon steel now commonly used in nurse tank fabrication.
- Fabrication of 56 SCC test specimen coupons. These were held under tensile stress and placed either in anhydrous ammonia liquid or vapor for 7 months in the testbed tank. They were then analyzed to determine their SCC behavior (i.e., to determine the rate of crack initiation and growth).
- Assessing the data acquired from the above steps and formulating recommendations for best inspection practices to reduce future occurrences of nurse tank failures.
- Performing a search of the technical literature addressing past nurse tank failures and SCC in nurse tanks. A report of the findings from the literature survey are in Appendix E. They are summarized in the body of this report.

RATIONALE AND BACKGROUND

Past studies of nurse tank failures concluded that SCC is the primary threat to tank integrity. However, many of these studies focused on examining pieces of failed nurse tanks. This is the first comprehensive study of representative nurse tanks that were operating satisfactorily in regular service. This study was designed to:

- Perform a sampling of tanks over a range of ages to determine their state of residual stress, the number and location of indications of possible cracks in such tanks, and the strength and microstructure of the steel in those tanks.
- To perform a 7-month-long assessment of stress corrosion cracking initiation and propagation in steel specimens immersed in either anhydrous ammonia liquid or vapor.

The study was designed to determine whether angle-beam ultrasonic testing could be a practical alternative non-destructive testing method. The method now used is visual inspection and hydrostatic pressure test inspection at 375 psig. This is required only for the minority of tanks without legible American Society of Mechanical Engineers (ASME) data plates.

STUDY FINDINGS

Key findings from the investigation are as follows:

- The 20 nurse tanks examined were fabricated from steel that in almost all cases met its published design standards for tensile strength and ductility. In the rare instances where the steel fell below minimum performance levels, the measured values were only very slightly lower than expected levels. The steels used over the years have changed from high-strength, which is more susceptible to SCC, to lower-strength, which is less susceptible to SCC.
- Four of the nurse tanks examined contained cracks detected by external angle-beam ultrasound. As explained in detail in Appendix A, each of these cracks was too small to pose a 10-year safety concern. Nevertheless, such cracks could potentially expand during future service and could potentially cause tank failure.
- Neutron diffraction analysis performed on hoop sections from two nurse tanks showed that they contained extremely high residual tensile stresses in the heat affected zone of the steel immediately adjacent to the unannealed welds used to assemble the heads to the shell during the manufacturing process. Tensile stress is a necessary factor in SCC in terms of crack initiation and crack growth.
- In the 20 nurse tanks examined, there was no significant decarburization in the steel near the tank's inner wall. Decarburization is a diffusion-driven process that slowly removes the carbon from regions near a steel specimen's surface, making the steel weaker.
- SCC studies on steel sample test coupons immersed in anhydrous ammonia liquid or vapor generated some cracks that grew in a minority of the specimens; however, most specimens did not initiate or grow cracks. Continued monitoring of the cracked specimens allowed measurement of their crack growth rates under conditions matching

actual nurse tank service conditions. These data in turn allowed for the formulation of a recommended nurse tank inspection procedure that could mitigate future tank failure rates.

CONCLUSIONS

Findings from this study illustrate the great need for additional anhydrous ammonia/steel SCC studies to determine a fuller picture of crack growth rates over a larger sample of sample test coupons and for a longer period of time. The findings also indicate that a more detailed assessment should be made to determine whether future nurse tank manufacturing processes would benefit if they included whole-tank stress relief annealing after welding the tank heads to the shell. These and other issues are included in two follow-on task orders. The initial one was authorized on February 17, 2011 and both are now scheduled to be completed August 2013.

This project developed a preliminary set of recommended inspection procedures based on the limited data collected in this study. These new procedures are based on inspection of the tanks using an ultrasonic angle beam to search for and measure the dimensions of indications for possible cracks in the high stress areas near unannealed welds. The major question associated with these recommended inspection procedures is whether they should be implemented now or should wait until the larger dataset of cracks in sample coupons from the new task order research becomes available as part of the work to be completed in later 2013. It is the recommendation of the researchers that the wiser course of action would be to wait until the additional data are available and can be used as a guide for formulation of inspection procedures that might be included in a rulemaking. The rationale behind this recommendation is summarized as follows:

- The SCC testing performed in this study exposed 56 specimens to tensile stress in anhydrous ammonia, some in liquid and others in vapor for a period of 7 months. Of these specimens, seven initiated and grew cracks, and the growth rates of those cracks were then measured. This is a sufficient dataset to be useful; however, it is still a very small statistical base (both in terms of the number of expanding cracks and the length of time the cracks were exposed to anhydrous ammonia) to use in formulating required inspection procedures for the estimated 200,000 nurse tanks of various ages and types of steel in use today in the United States.
- Nurse tank failures are relatively infrequent events. In the research team's opinion, the probability is not excessively high for life-threatening failures occurring during the time period while the second set of investigations specified under the follow-on task order are performed. The current testing procedures for tanks without legible ASME data plates will continue while the larger database is acquired and analyzed.
- There will be an extensive learning process associated with implementing and enforcing any new set of inspection procedures. It would be potentially confusing and counterproductive to begin the process for implementing a new inspection procedure now, only to need to revise the procedure in a short period of time based on the new data from the new task order study. We recommend it would be better to wait until a more complete body of data is available to formulate and propose adoption of new inspection procedures.

DEPLOYMENT STRATEGIES

Recommended inspection procedures are based on a combination of visual inspection and angle beam ultrasound inspection where warranted. The time interval between such ultrasound inspections is correlated to the estimated crack growth rates determined in this study. These inspection procedures could be used either in addition to current procedures, or as a replacement for current procedures.

1. INTRODUCTION

Anhydrous ammonia (NH_3) is widely used as an agricultural nitrogen-rich fertilizer for crops needing nitrogen soil supplements. It is locally distributed from agriculture cooperatives to farm fields via nurse tanks. Nurse tanks are cylindrical steel tank shells with hemispherical or elliptical end caps referred to as heads, designed to hold NH_3 in liquid form under pressure. Typical steels that have been used to construct nurse tanks include ASTM A285, ASTM A455, and ASTM A516 grade 70. (ASTM is formerly known as the American Society for Testing and Materials.) The lower-strength, low-carbon A455 is now more common. The 56 coupons tested in NH_3 by this study used A455 steel. However, the data calculations in Appendix A for minimum critical crack sizes are based on the very similar A516 grade 70 steel. The 455 and 516 grade 70 steels are quite similar in composition, mechanical properties, and corrosion behavior. Thus, we believe the Appendix A calculations are representative of the A455 steel.

In the 1960s, a quenched and tempered ASTM A517 grade F higher-strength steel was used to construct nurse tanks and is still used today in NH_3 tank trailers subject to U.S. Department of Transportation (USDOT) motor carrier (MC) MC-331 requirements for high-pressure vessels. Data on SCC of this steel is reported in Tables 3 and 4 in Appendix E. ASTM A517 Grade F has significantly lower carbon content and higher chromium, molybdenum, and nickel contents that could make its SCC behavior differ from that of A455 and A516 steels. However, the general finding of what causes SCC, reported in Appendix E, still holds.

The Fertilizer Institute (TFI) previously estimated that about 200,000 nurse tanks are in operation across the United States, many of which are 3 to 5 decades old. An international survey conducted in 1982 found that more than half of all inspected spherical NH_3 tanks were reported to have cracks.⁽¹⁾ The Hazardous Substances Emergency Events Surveillance branch of the U.S. Department of Health and Human Services reported NH_3 as the number one released hazardous substance in 1997.⁽²⁾

Liquefied NH_3 flash vaporizes upon depressurization and causes severe freeze burns when in contact with human tissue. NH_3 is also very caustic and most severely affects the high-moisture-bearing eye, skin, gastrointestinal, and respiratory systems. Exposure to greater than 140 parts per million (ppm) of NH_3 can cause corneal ulcerations, iritis (swelling and irritation of the uvea, the middle layer of the eye, which provides most of the blood supply to the retina), cataracts, glaucoma, and retinal atrophy. An article in the publication "*The Nurse Practitioner*" says that exposure to 1,700 ppm (1/6 of 1 percent) of NH_3 can result in permanent respiratory damage.⁽³⁾ In the National Transportation Safety Board (NTSB) report on the Calamus, Iowa, anhydrous ammonia incident, NTSB recommended a rulemaking to require non-destructive testing of all nurse tanks. That report also states that according to the National Institute for Occupational Safety and Health (NIOSH), the "low lethal" concentration (LCLO) of anhydrous ammonia for humans is 5,000 ppm ($1/2$ of 1 percent) for a period of 5 minutes.⁽¹²⁾ Therefore, the safe storage of NH_3 in nurse tanks is of great concern to anyone dealing with its handling or transportation.

Nurse tanks can fail from cracks for several reasons:

- There can be a flaw in the manufacture (e.g., a weld is not properly executed).
- The tank can be damaged in use (e.g., dented by an impact).
- The tank can spontaneously initiate and grow small existing cracks due to the high residual stresses, high operational stresses in the tank, and corrosiveness of the NH₃ solution. This initiation of and growth of cracks is commonly referred to as SCC.

The American Society of Mechanical Engineers (ASME) code for some time has provided the nurse tank manufacturer a choice regarding what level of radiography to use to inspect welded joints on the tanks. If they use 100-percent radiography on the longitudinal seam, then they can meet the minimum safety requirements using thinner steel for the shell wall than if they do not perform a 100-percent radiograph of the longitudinal weld seam. According to 49 CFR 171.7 the finished tank is then supposed to be subject to a hydrostatic acceptance test at 1.5 times the maximum working pressure of 250 pounds per square inch, or 375 pounds per square inch (psi).

At one of the manufacturers of nurse tanks, radiography equipment was developed (in the late 1980's) that practically allows 100-percent radiography of the longitudinal seam in a production line environment. The result of that development, together with the safety design provisions of the code, has led both the remaining U.S. manufacturers of nurse tanks to make the business decision to use 100-percent radiography of the longitudinal seam, and thus take advantage of the ASME specification for thinner steel for the shell.

The amount of radiography used in inspecting the longitudinal weld seam during manufacture is recorded on the nurse tank's data plate. Thus, owners and inspectors of nurse tanks can easily distinguish which tanks received a 100-percent radiograph of the longitudinal seam as part of their manufacture.

Head-to-shell welds continue to be spot x-rayed at one 6-inch length of weld for every 50 feet of weld. This means it is possible for the head seams on a given tank to have no spot x-ray applied. Because head-to-shell welds are not 100-percent x-ray inspected, a variety of crack-like flaws can exist in these welds, even in new tanks. These cracks can be encouraged to grow by operational stresses and SCC. The same is true for welds that join two or more shell sections together. Unlike the head welds, which are welded only from the outside, the welds joining shell sections together are performed from both the inside and outside.

The same is also true for cracks around welds that attach the running gear feet to the tank body. ASME offers a number of examples of guidance for how running gear feet may be attached to the tank shell, but none constitutes a specification. Running gear feet failures generally cannot be attributed to SCC, because the NH₃ is on the inside of the tank, which does not reach the leg feet mount welds. However, because these are unannealed welds, there is the possibility of creating a higher stress heat-affected zone (HAZ) through the steel, making the inner surface where the running gear feet are attached more susceptible to SCC. However, failures around these welds seem more likely to be metal fatigue related from the repeated stresses placed on the tank shell through repeated transient stresses associated with traversing rough terrain.

There are visual inspection standards applied to dents in nurse tanks without data plates. They specify the maximum dent depth, size, and ratio of depth to size. This visual inspection standard could be logically applied to all tanks if the decision is made to require all nurse tanks to be periodically inspected, as recommended by the National Transportation Safety Board (NTSB).

There is also an inspection standard found at 49 CFR 173.315(m)(2) for hydrostatically testing nurse tanks without data plates at 375 psi. This too could be applied to all nurse tanks. TFI petitioned the Pipeline and Hazardous Materials Safety Administration (PHMSA) for adoption of such a standard. The specification found at 49 CFR 173.315(m)(2), "Nurse tanks with missing or illegible ASME plates," says:

Nurse tanks with missing or illegible ASME plates may continue to be operated provided they conform to the following requirements:

- (i) Each nurse tank must undergo an external visual inspection and testing in accordance with §180.407(d) of this subchapter.
- (ii) Each nurse tank must be thickness tested in accordance with §180.407(i) of this subchapter. A nurse tank with a capacity of less than 1,500 gallons must have a minimum head thickness of 0.203 inch and a minimum shell thickness of 0.239 inch. A nurse tank with a capacity of 1,500 gallons or more must have a minimum thickness of 0.250 inch. Any nurse tank with a thickness test reading of less than that specified in this paragraph at any point must be removed from hazardous materials service.
- (iii) Each nurse tank must be pressure tested in accordance with §180.407(g) of this subchapter. The minimum test pressure is 375 pounds per square inch gauge (psig). Pneumatic testing is not authorized.
- (iv) Each nurse tank must be inspected and tested by a person meeting the requirements of §180.409(d) of this subchapter. Furthermore, each nurse tank must have the tests performed at least once every 5 years after the completion of the initial tests.
- (v) After each nurse tank has successfully passed the visual, thickness, and pressure tests, welded repairs on the tank are prohibited.
- (vi) After the nurse tank has successfully passed the visual, thickness, and pressure tests, it must be marked in accordance with §180.415(b), and permanently marked near the test and inspection markings with a unique owner's identification number in letters and numbers at least 1/2 inch in height and width.
- (vii) Each nurse tank owner must maintain a copy of the test inspection report prepared by the inspector. The test report must contain the

results of the test and meet the requirements in §180.417(b) and be made available to a DOT representative upon request.

Note. The current hazmat regulation at 49 CFR 171.7 incorporates the 1998 ASME specification for hydrostatic testing by the manufacturer at 1.5 times the maximum allowable working pressure of 250 psig, or 375 psig, as a final quality control check after the tank is fabricated at the manufacturing facility. (PSIG is generally interpreted to mean the same as PSI. It specifically means the internal pressure minus the external atmospheric pressure, i.e., the difference in pressures.)

ASME has issued an update to the 1998 code that lowered the initial manufacturer's quality control or acceptance pressure testing to 325 psi. FMCSA reports the remaining two U.S. nurse tank manufacturers have adopted the newer ASME specification of 325 psi for initial acceptance testing. The existing PHMSA regulation at 49 CFR 171.7 still references the 1998 ASME specification that requires 375 psi hydrostatic initial manufacturer acceptance testing. The more recent PHMSA regulation at 49 CFR 173.315(m)(2) also specifies hydrostatic testing at 375 psi for tanks with missing or illegible data plates.

1.1 PRIOR STUDIES OF STRESS CORROSION CRACKING IN NURSE TANKS

Most studies of NH₃ SCC were performed in the 1960s and 1980s. Current literature on the topic is scarce, suggesting the need for further investigation of the structural integrity of aging nurse tanks. Different steels and manufacturing quality control methods were employed over the years by multiple companies. The number of U.S. nurse tank manufacturers is now reduced to two.

1.1.1 Stress Corrosion Cracking (SCC)

SCC results from a process that simultaneously involves a corrosive environment and tensile stress on the steel from residual and/or applied tensile stresses. The extent to which SCC damages a material is determined by the material type, environment, and amount of tensile stress. SCC can be classified according to three broad categories: active path dissolution, hydrogen embrittlement, and film-induced cleavage.

1.1.1.1 Active Path Dissolution

Active path dissolution occurs in active metals that have passive protective layers. Accelerated corrosion occurs along crack tips, grain boundaries, or other paths of high corrosion susceptibility where the passive protective layer is compromised.⁽⁴⁾ When a metal is surrounded by a corrosive solution (e.g., NH₃) and a tensile stress is applied, the stress serves to open up small cracks in the protective layer. The crack tips act as stress risers and provide a pathway for accelerated corrosion (dissolution of the active metal). Thus, the combined effect of corrosive solution and stress serve as an "electrochemical knife" that slices through the metal.⁽⁵⁾ The speed of active path dissolution is limited by the rate of corrosion that can occur at the crack tip. Thus, cracks in steel used for nurse tanks generally grow at rates of less than 1 millimeter (mm) per year.⁽⁴⁾

1.1.1.2 Hydrogen Embrittlement

Hydrogen embrittlement is the process by which various metals, most importantly high-strength steel, become brittle and fracture following exposure to hydrogen in environments that facilitate its infusion into the metal. Thus, hydrogen embrittlement may have been a larger problem in the past when nurse tanks were made out of high-strength steels.

Hydrogen embrittlement occurs when a source of hydrogen is present in a metal's environment, which is true in nurse tanks containing both NH_3 and 0.2 percent water. Hydrogen can damage nearly all metals by filling interstitial sites associated with the cracks (these are the spaces between the atoms and the grains of the metal), which causes the metal to become more brittle. Because of their small size, hydrogen atoms can diffuse into metals very quickly. Furthermore, hydrogen easily diffuses into regions ahead of crack tips due to local stresses and lattice dilations (stretching of the spacing between the metal atoms by the tensile stress).⁽⁴⁾

1.1.1.3 Film-induced Cleavage

Film-induced cleavage occurs in ductile materials that form brittle films in the presence of a corrosive substance. When stresses crack open the brittle outer protective layer, the active ductile material underneath blunts the crack tip. The film reforms, and the process repeats, causing the metal to continually corrode away.⁽⁴⁾

1.1.2 Mechanisms of Anhydrous Ammonia Stress Corrosion Cracking in Steel

Wilde concluded that hydrogen embrittlement does not contribute to NH_3 SCC, and that NH_3 SCC in steel is of the active path dissolution type.⁽⁶⁾ Thus, film-induced cleavage is also eliminated as the mechanism by which SCC advances. However, not all investigators agree with Wilde's conclusions (see Appendix E).

Both intergranular and transgranular cracking occur as the result of NH_3 SCC:

- Intergranular is a crack that runs through a metal by following a path along grain boundaries. Grain boundaries are individual crystals of metal. A typical piece of metal contains thousands or even millions of very small grains. A grain boundary is the place where one grain ends and a new grain begins. This could be thought of as somewhat like a person who travels across a State by driving only on county-line roads.
- Transgranular is a crack that runs through the grains of a metal and does not follow a path along grain boundaries. It could be thought of as somewhat like a person who travels across a State ignoring county-line roads and driving a four-wheel-drive vehicle across field and stream.

Pure NH_3 does not cause SCC. But when NH_3 is mixed with as little as 0.5 ppm oxygen, it does cause SCC. Adding 0.1 percent water by weight to NH_3 was shown to inhibit SCC completely in such ammonia solutions. Thus, oxygen serves two roles in NH_3 SCC; it forms protective oxide layers on metal, but when those layers are cracked or broken, it acts as the oxidizing agent to cause corrosion.

However, the inhibition of corrosion by the addition of water to NH_3 only works in the portion of the tank where the ammonia solution is in the liquid phase that contains the water. Since ammonia has a much higher vapor pressure than water, the vapor area of the tank does not contain the necessary water to inhibit the SCC caused by the NH_3 .

Lunde and Nyborg demonstrated that the addition of water to liquid NH_3 does not provide protection against SCC in regions of the tank above the liquid level because vaporized NH_3 (free of the added water) can condense on the upper surfaces of the tank.⁽⁷⁾ Oxygen dissolved in NH_3 increases the corrosion potential of steel, while dissolved nitrogen has little effect on the polarization potential.

Though nitrogen has no electrochemical effect, it accelerates SCC when in the presence of oxygen.^(8,9) Only oxygen and oxygen-nitrogen contaminations of ammonia have been shown to cause SCC. Though carbon dioxide (CO_2) has been shown to be generally corrosive, it does not appear to contribute to NH_3 SCC.⁽⁶⁾

Several theories have developed to explain the process of NH_3 SCC. A film-rupture model was proposed by Wilde based upon electrochemical studies, and it proceeds as follows. Steel in NH_3 exists in both a film-free active state, and a covered passive state formed by dissolved oxygen. The oxygen forms a noble adsorbed film on all steel surfaces (adhering to the surface but not penetrating beneath the surface). When the steel is stressed enough to create plastic deformation at slip steps, the protective oxygen film rendering the steel passive is ruptured at that point. Direct galvanic coupling between the bare steel at the slip step and the still intact portion of the adsorbed oxygen film causes anodic dissolution of the steel until the oxygen film reforms.

Nitrogen is proposed to compete with oxygen to adsorb to the steel, but without forming a protective film itself, thus hindering repassivation of the exposed steel with an oxygen film. When the passive protective oxygen film is ruptured by an applied stress, nitrogen adsorbs in place of oxygen and anodic dissolution is allowed to continue for a much longer time. In the absence of dissolved nitrogen, the oxygen film passivating the steel quickly recovers and crack growth is slow. The nitrogen-oxygen combination causes more rapid dissolution of steel and thus more severe cracking. A regular source of free N_2 nitrogen introduction occurs when air enters the tank as part of hydrostatic pressure tests. A tank interior completely devoid of oxygen gas would not passivate well, but would also lack the oxygen needed to drive SCC; thus, purging tanks with nitrogen after exposing the inner surface to air has been suggested as an effective step to reduce SCC damage in nurse tanks.

Water also has an affinity for adsorption (adhering to the surface but not penetrating beneath the surface) on steel since it is a polar molecule, and it acts as an additional passive film, thus aiding oxygen in slowing SCC, thus, the value of adding water to the NH_3 .

1.2 EXAMPLES OF CATASTROPHIC FAILURE CAUSED BY STRESS CORROSION CRACKING

In 1956, Dawson reported that 3 percent of anhydrous nurse tanks (possibly being used for cotton) failed within 3 years of service in a southern State that has a large number of such vessels.⁽¹⁰⁾ Revised ASME specifications were put in place for future tanks manufactured, but

failures continued to occur. Fuller versions of the following summaries are contained in Appendix E.

1.2.1 Calamus, Iowa Incident

In the spring of 2003, a cooperative worker in Calamus, Iowa, was killed when the nurse tank he and another man were filling ruptured. The catastrophic rupture of NH₃ gas threw one man against a truck, knocking him unconscious. A coworker who pulled him to safety inhaled NH₃ gas at a sufficient concentration (presumably between 1,700—1/6 of 1 percent—and 5,000 ppm 1/2 of 1 percent) that caused him to eventually die of pneumonia due to inhalation burns in his lungs.

After the accident, a detailed investigation was performed by the NTSB. The tank was constructed of 3/8-inch SA-455 steel in 1976 and was designed to withstand 250 psig as specified by the ASME *Boiler and Pressure Vessel Code: Section VIII, “Rules for Construction of Pressure Vessels.”* Furthermore, the tank was hydrostatically pressure tested by the manufacturer at the then-specified 375 psig after manufacture. About 27 years after construction, the nurse tank ruptured along the tank’s longitudinal weld seam that ran along the bottom of the tank for 53.5 inches (see Appendix E, Figure 86, for a photo).⁽¹¹⁾

The NTSB determined that the probable cause of the sudden failure of the nurse tank was inadequate welding and insufficient radiographic inspection during the tank’s manufacture, as well as lack of periodic inspection testing during the tank’s service life to detect deterioration of the inadequate weld. They recommended in their 2003 report that a 100-percent radiosopic inspection of longitudinal welds should be required in place of spot radiography.⁽¹²⁾

Current ASME specifications still allow using only spot checks. But, it also provides an incentive for using a 100-percent radiosopic check of the shell’s longitudinal weld seam. Namely, if 100-percent radiosopic inspection is completed, then it allows for use of slightly thinner steel for the tank shell.⁽²³⁾ Both existing U.S. manufacturers have adopted using a 100-percent radiograph of the longitudinal welded seam and the thinner steel for the tank shell.

1.2.2 Morris, Minnesota Incident

On June 6, 2005, at approximately 6 p.m., a 1,000-gallon NH₃ tank catastrophically ruptured in Morris, Minnesota, at the Cenex Cooperative site. The tank had been filled to the recommended maximum of 85 percent capacity 3 hours before it ruptured. When the tank ruptured, a portion of the rear head blew off, releasing the entire contents of more than 841 gallons of NH₃. The nurse tank shot 100 yards across the lot, split a utility tractor in half, and hit a parked automobile before coming to rest. The tank’s path missed other filled nurse tanks by only 25 yards. Since the rupture happened in the evening, no employees were in the area, and no workers were injured or killed. However, a farmer living three-tenths of a mile to the west of the Cenex Coop was hospitalized for NH₃ inhalation treatment. The tank was coined the “Morris Missile” because of its ballistic nature (see Appendix E for a photo).⁽¹³⁾

1.2.3 Silver Lake, Minnesota Explosion

On December 21, 2007, the rear-facing head of a 1,000-gallon nurse tank, towed by a farmer with his pickup truck, catastrophically ruptured. The tank tore away from its running gear,

slammed into the back of the truck, and then shot across the farmer's front yard. The NH₃ in the tank vaporized, and the farmer was hospitalized for NH₃ exposure. Packer Engineering performed an investigation of the accident for the USDOT. The tank was constructed in 1973 by Chemi-Trol Chemical Co. in Ohio. The ASME nameplate information indicated that upon manufacture, like all such welds, the tank's head to shell weld was spot-inspected by radiography, but additionally the welds had been stress-relieved (annealed).

Visual examination of the head revealed that the crack originated on the inside diameter of the rear head at a region that had previously been damaged by an impact with some other object.

This is critical, because significant dents create considerable local stresses in the steel, which can facilitate the initiation of a crack. This is why the visual inspection standard for nurse tanks without data plates specifies the maximum allowed size and depth for dents. Metallographic examination of the crack initiation site revealed that severe crack branching, as well as intergranular and transgranular brittle fracturing had occurred because of the dent damage, and thus the induced stress. The cause of the accident was reported as rupture due to SCC, accelerated by residual stresses induced from the dent (see Appendix E, Figure 92, for a photo).⁽¹⁴⁾

1.2.4 Middleton, Ohio Tanker Accident

On August 22, 2003, a USDOT MC 331 cargo tank head ruptured while the tank was being filled with NH₃ in Middleton, Ohio. The tank was manufactured in 1977 of ASTM A516 grade 70 quenched and tempered steel. It had a nominal shell thickness of 0.399 inches, minimum head thickness of 0.250 inches, and maximum allowable working pressure of 265 psig at 150° F. The tank's capacity was 10,600 gallons. The head failure occurred when the tanker was about half-full of NH₃ at 80° F, with an internal pressure of 170 psig. The release of NH₃ caused the evacuation of 100 employees from buildings downwind of the tank. Five people received medical treatment for inhalation injuries, but no one was seriously hurt. The damage from the tank rupture caused an estimated \$25,000 in damages to equipment.

Before the accident, the tank had been inspected externally with magnetic particle testing and internally with hydrostatic testing in March 2002. It had received the annual external visual inspection in 2003 in accordance with USDOT mandates. An NTSB investigation into the accident revealed that a 16-inch through-wall crack next to a radial weld on the head had developed. Post-mortem magnetic particle inspection revealed cracks along other radial head welds that had not yet penetrated completely through the wall.

When investigators opened up the 16-inch through-wall crack for examination with a scanning electron microscope (SEM), a previously undetected 3-inch through-wall crack opened up as well. Both through-wall cracks exhibited intergranular corrosion and separation (see Appendix E, Figure 98, for photo).

Investigation into the NH₃ filling process revealed that the required amount of water needed to prevent SCC was not being added to the liquid NH₃, even though the tanker company handbook stated that 0.2 percent water by weight must be added to NH₃ carried in its liquid petroleum gas (LPG) tanks. When it ruptured, the NH₃ being pumped into the tanker contained less than 0.1 percent water. The reported cause of the failure was SCC, which presumably developed because

company practices were not established to explicitly prohibit quenched and tempered high-strength steel tankers from carrying NH₃ with less than 0.2 percent water.⁽¹⁵⁾

[This page intentionally left blank.]

2. TANK ACQUISITION AND METALLURGICAL EVALUATIONS

2.1 TANK ACQUISITIONS

The design of this project was to study nurse tanks with a wide range of ages. Twenty tanks were acquired, some by donation and some by purchase. Two were manufactured in the early 1950s, one was manufactured in 2009, and the rest were manufactured between 1960 and 1990. Tanks manufactured during the 1990's and 2000's were difficult to acquire because owners were reluctant to sell or donate newer tanks. Consequently, the sample includes more tanks manufactured during the 1960's and 1970's and fewer tanks manufactured in the 1990's and 2000's than intended in the design specifications for the project. Most of the tanks had been in service in Iowa, although information about the tanks' histories was difficult to acquire.

A follow-on task order to this one performed angle-beam measurements on a number of tanks, thus supplementing information available about tanks manufactured during the 1990's and 2000's. Observations about these tanks will be provided in the final report from that follow-on task order.

2.2 TANK EVALUATION BY THE ANGLE-BEAM ULTRASOUND TECHNIQUE

Tanks were inspected visually upon delivery at the Jordan site, and the heat-affected zones adjacent to welds were examined by angle-beam ultrasound on the tank's exterior surface in an effort to detect indications of possible cracks. Most cracks initiate in the high residual stress heat-affected zones, so only this region was examined for all weld joints. Examining all regions of the tanks would have been prohibitively time-consuming. Cracks were found in 4 of the 20 tanks. These cracks varied in size from a few millimeters (mm) long to 150 mm long.

2.3 TANK EVALUATION BY METALLOGRAPHY

After completion of the visual and ultrasound inspections, the tanks were cut with an oxy-acetylene torch to obtain test specimen coupons of the steel tank shell walls for metallographic analysis. Tank heads were not analyzed metallographically. These test coupons displayed the expected mixed microstructure (ferrite plus pearlite regions) typical of slow-cooled low-carbon steel. Some metallographic sections were taken from flawless regions, others around cracks.

A mixture of nitric acid and methanol, known as nital, was used to etch the specimens to reveal their phase structure. The clear regions in Figure 1 show a crack that appears to have followed the grain boundaries in the metal, although it is difficult to discern clearly if that is true along the entire crack length. The figure shows ferrite (Fe) and nearly pure Fe with trace amounts of carbon dissolved in the metal. The darker regions are a mixture of Fe₃C (carbide) and ferrite, a two-phase microstructure called *pearlite*.

Pearlite is a banded structure of alternating layers of nearly pure Fe and Fe₃C. Each layer is about 1 micrometer thick, similar to a stack of bread slices, where the first, third, fifth, etc., slices are white bread, and the second, fourth, sixth, etc. slices are rye bread. In lower-carbon steels with less than about 0.75 percent carbon content, like A455 now commonly used in nurse tanks, there is not enough carbon available to make the steel totally comprised of pearlite colonies. In these lower-carbon steels, these pearlite colonies will be mixed with other grains that are nearly pure Fe (no Fe₃C platelets in those grains). Both microstructures (i.e., all pearlite colonies or mixed pearlite colonies+pure Fe) are called “pearlite.”

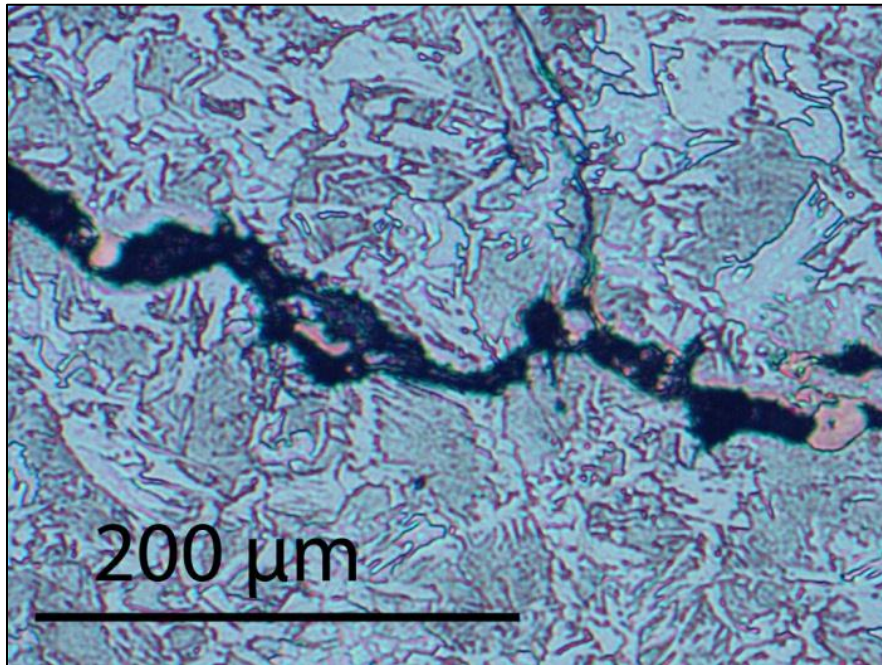


Figure 1. Photograph. Metallographic cross-section of tank wall steel containing a crack.

Both in regions with cracks and regions without cracks (the great majority of specimens), the steel showed a consistent ferrite plus pearlite microstructure. This is the normal microstructure and indicates that the steel was consistently in the expected microstructural condition in all areas inspected by metallographic inspection.

One previous study of steel from a failed nurse tank⁽¹⁴⁾ was reported to have detected decarburized regions (i.e., showing lower than normal pearlite phase content, presumably because of removal of the carbon) near the inner tank surface. No such decarburized regions were seen in any of the 20 tanks studied in this project, as explained in the next section. Decarburization is a diffusion-driven process that slowly removes the carbon from regions near a steel specimen’s surface. Such a state would weaken the steel.

2.4 TANK EVALUATION BY GLOW DISCHARGE SPECTROSCOPY

Coupons cut from the tank walls were also studied by analyzing their compositions using glow discharge spectroscopy. This method bombards the steel’s surface with high-velocity argon gas atoms, which sputter metal from the steel surface. This method is similar to sandblasting—only

in this case the abrasive is argon gas, not sand. This sputtered metal is then analyzed for its elemental content. This “sandblasting” allows metal to be removed in thin sections (small fractions of a micron) so the composition profile as a function of depth can be determined for the metal near the surface.

This technique is a particularly sensitive method for determining carbon content in shallow depths below the metal’s surface, and it was thought that any decarburized regions could be analyzed accurately with this method. The glow discharge results were consistently similar to the example seen in Figure 2. Aside from a very thin (less than 1 micron thick) oxidized layer near the inner tank surface, there were no significant deviations from the expected carbon content of the metal. This oxidized layer is the sort that forms on nearly all free metal surfaces exposed to the atmosphere and is not the same as the adsorbed oxygen discussed earlier in this document. The content of other elements was also consistent with what one would expect for steels of these nominal compositions.

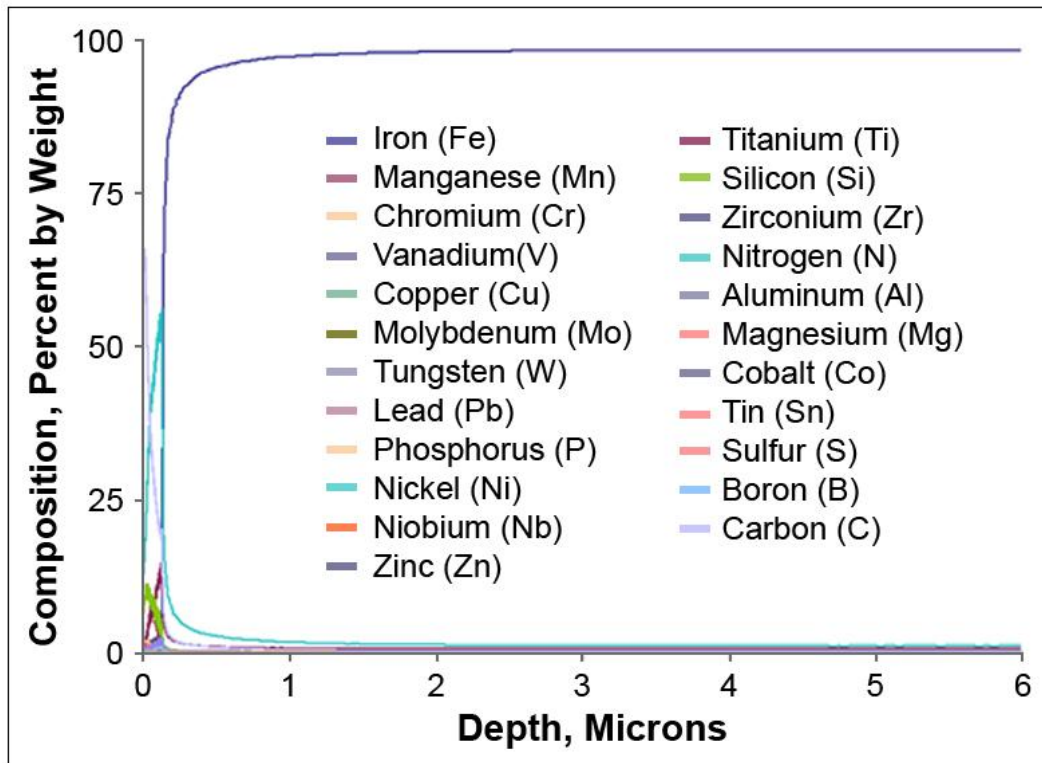


Figure 2. Graph. Glow discharge spectroscopy results from first 6 microns of steel at the inner tank wall.
 Depth = 0 corresponds to the surface in direct contact with anhydrous ammonia during service; depth = 6 corresponds to steel 6 microns below the anhydrous ammonia-contact. (A standard 3/8 nurse tank is 9,525 microns.)

2.5 TANK EVALUATION BY TENSILE TESTING

Test specimen coupons cut from the tank walls were also studied by fabricating them on a lathe into round tensile test specimens and pulling them with a tensile testing machine until they fractured (Figure 3). This allowed measurement of the steel’s tensile yield strength, tensile

ultimate strength, and tensile ductility by elongation. (Ductility is the degree to which a material can be deformed, dented, twisted, or stretched without breaking. A high-ductility material is a copper wire; a low-ductility material is a glass pane.) The data acquired by tensile testing (see Appendix B) were almost entirely within the expected performance range for these steels. The few specimens that fell below the minimum expected strength values were within 1 to 2 percent of the minimum strength value.

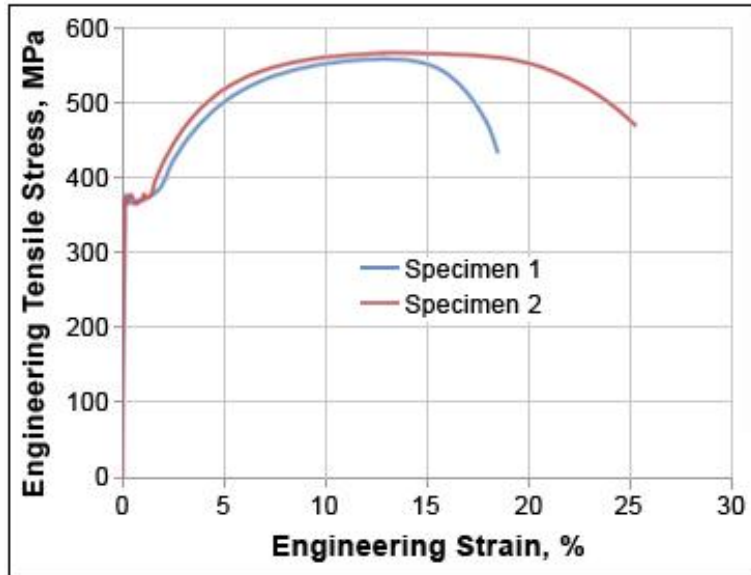


Figure 3. Graph. Tensile test results from a 1,000-gallon nurse tank manufactured in 1966.

2.6 TANK EVALUATION BY MAGNETIC PARTICLE-FLUORESCENT DYE PENETRANT TESTING

Once the tank interiors were accessible on the test specimen coupons, it was possible to use magnetic particle fluorescent dye penetrant testing to reveal cracks on the interior surface. This technique magnetizes the tank steel to attract magnetic powder particles to the edges of cracks; once there, the particles can be detected visually by shining an ultraviolet light onto the surface (Figure 4) to make the particles poised at the crack's edges fluoresce. This method provided a corroborating cross check on the accuracy of the angle-beam ultrasound inspection for cracks detected from the tank's exterior surface.

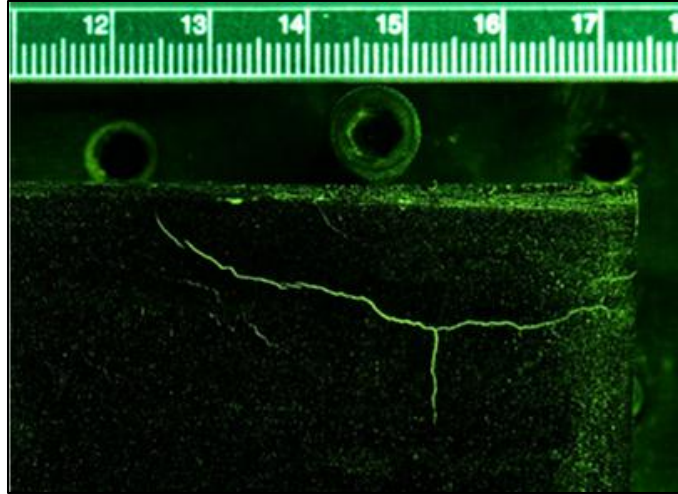


Figure 4. Photograph. One of several cracks made visible by ultraviolet-light-induced fluorescence of magnetic particles poised at the crack edges.

The scale at left is calibrated in centimeters; the finest divisions are 1 millimeter apart.

2.7 TANK EVALUATION BY SCANNING ELECTRON MICROSCOPY (SEM) OF FRACTURE SURFACES

The cracks revealed in the previous evaluations were forced open to separate the two surfaces of the crack. This is done by dramatically lowering the temperature of the steel by immersing it in liquid nitrogen. This makes the steel dramatically more brittle, thus enabling it to be mechanically forced to crack along the weakened crack.

This allowed examination of the fracture surfaces in the SEM. The fracture surfaces showed the faceted surface (Figure 5) characteristic of the intergranular cracking that occurs with SCC.

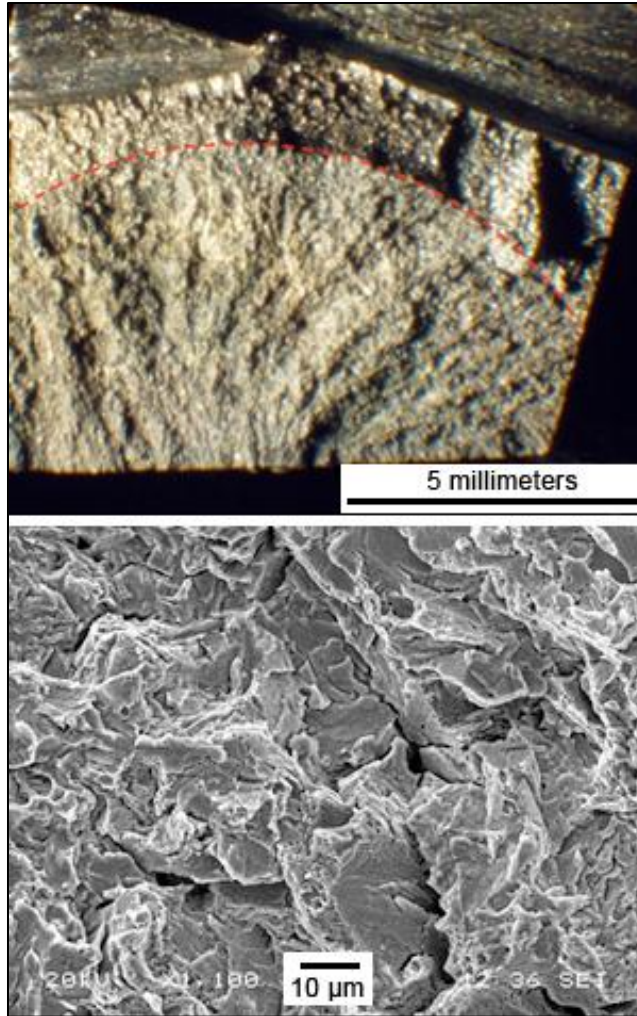


Figure 5. Image. Photographs of a typical fracture surface in one of the tanks examined.

The top image is a low-magnification image showing the boundary (dashed line) between the SCC crack region metal newly exposed by forced opening of the crack. The bottom image is a high-magnification image of the SCC surface showing the intergranular nature of the fracture along the SCC growth path.

3. TANK EVALUATION BY NEUTRON DIFFRACTION ANALYSIS

3.1 RESIDUAL STRESS IN WELDMENTS

When welds are used to join two pieces of metal, the heated regions of the metal (heat-affected zone or HAZ) expand as the temperature rises, while the cooler regions distant from the weld do not expand. These differences in expansion generate stresses in the metal that, unless relieved by heat-treating (annealing), remain essentially unchanged from the moment the weld is completed until the tank is retired from service several decades or more later.

Regions in the HAZ near a weld's fusion line (actual melting of the metal occurs only in the fusion zone) have the highest residual stresses. Some regions near a weld retain a tensile residual stress, and other regions retain a compressive residual stress. Tensile stresses are essential for SCC initiation and growth, so regions with tensile residual stresses are the ones vulnerable to SCC attack.

Regions in a metal with tensile residual stresses are distinguished by atom spacings that are approximately 0.1–0.2 percent longer than normal. Regions in a metal with residual compressive stresses are distinguished by atom spacings that are approximately 0.1–0.2 percent shorter than normal. These net differences in spacing are, at most, only a few picometers (one picometer equals one trillionth of a meter), so very sensitive instrumentation that can penetrate the steel is needed to make such measurements accurately.

The only accurate way these atom spacings can be accurately measured is with sufficient energy to penetrate the metal to a sufficient depth. The only two possible methods are x-ray diffraction or neutron diffraction. The literature search performed for this project (see Appendix E) indicated no nurse tank had ever been evaluated for tensile residual stresses in the HAZ by using either neutron or x-ray diffraction methods. Diffraction methods provide precise information on the spacing between neighboring atoms in a material. As normally applied, x-ray diffraction has a limited penetration capability. Thus, to see all the way through the metal it is necessary to use neutron diffraction.

3.2 RESIDUAL STRESS MEASUREMENTS

The Los Alamos Neutron Science Center (LANSCE) operates a neutron beam, supporting instrumentation, and technical staff to assist scientists in making neutron diffraction measurements. Demand from researchers for beam time is greater than the amount of beam time available, so prospective users must compete for allocations of the available beam time by writing proposals, which are ranked by a review panel. Two proposals were written to LANSCE to measure residual stresses in the hoop welds (Figure 6) of 1,000-gallon nurse tanks, one manufactured in 1986 and the other in 1966. The size of the hoops (more than 1 meter in diameter) posed challenges for fixtures to hold the large specimen in the correct orientations in the neutron beam (Figure 7), but these problems were overcome, and extensive data were acquired on residual stress distributions in and near the hoop welds of these tanks (Figure 8).

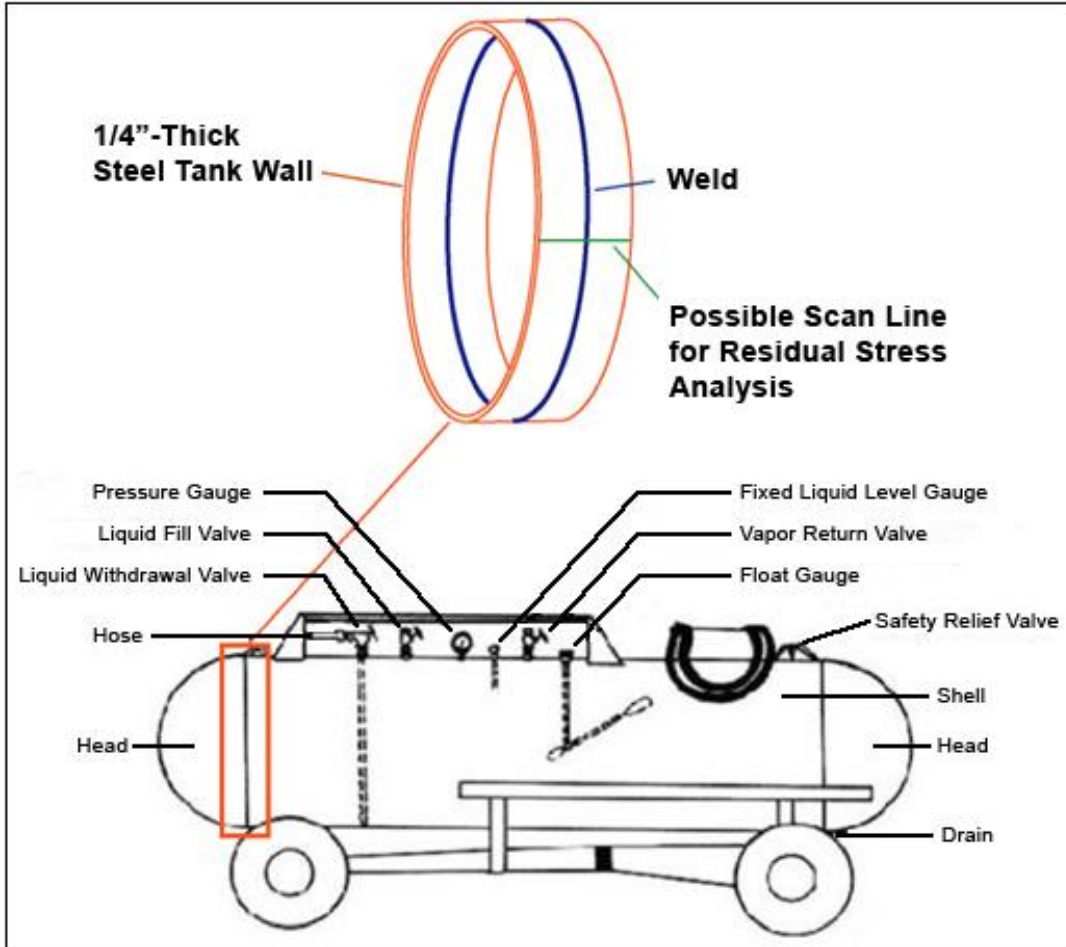


Figure 6. Diagram. Location of hoop weld sections cut from tanks.



Figure 7. Photograph. Nurse tank hoop section in the neutron beam line at LANSCE.

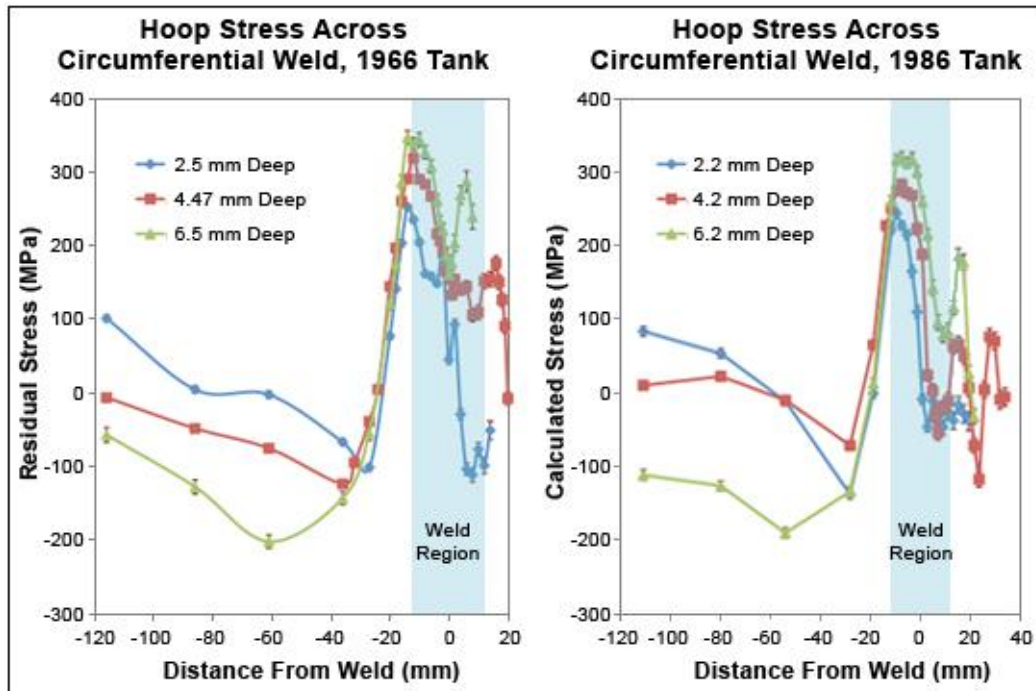


Figure 8. Graph. Residual hoop stress distributions measured by neutron diffraction at LANSCE.

The stress distributions shown in Figure 8 are quite similar for the two different tanks studied using diffraction. In each case the residual tensile stresses (denoted by the positive stress values on the plots) are nearly as large as the tensile yield strength of the steel. (Tensile yield strength is the stress value at which the steel begins to permanently deform under load. If that deforming load is then removed, the steel will not elastically recover its original dimensions.)

When tanks are pressurized with anhydrous ammonia (NH_3), additional stresses are imposed on the metal such that the yield strength of the metal is exceeded, and the ultimate strength that the metal can hold is approached (Figure 9 and Table 1). Thus, the combination of the very high residual stress near the weld and the pressure of the NH_3 , places the metal adjacent to the weld at nearly the highest possible tensile stress state, making it especially susceptible to the initiation of stress corrosion cracking in these regions.

It is significant that the highest tensile stresses are found at the boundary of the HAZ, not in the weld's fusion zone. This information can guide future inspection methods, indicating that the most productive search for cracks would be performed along the unannealed HAZ.

There is a separate issue with the feet welded to the shell of the nurse tank. Just as with the head-to-shell welds, those welds are also only on the external surface of the shell body. Although the head-to-shell welds are only from the outside of the tank, they are joining the surfaces of the two overlapped structures (shell and head) together. The HAZ created from the feet welds may be different than the HAZ for the shell-head welds. This is because the metal forming the feet mounts are perpendicular to the shell and welded long both sides of the foot mount. Plus, the stresses placed on the metal where the feet are attached are also going to be significantly influenced by the variable loading and twisting caused by traveling over bumps and uneven

terrain. The issue of possible SCC on the feet mountings is not addressed in this task order. It is examined a bit in the follow-on task order.

In Figure 9, the upper horizontal line shows the sum of the residual tensile stress in the weld heat-affected zones, plus the stress imposed by pressurizing the tank with NH₃; this is the net stress on the steel in a nurse tank in service, neglecting transient stresses on these parts associated with towing the tank over rough ground in farm fields. As noted above the stresses on the feet are not addressed.

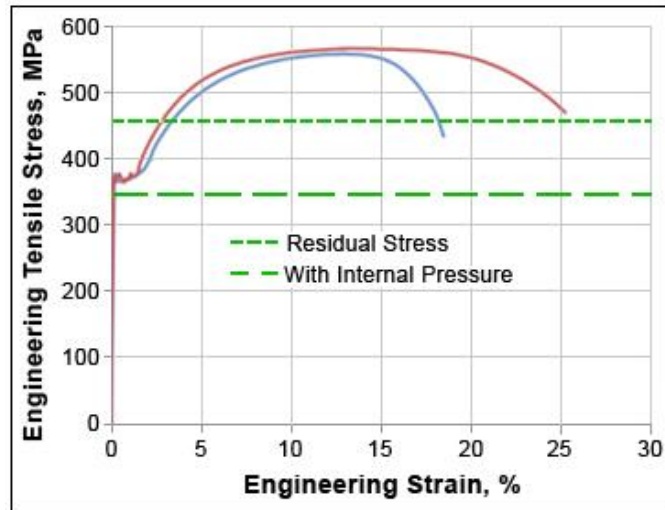


Figure 9. Graph. Superimposition of the maximum residual tensile stress measured at LANSCE (lower horizontal line) with the stress-strain plot for the steel coupons measured from that tank in tensile testing.

Table 1. Maximum hoop, axial, and radial stresses in a nurse tank resulting from internal pressure and from residual stress in the heat-affected zones near welds.

I. Stress Direction	II. Internal Pressure in MegaPascals (MPa)	III. Residual Stress in Heat-Affected Zones	Percent of Ultimate Tensile Strength of the Steel Due to (II + III)
Hoop	110 MPa	350 MPa	82%
Axial	50 MPa	250 MPa	54%
Radial	2 MPa	23 MPa	4.5%

3.3 IMPLICATIONS OF THE RESIDUAL STRESS FINDINGS FOR STRESS CORROSION CRACKING IN NURSE TANKS

The very high stresses in the heat-affected zones of the unannealed hoop weld sections measured at LANSCE are not a surprise. Other welds have been measured with this neutron diffraction technique, and in unannealed welds it is common to see stresses created near the yield strength of the metal. This indicates that thermally-induced hoop stresses during welding are high enough to

permanently deform the metal by a small amount. Stresses are lower in the axial direction (parallel to the tank's length) and radial direction (parallel to the cylinder's radius).

It is very undesirable to have such high stresses in nurse tank steel. These high stresses make initiation of SCC from exposure to NH_3 in the welded nurse tanks more likely, because the tanks are stressed to almost the highest possible values during most of their service life. This leads to accelerated SCC initiation and, to a lesser extent, growth of the cracks.

There is some consolation to be found in the fact that the high residual tensile stresses fall rapidly to compressive stress values as one moves to regions farther from the weld; thus, crack initiation conditions are severe near welds, but the stresses tending to grow the cracks diminish and reverse with distance from the weld. This would be expected to diminish the speed of SCC as the crack grows outward from the weld.

Steel is a high-toughness material, and therefore the critical crack size (the critical size is the minimum crack dimension that results in instantaneous failure of that material) is quite large. In materials science and metallurgy, toughness is the ability of a material to absorb energy and plastically deform without fracturing.⁽¹⁾ Material toughness is defined as the amount of energy per volume that a material can absorb before rupturing. It is also defined as the resistance to fracture of a material when stressed.

Therefore, these findings suggest that in unannealed nurse tanks, crack initiation conditions from stress are severe. Small cracks (once initiated) generally will grow into lower stress areas, and thus will be slow to expand to the critical size that will cause failure. The stresses on the feet welds may be influenced by significant additional transitory operational stresses.

Next, it is important to determine the likelihood that *some* cracks may NOT be slow to expand to the point of becoming a critical crack size that will cause a tank to fail.

1. "Toughness," NDT Education Resource Center, Brian Larson, Editor, 2001–11, The Collaboration for NDT Education, Iowa State University.

[This page intentionally left blank.]

4. STRESS CORROSION CRACKING EXPERIMENTS

4.1 THE STRESS CORROSION CRACKING EXPERIMENTAL PLAN

To measure crack formation and initiation rates in the steel now most commonly used to manufacture nurse tanks (SA455), test specimens were prepared and held in tensile stress while immersed in anhydrous ammonia (NH_3) vapor or ammonia liquid solution for a period of 7 months. To facilitate crack formation (in order to get measures of crack growth rates), V-shaped notches were machined into the test specimens. This was done in order to concentrate stresses at the tip of the V, thus encouraging crack nucleation and growth. The same happens in the life of the nurse tanks from random scratches, nicks, microscopic voids and inclusions, or from machining marks on standard nurse tanks. These test specimens were periodically removed, examined for crack nucleation and growth, and measured. They were then returned to the NH_3 environment. The goals of this work were to determine how rapidly cracks began, and to measure crack growth rate.

Growth rate information, in particular, is valuable in predicting likely failure times for sub-critical-sized cracks. Many nurse tanks contain cracks, but the cracks are usually too small to pose any immediate safety threat. Such cracks can eventually grow to dangerous dimensions. Information on how fast such growth is likely to occur is needed to guide inspection procedures to assure that cracked tanks are repaired or removed from service when that becomes necessary.

This SCC testing was performed in a custom-built 470-gallon test tank with a manway that permitted specimens to be placed into the tank and subsequently removed (this would be next to impossible in a normal nurse tank because access ports are so small). The test specimens were placed on a rack that held 56 prepared, direct tension samples preloaded to various stresses. These were periodically removed from the tank, and each specimen was examined using a stereographic optical microscope to determine if SCC had occurred in that sample. These examinations showed that seven specimens developed cracks during the test period.

At the end of the test, crack lengths were checked by opening (stressing to failure after immersing the sample in liquid nitrogen) specimens that contained cracks to check whether external evidence of crack length matched actual crack dimensions (which can be viewed completely only by opening the specimens). In every case, the crack lengths determined by measuring crack lengths from the metal's surface with angle-beam ultrasound were confirmed by crack opening results.

4.2 THE STRESS CORROSION CRACKING EXPERIMENTAL RESULTS

The crack sizes measured in this experiment are displayed in Figure 10 as a function of the stress intensity factor imposed on the specimen (a higher stress intensity factor correlates to a higher stress on the specimen). This figure also indicates the location of the cracked specimen in the tank (i.e., whether it was above, at, or below the tank's vapor-liquid level).

The location of the specimens in the tank may be significant. This is because of the theory explained earlier about lack of water in the NH_3 vapor, and because we received an anecdotal report from the “R” stamp tank repair person on the review team that most cracks observed in tanks that require repair occur in the vapor space above the liquid rather than on tank surfaces covered by liquid ammonia with 0.2 percent water. As reported above, NH_3 vapor promotes SCC more aggressively since it contains little or none of the 0.2 percent water content intentionally added to NH_3 liquid to suppress SCC.

The symbols in Figure 10 indicate whether the cracked specimen was tested in NH_3 vapor only, in ammonia liquid solution only, or partially in vapor and partially in liquid (interface).

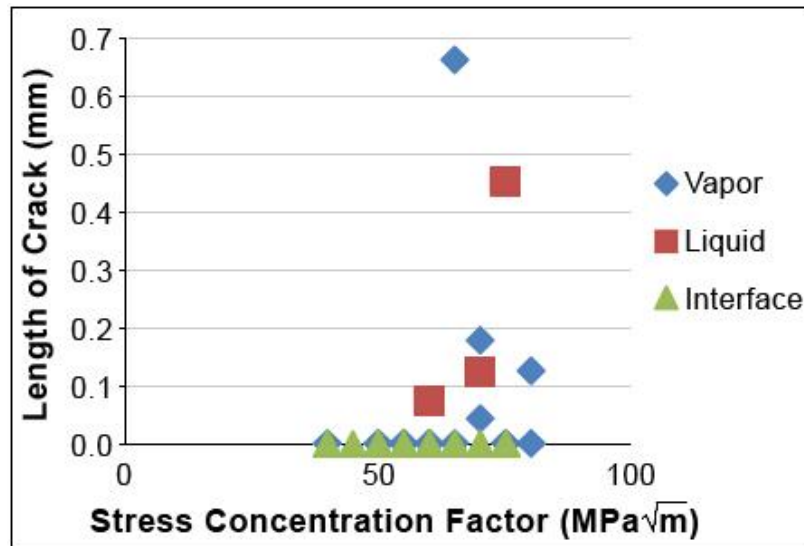


Figure 10. Graph. Crack size as a function of stress intensity factor after 4 months of exposure to NH_3 .

Seven specimens had cracks that formed and grew in the test coupons, and those cracks were small (Figure 11) with modest growth rates. This is consistent with what would be expected during a trial that lasted only 7 months on only 56 coupons. It was, however, possible to obtain estimates of growth rate values from this experiment, and these estimated growth rates were used to formulate the recommendations described in Section 6 of this report.

The data show only a loose correlation between stress intensity factor and crack size. This is typical of SCC data and reflects the stochastic (random) nature of SCC crack growth rates, which illustrates why significantly more data is needed. It also illustrates that it is possible for a particular crack to grow much faster than most other cracks, and thus establishes the importance of an inspection protocol to detect such cracks before they lead to rupture of the tank.

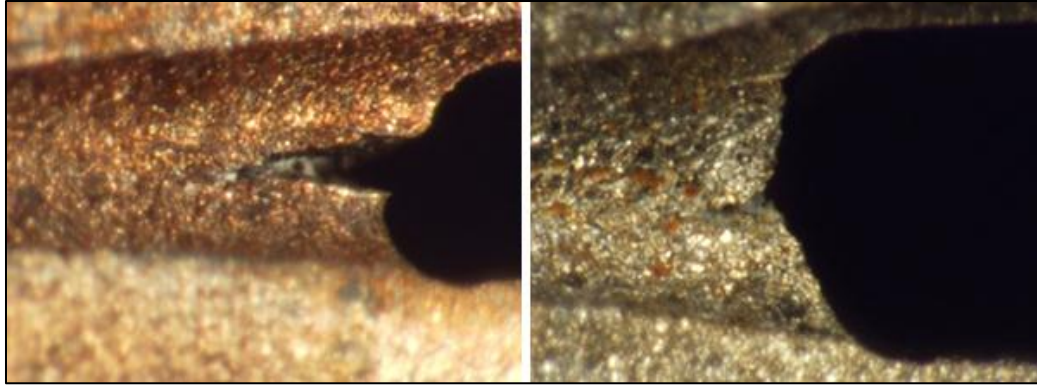


Figure 11. Image. Two cracks that initiated and grew during the stress corrosion cracking test.

The crack on the left in Figure 11 was observed after being exposed for only 2 months in NH_3 vapor on a specimen with a stress intensity factor of 65 megapascals (MPa) times the square root of m [$65 \text{ MPa}(m)^{1/2}$] (m =critical crack length in meters [remember the critical size is the minimum crack dimension that results in instantaneous failure of that material]). (How to approximate this length under different conditions is explained in Appendix A, along with a discussion of the role of stress intensity factor.) The crack on the right was also observed after being exposed for only 2 months, but at the NH_3 vapor/liquid interface on a specimen with a stress intensity factor of $75 \text{ MPa}(m)^{1/2}$. It may be that the water available at the vapor/liquid interface may have retarded the formation of a crack, plus it illustrates that even at a higher stress level there is variability in the formulation and growth of cracks.

A comparison of these stress intensity factor values with the values shown in Table 1 indicates that both are relatively low values compared to the stresses that exist at unannealed welds in nurse tanks. Yet, even at these relatively low stress-intensity factor values, they still resulted in crack growth in one of the test coupons (the V-shaped notches in the sample coupons were induced mechanically to create a concentrated stress point; the value of particular interest for this test is the growth of the crack).

The data obtained from these tests can only be usefully applied to actual situations of nurse tank crack growth if the stress intensity factors are known for steel at various locations in the tank. A summary of stress intensity was presented in Section 3 above, and an analysis of stress intensity factors is presented in detail in Appendix A, which describes the mathematical relationships of how the SCC test data were combined with the residual stress analysis data from LANSCE to formulate the recommended best practices for tank inspection presented in Section 6.

[This page intentionally left blank.]

5. CONCLUSIONS

This study delivered the following key findings:

- The 20 nurse tanks examined were fabricated from steel that in almost all cases met its published design standards for carbon content, microstructure, tensile strength, and ductility. In the rare instances where the steel fell below minimum performance levels, the measured values were outside the expected range by trivially small amounts.
- The 20 nurse tanks examined contained a limited number of cracks. Fractography is the study of cracks and fracture surfaces of materials. One of the aims of fractographic examination is to determine the cause of failure by studying the characteristics of a fracture surface. Different types of crack growth (e.g. fatigue, SCC, hydrogen embrittlement) produce characteristic features on the surface, which can be used to help identify the failure mode.

Fractographic examination of the cracks found in the 20 nurse tanks acquired for this study in the SEM indicated that the cracks were intergranular, which is the crack mode seen in SCC. Each of these cracks was too small to pose an immediate safety concern, but such cracks can potentially expand during future service to critical sizes that could cause tank failure.

- Neutron diffraction analysis performed on hoop sections from two nurse tanks showed that the unannealed welds joining the shell and head of the nurse tanks contained high residual tensile stresses. These high stresses were in the steel immediately adjacent to the welds used to assemble the tanks during the manufacturing process. In certain regions of the tank in the weld HAZ, these stresses are high enough that with the pressure of the anhydrous ammonia (NH_3), they could push the steel beyond its yield strength. Tensile stress is one of two necessary factors for stress corrosion cracking to occur; the other is a corrosive environment (e.g., NH_3).
- In the 20 nurse tanks examined, there was no significant decarburization in the steel near the tank's inner wall that would weaken the steel.
- SCC studies on steel test specimen coupons immersed in NH_3 liquid or vapor generated cracks in a minority of the specimens; most specimens did not form cracks at the tips of the V-shaped notches. Continued monitoring of the cracked specimens allowed measurement of their crack growth rates under conditions simulating actual nurse tank service conditions. These data in turn allowed formulation of a recommended nurse tank inspection procedure that could reduce the number of future tank failures.

[This page intentionally left blank.]

6. RECOMMENDATIONS

The data acquired in this study were analyzed, as detailed in Appendix A, to develop a preliminary recommended inspection procedure based on angle-beam ultrasound examination of tanks at time intervals dictated by the condition of the tanks. That is, it is recommended that tanks with no indications of possible cracks be allowed longer time periods between inspections than tanks with indications of possible cracks; tanks with small cracks be allowed longer time periods between inspections than tanks with larger cracks; and tanks with cracks at or larger than the specified maximum are mandated to undergo immediate repair or removal from service. These inspection precepts are presented in Figure 12 in a flow chart format.

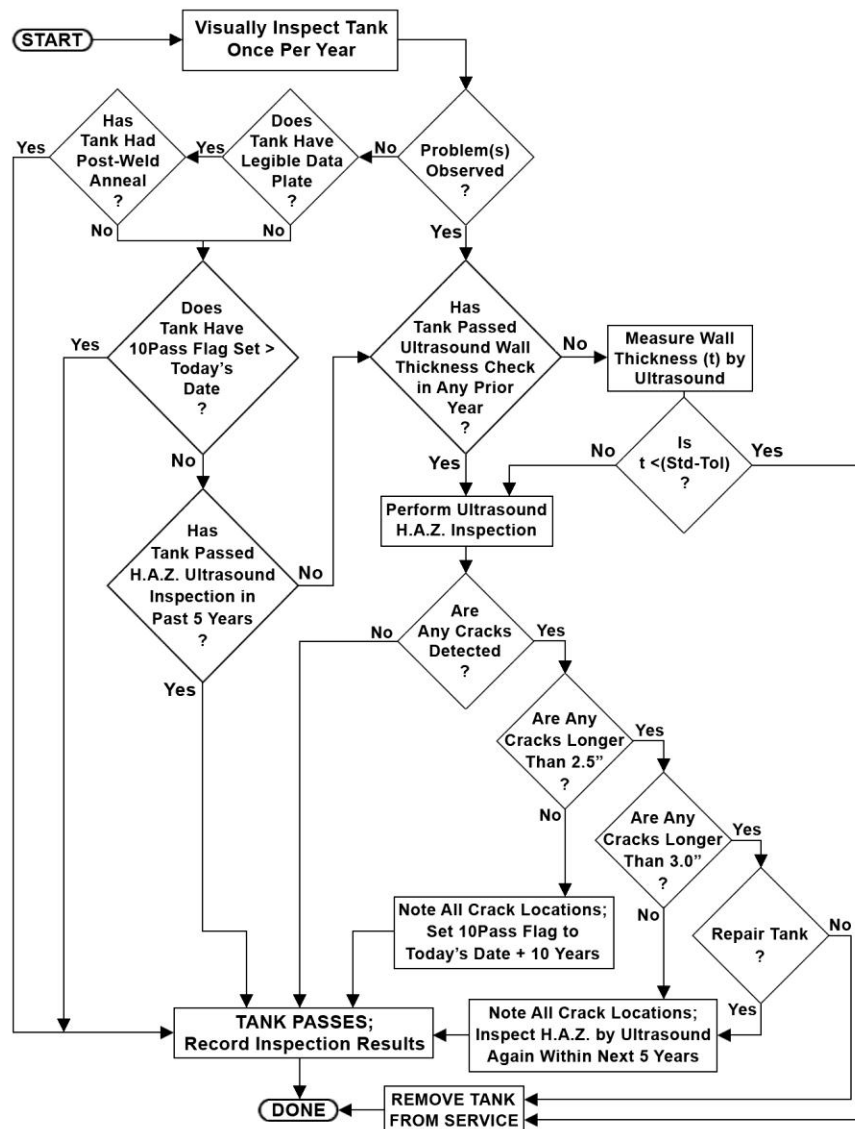


Figure 12. Flowchart. Preliminary recommended nurse tank inspection, repair, and retirement precepts based on the findings from this study.

H.A.Z.=heat-affected zone; STD=standard tank wall thickness; TOL=tolerance allowed for variation in tank wall thickness; 10PASSFLAG=date 10 years after finding a crack between 2.5" and 3.0" long

The database of crack growth for these recommendations is uncomfortably small, since only seven of the SCC specimens provided crack growth data. The other 49 specimens did not nucleate cracks at the tip of the V-shaped notch; however, these specimens were immersed in NH₃ for a total of only 7 months.

Additional follow-on research was awarded on February 17, 2011. That research will provide data from 200 SCC specimen coupons exposed to NH₃ for a 12-month period. Half will be in the fluid and half will be in the vapor area. More field-observed crack growth should be completed to create a larger database of SCC specimens to more accurately predict crack growth.

The “heat-affected zones inspection” in the flowchart is recommended to be performed with an angle-beam transducer scan along both sides of all welds to search the heat-affected zones for indications of possible cracks. If an indication of a possible crack is located, the area near that indication needs to be searched by rotating the transducer 360 degrees to define the dimensions of cracks that may turn and run at different angles. This would assure that if it is a crack the entire crack is imaged by ultrasound, not just the portion that happens to be perpendicular to the initial scan line.

Theory and some anecdotal evidence indicate that perhaps most cracks not caused by flaws in manufacture or damage to the tank occur in the vapor space. That would be consistent with the earlier explanation that anhydrous ammonia (NH₃) vapor does not contain the necessary water, and thus is expected to be more corrosive. (This study did not consider the welded feet pads for the running gear attachment.)

Discussion of the above theory with the peer review committee led to a recommendation for carrying out a field test on a number of nurse tanks to see if there is a clear preponderance of cracks in the vapor area. As a result, the original follow-on work was expanded by new work awarded on September 30, 2011 to carry out such a field measuring project. Based on findings from that expanded follow-on research, it is possible that future recommendations could recommend restricting the areas of the tank to examine.

The hypothesis to be examined is whether it might be sufficient to inspect only along welds in the vapor space for indications of possible cracks (i.e., on the upper portion of shell-head weld seams). We also need to develop recommendations for the weld’s made-to-join sections of shells.

Additionally, newer nurse tanks are now 100-percent radiographed on the longitudinal weld seam to detect possible weld flaws, and thus they use thinner steel for the shells. However, until the validity of the longitudinal weld seam can be more clearly demonstrated, we feel it would be prudent for this preliminary recommendation to inspect both sides of every weld, both over the liquid zone and over the vapor zone.

At present, the regulations at 49 CFR 171.7 incorporate by reference the 1998 version of the ASME code that specifies every tank is to be initially hydrostatically tested by the manufacturer at 1.5 times the maximum allowable working pressure of 250 psig, or 375 psig, as a final quality control check after the tank is fabricated at the manufacturing facility. FMCSA reports that U.S.

nurse tank manufacturers have adopted newer ASME guidance that under certain conditions allows initial acceptance hydrostatic testing to only 325 pounds.

Additionally, in-service hydrostatic testing is required on tanks that do not have the ASME data plate. The recommended new inspection procedure shown in Figure 12 could be adopted for use instead of the present hydrostatic testing procedure, or in addition to the present hydrostatic procedure.

Since the angle-beam ultrasound inspection procedure reveals more information than hydrostatic testing, it may be that performing both kinds of tests is duplicative and needlessly costly for the tank owner. Two of the advantages of angle-beam ultrasound testing are that it is not necessary to drain NH₃ from the tank to perform the inspection, and the inspection does not vent air containing oxygen and nitrogen into the tank. The presence of both nitrogen and oxygen is thought to pose the greatest SCC challenge to the metal, since nitrogen in the absence of oxygen does not cause the oxidation necessary for SCC to progress, and oxygen in the absence of nitrogen more effectively repassivates (seals) the surface of the inner tank wall.

If both angle beam ultrasound and hydrostatic testing are required, the two cost advantages of angle beam ultrasound testing would be lost. For these reasons, we recommend eventual replacement of the hydrostatic test with the new procedure.

The preliminary recommendations incorporated in Figure 12 are conservative and are based on the following assumptions and boundary conditions:

- The estimates are for through-wall cracks, even though most cracks in nurse tanks do not penetrate the entire tank wall.
- They are based on calculations that used the highest crack growth rate recorded in the SCC study rather than the average crack growth rate recorded in the SCC study.

They are calculated for 250-psig tank pressure throughout the crack growth period. This is the rated maximum operating pressure for nurse tanks, but most nurse tanks operate at somewhat lower pressures during most of their service lifetimes. For example, in Iowa it is reported by the tank operators that an 85 percent full tank in full sun generally does not exceed 150 psig. The pressure will drop further overnight.

However, we recommend delaying implementation of these preliminary recommended test procedures shown in Figure 12 until the underlying estimates can be better verified based on the forthcoming larger database of crack initiation and propagation, and the field test of crack locations in tanks. Both of these will be provided by the research under the follow-on task orders.

[This page intentionally left blank.]

APPENDIX A—STRESS INTENSITY FACTOR ANALYSIS AND APPLICATION OF THIS ANALYSIS TO PREDICT CRACK PROPAGATION RATES IN NURSE TANKS

The discipline of fracture mechanics uses stress intensity factors to evaluate the stress states of materials near crack tips. (In this case we are addressing stress created by pressure of material being contained by the tank, not residual stresses left in the tank’s steel by welding processes used in the manufacturing.) The stress state at crack tips is important because it is at the crack tip that the crack grows. Stress intensity factors are theoretical constructs and have units of *stress* multiplied by the square root of the crack length. The stress intensity factor for axial flaws in thin-walled cylinders subject to internal pressure can be approximated by the equation in Figure 13 (Anderson, 1991).

$$K_I = \sigma_h \sqrt{\pi \alpha} \sqrt{1 + 0.52\chi + 1.29\chi^2 - 0.074\chi^3}$$

Figure 13. Formula. Formula for stress intensity caused by an axial through-crack in a thin-walled cylindrical pressure vessel.

Where lowercase *sigma* subscript *h* is the hoop stress, as given by Figure 14,

alpha is one-half the flaw (crack) length as shown in Figure 16, and

chi is given by Figure 15.

In tanks such as nurse tanks where the radius is many times larger than thickness of the tank wall (Figure 16), the hoop stress can be approximated by,

$$\sigma_h = \frac{pR}{t}$$

Figure 14. Formula. Formula for hoop stress in a thin-walled cylindrical pressure vessel.

Where *p* is the internal pressure,

R is the internal radius of the tank, and

t is the thickness of the tank wall.

$$\chi = \frac{\alpha}{\sqrt{Rt}}$$

Figure 15. Formula for chi, a fitting parameter for stress intensity of axial through-cracks in thin-walled cylindrical pressure vessels.

Hoop stresses are perpendicular to axial flaws and therefore cause axial cracks to open. Axial stresses are perpendicular to hoop flaws and cause hoop cracks to open. As illustrated in Table 1 in the body of the report, the hoop stress measured by neutron diffraction is twice the magnitude

of the axial stress, and therefore is a far more likely source of crack originations. For this reason, this appendix only calculates the stress intensity factors for axial flaws.

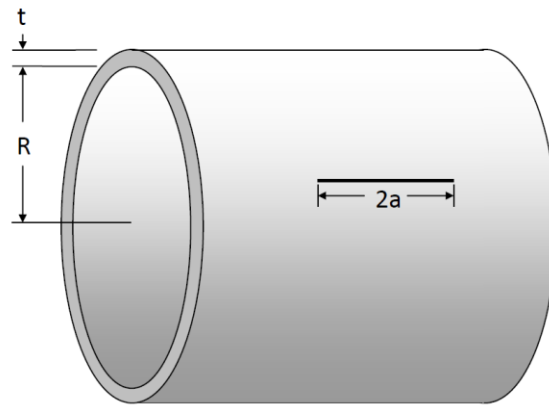


Figure 16. Diagram. Axial flaw in a cylinder subjected to internal pressure.

A pressure relief valve regulates the internal pressure in a nurse tank so that the maximum internal pressure will not exceed 250 psig, which is equal to 1.72 MPa. MPa=megapascals, a unit of stress equivalent to one Newton of force applied over a cross sectional area of one square millimeter. Thus, for a typical 1,000-gallon nurse tank, with an inner diameter of 41 inches (i.e., a radius of 20.5 in [520 mm]), and a shell thickness of 5/16 (0.3125) in. (7.94 mm), the hoop stress caused by the internal pressure is calculated by Figure 17.

$$\sigma_h = \frac{pR}{t} = \frac{(1.72 \text{ MPa})(520 \text{ mm})}{7.94 \text{ mm}} = 113 \text{ MPa}$$

Figure 17. Formula. Example calculation of hoop stress for a specific nurse tank.

The fracture toughness, J_{IC} value, of A516 Grade 70 steel at 20° C (68° F) is 114 kiloNewtons per meter (kN/m) (Seok, 2000). This corresponds to a K_{IC} value of 158 MPa $m^{1/2}$ (m = the minimum crack length in meters that will lead to fracture at a specific temperature). How to approximate the length of m under different temperature conditions is discussed below.

Note, the A455 steel used for the coupon tests described in the body of the report and the A516, Grade 70 steel used as the reference for calculations in this appendix are similar steels. A455 has a carbon content of 0.28–0.33 percent with 0.85–1.2 percent manganese, 0.040 percent phosphorus maximum, 0.050 percent sulfur maximum, and 0.10–0.30 percent silicon. A516, Grade 70 has a carbon content of 0.31 percent with the same 0.85–1.2 percent manganese, 0.035 percent phosphorus maximum, 0.040 percent sulfur maximum, and 0.15–0.30 percent silicon. These small variations in composition are not expected to cause significant differences in SCC behavior or fracture toughness.

Fracture toughness of steel changes substantially when a breach occurs in the wall of a tank with anhydrous ammonia in it. Leakage through the breach in the tank wall causes the anhydrous ammonia (NH₃) to evaporate through the breach. This can cause the temperature in the local zone of the breach to fall to -67° C (-89°F) due to localized cooling (Basko, Larionov, &

Lazutin, 2007). Basko (Basko, Demygin, & Gonchara, Increase in safe operation life of vessels for storage of liquid NH₃ under pressure, 1997) found that at temperatures of -70° C (-94° F) the steel becomes much more brittle, with a correspondingly lower critical stress intensity factor K_C of 85 MPa m^{1/2}.

Thus, we can solve for the minimum crack size that would cause the nurse tank to rupture at -70° C (-94° F). In a nurse tank with an internal pressure of 250 psig, diameter of 41 inches, a wall thickness of 0.238 inches, and a critical stress intensity factor K_{IC} 85 MPa m^{1/2}, then *m* (the axial crack length) is 3.7 inches (Figure 18). **Note:** The steel wall thickness used here is thinner than the 0.325 inches in the 1966 tank tested or the 0.321 inches in the 1986 tank tested.

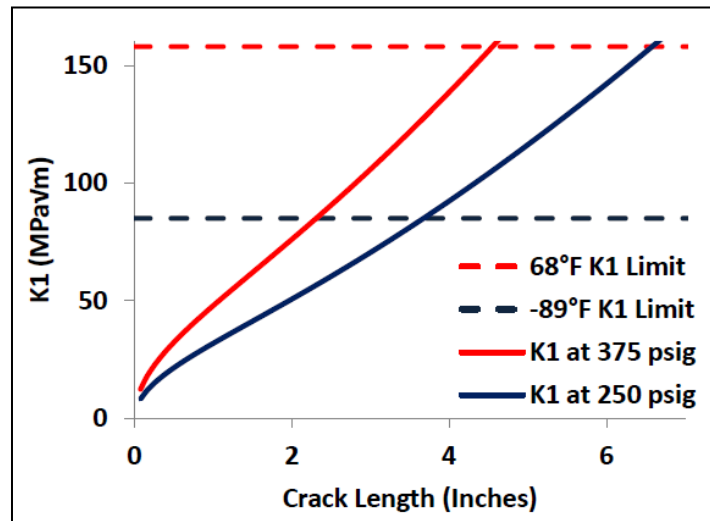


Figure 18. Graph. K1 versus crack length in a 1,000-gallon nurse tank.

Visual inspection cannot detect cracks that do not penetrate the surface. This means that dangerous tanks can easily be passed as safe by visual examination. This can occur when a crack grows to a critical length before penetrating through the tank wall.

Ultrasonic thickness testing will also miss nearly every crack. This is because it looks directly through the material to see the reflection of the opposite wall (i.e., the thickness). Cracks are edge-on in this inspection mode, thus, not detected.

Angled ultrasonic inspection is necessary to find cracks in order to receive reflection indications off crack surfaces.

Hydrostatic pressure tests will reveal the existence of some subcritical size flaws. By testing at pressures 50 percent higher than working pressures, some subcritical cracks may be revealed. For the 1,000 gallon tank described in Figure 18, at room temperature and 250 psig, the critical crack length is 6.25 inches long. However at the higher pressure when a tank is hydrostatically tested at 375 psig, then the critical crack length is 4.25 inches long. Thus, we would expect that all subcritical cracks between 4.25 inches and 6.25 inches long should be revealed. Note that for this tank, if localized cooling occurs because of a leak allowing anhydrous ammonia to evaporate and chill the steel, then the critical crack length at 250 psig is reduced to 3.7 inches.

There are two potential problems with hydrostatic tests. First, the tanks may contain cracks, which are not yet critical length at 375 psig, but will continue to grow over time. The hydrostatic test alone does not inform testers of how much time remains until any such existing cracks may grow to critical length. The second problem is that the test is performed at ambient temperature (20°C), and misses cracks that are already of a length that will become critical if there is a through-the-wall breach that locally lowers the temperature of the steel to -70° C (-94° F). Thus a 3.7 inch crack is unlikely to be revealed by hydrostatic pressure testing at normal temperatures. But such a crack, if subsequently cooled by a minor through breach, could cool the steel sufficiently to become brittle enough to catastrophically fail.

In Figure 18, a less than 4.25-inch-long crack is not critical at 20° C (68° F) and 375 psig, but cracks 3.7 to 4.25 inches long *are* critical at -70° C (-94° F) at 250 psig. If this crack develops a through-the-wall leak, localized cooling can cause the temperature at the crack tip to drop to -70° C (-94° F) and the fracture toughness to drop from 185 to 85 MPa $m^{1/2}$ resulting in a catastrophic failure.

A calculation of SCC growth rate in low-carbon steel immersed in NH₃ was made by Lunde and Nyborg and is shown in Figure 19:

$$a(y) = a_0 + 3.0 \times 10^{-7} K_{IC}^2 \sqrt{y}$$

Figure 19. Formula. The crack length after y years is equal to the initial crack length plus 3e-7 times the stress intensity squared times the square root of y years.

Where alpha sub-y (a_y) is the final crack length in meters; alpha sub-zero (a_0) is the initial crack length; and y is time in years.

The first derivative formula for predicting crack growth rate calculated by Lunde and Nyborg is shown in Figure 20:

$$\frac{\partial a}{\partial y} = 1.5 \times 10^{-7} K_{IC}^2 y^{-1/2}$$

Figure 20. Formula. This is the derivative with respect to y, time in years, of Figure 19.

Combining the equation from Figure 13 with the equation in Figure 19 results in the equation shown in Figure 21:

$$a'(y) = \frac{1.5 \times 10^{-7} \pi p^2 R^2}{t^2} \left(a(y) + \frac{0.52}{\sqrt{Rt}} a(y)^2 + \frac{1.29}{Rt} a(y)^3 - \frac{0.074}{(Rt)^{3/2}} a(y)^4 \right) \frac{1}{\sqrt{y}}$$

Figure 21. Formula. The change in length of the crack with respect to the time in years.

This equation does not cover crack initiation, only crack growth.

Given the initial value of $a(y) = a_0$, we can solve this nonlinear first order differential equation for a number of initial crack lengths at different temperatures, which gives Figure 22 and Figure 23. In these figures, the plot cuts off at the 20° C (68° F) critical crack length. The critical crack

length at -70°C (-94°F) is displayed as a horizontal blue line near the center of the plot. A horizontal dotted blue line near the bottom third of the plot is the critical crack length with a factor of safety of 3 at 20°C (68°F).

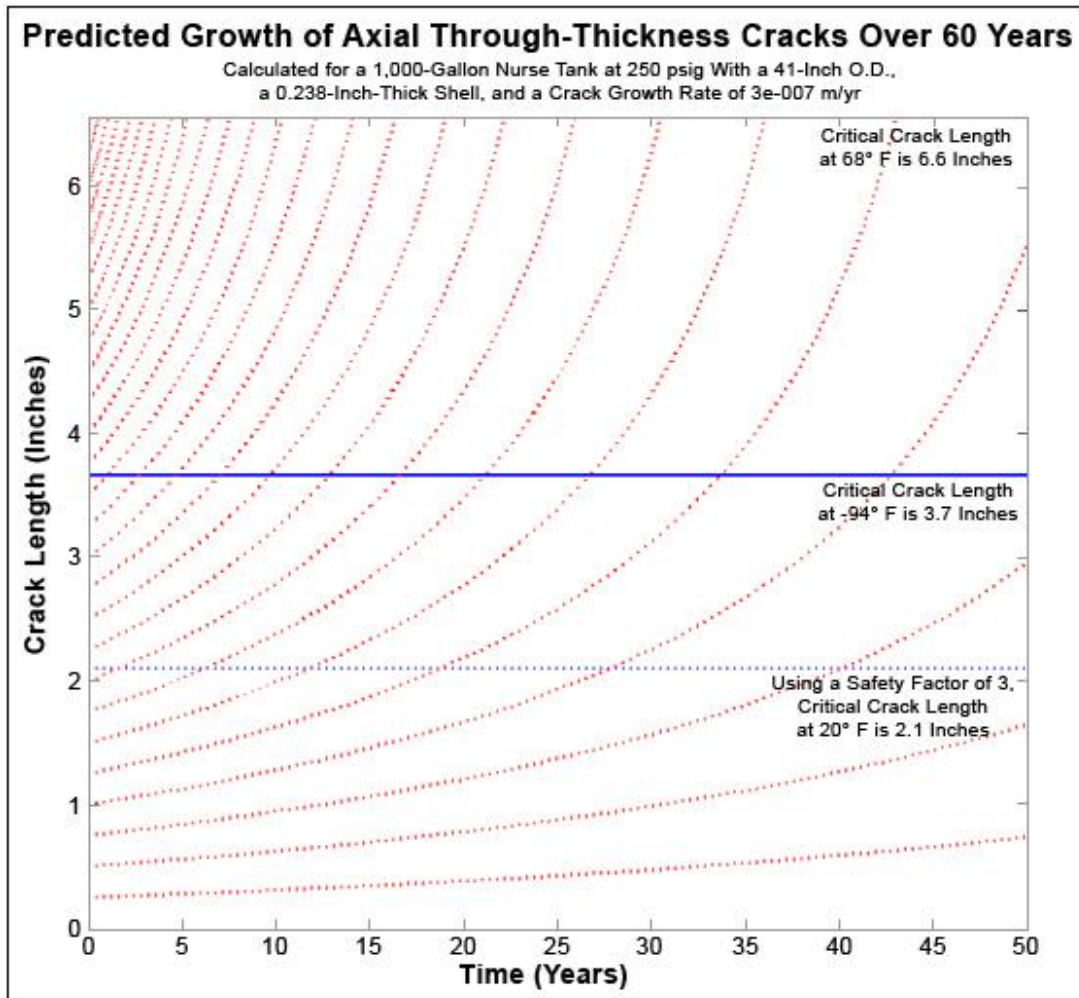


Figure 22. Graph. In this representative 1,000-gallon tank, cracks less than 2.75 inches long will not grow to the critical crack length at -94°F for at least 10 years.

Two-inch-long cracks will not grow to this critical length for 50 years.

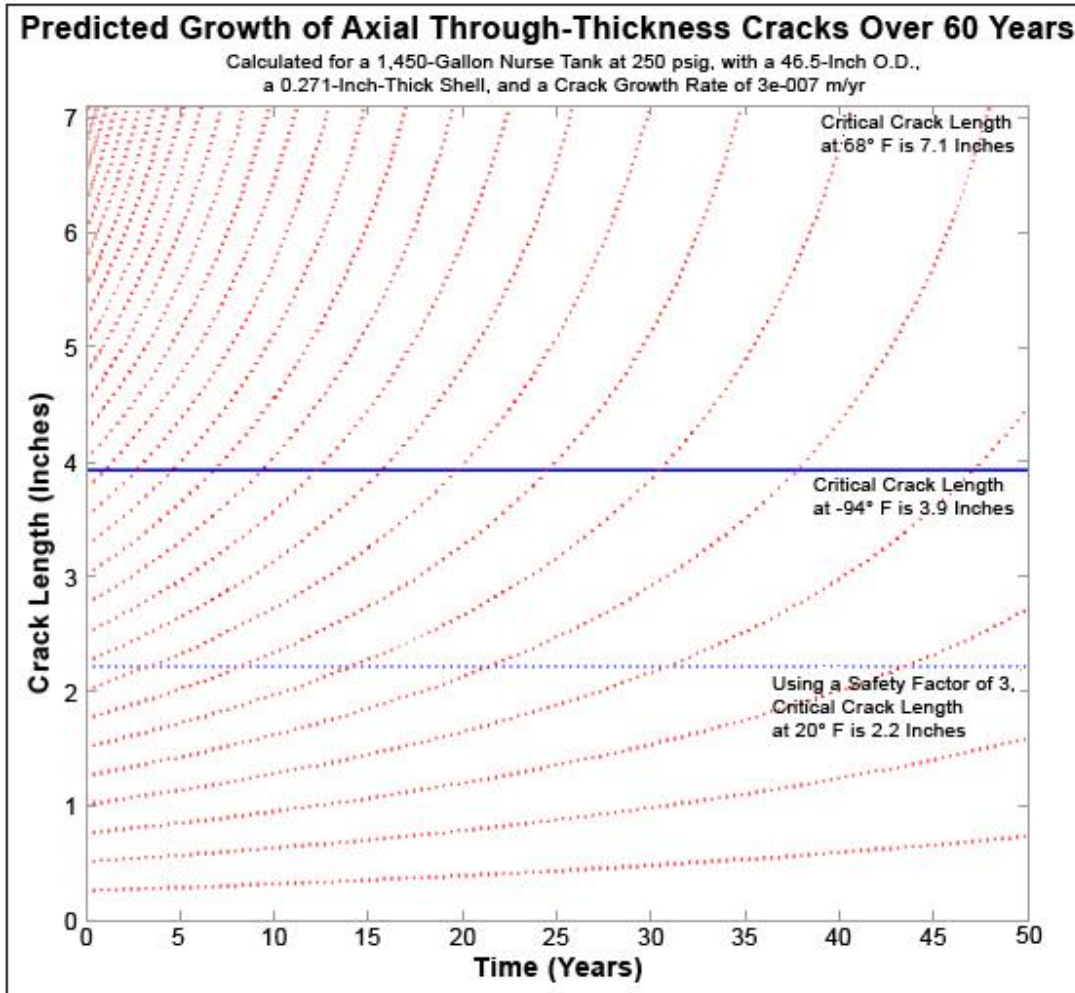


Figure 23. Graph. In this representative 1,450-gallon tank, cracks less than 3 inches long will not grow to the critical crack length at -94° F for at least 10 years.

2.25-inch-long cracks will not grow to this critical length for 50 years.

These calculations predict that in a 1,500-gallon tank with a 3-inch crack, the length of the crack will not become critical until about 10 years later. However, this prediction assumes that the crack grows equally in both directions and that the internal pressure remains at 250 psig throughout the life of the tank. It also assumes that crack growth slows over time, as this was what Lunde and Nyborg’s research found. However, they mentioned that their tests maintained a constant stress intensity factor, K_{IC} . In actuality, in a nurse tank without external imposition of force that maintains constant stress intensity as the crack grows, the stress intensity would also increase. Thus, in normal field experience we would expect to observe a higher crack growth rate.

If the crack growth rate remains constant and does not slow down with time, then the equations change to the following:

$$\frac{\partial a}{\partial y} = 3.0 \times 10^{-4} K_{IC}^2$$

Figure 24. Formula. The crack growth rate in millimeters per year is equal to 3e-4 times the stress intensity squared.

$$a'(y) = \frac{3.0 \times 10^{-7} \pi p^2 R^2}{t^2} \left(a(y) + \frac{0.52}{\sqrt{Rt}} a(y)^2 + \frac{1.29}{Rt} a(y)^3 - \frac{0.074}{(Rt)^{3/2}} a(y)^4 \right)$$

Figure 25. Formula. The crack growth rate as a function of thickness, internal pressure, and crack length.

This causes the plots of crack growth to change significantly to indicate this faster growth rate.

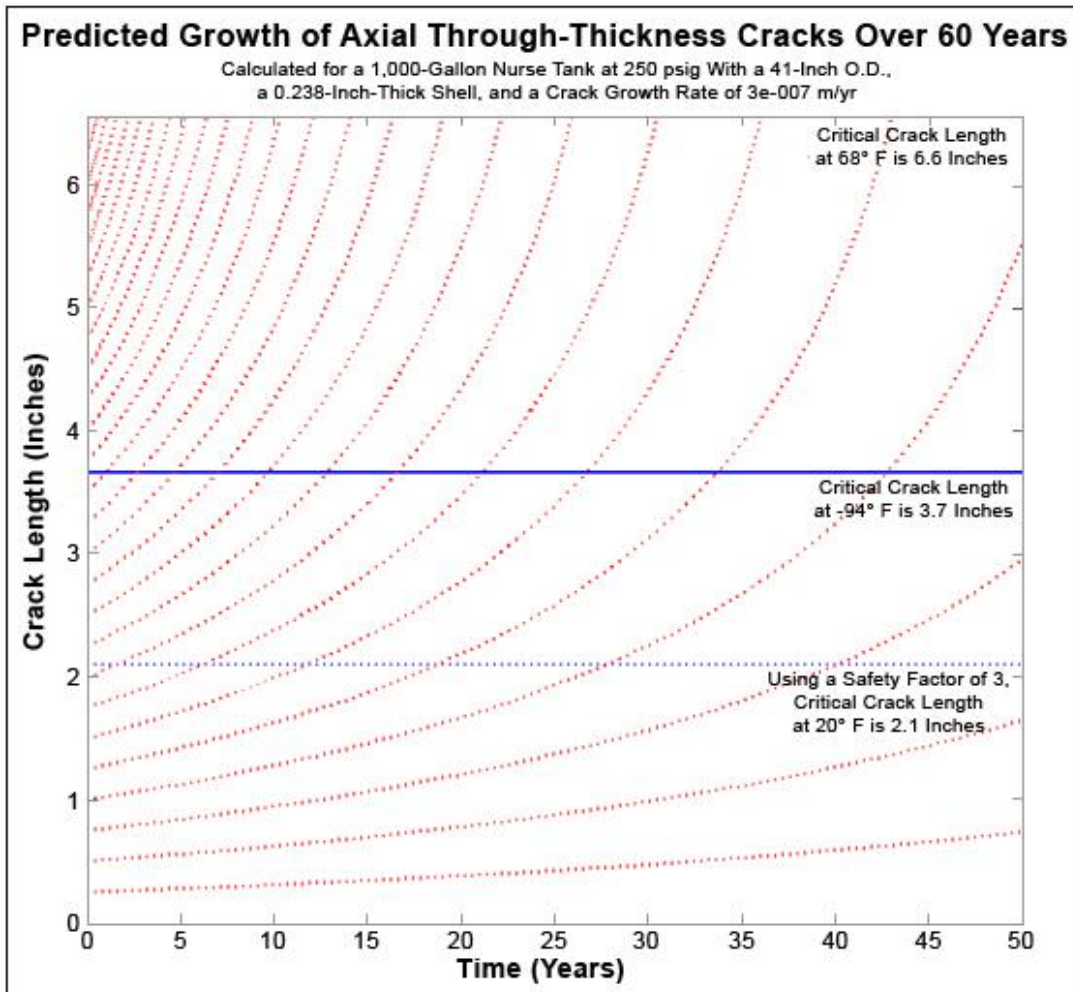


Figure 26. Graph. In this representative 1,000-gallon nurse tank with the revised prediction of crack growth rate, cracks less than 2.25 inches long will not reach critical length at -94° F for at least 10 years.

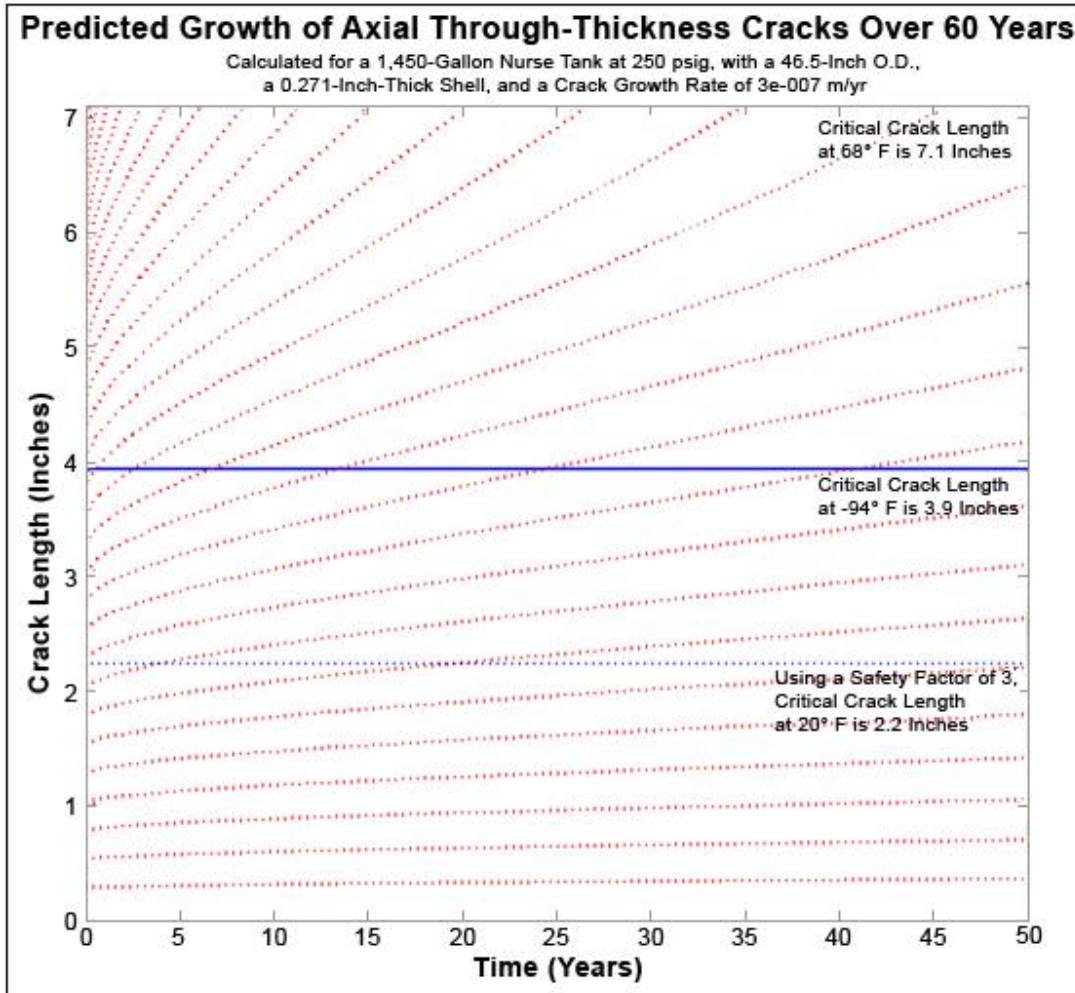


Figure 27. Graph. In this representative 1,450-gallon nurse tank with the revised prediction of crack growth rate, cracks less than 2.5 inches long will not reach critical length at -94° F for at least 10 years.

The resulting plots are not as forgiving as the original assumption. They indicate that a 1,000-gallon tank with a 2.25-inch crack, or a larger 1,500-gallon tank with a 2.5-inch crack, can fail in 10 years. A 1,500-gallon tank with a 3-inch-long crack can fail in 5 years.

A third possibility for crack growth rate is to instead use the most extreme case of crack growth recorded in this project’s tests for conservative safety reasons. That would result in the following equations:

$$\frac{\partial a}{\partial y} = 9.41 \times 10^{-4} K_{IC}^2$$

Figure 28. Formula. The highest crack growth rate in meters per year was 9.41e-7 times the stress intensity squared.

$$a'(y) = \frac{9.41 \times 10^{-7} \pi p^2 R^2}{t^2} \left(a(y) + \frac{0.52}{\sqrt{Rt}} a(y)^2 + \frac{1.29}{Rt} a(y)^3 - \frac{0.074}{(Rt)^{3/2}} a(y)^4 \right)$$

Figure 29. Formula. This equation describes the change in length of the crack with respect to the time in years.

The resulting plots are even less forgiving and indicate that a 1,000-gallon tank with a 1.25-inch crack, or a larger 1,500-gallon tank also with a 1.25-inch crack, can fail in 10 years. A 1,500-gallon tank with a 2-inch-long crack can fail in 5 years.

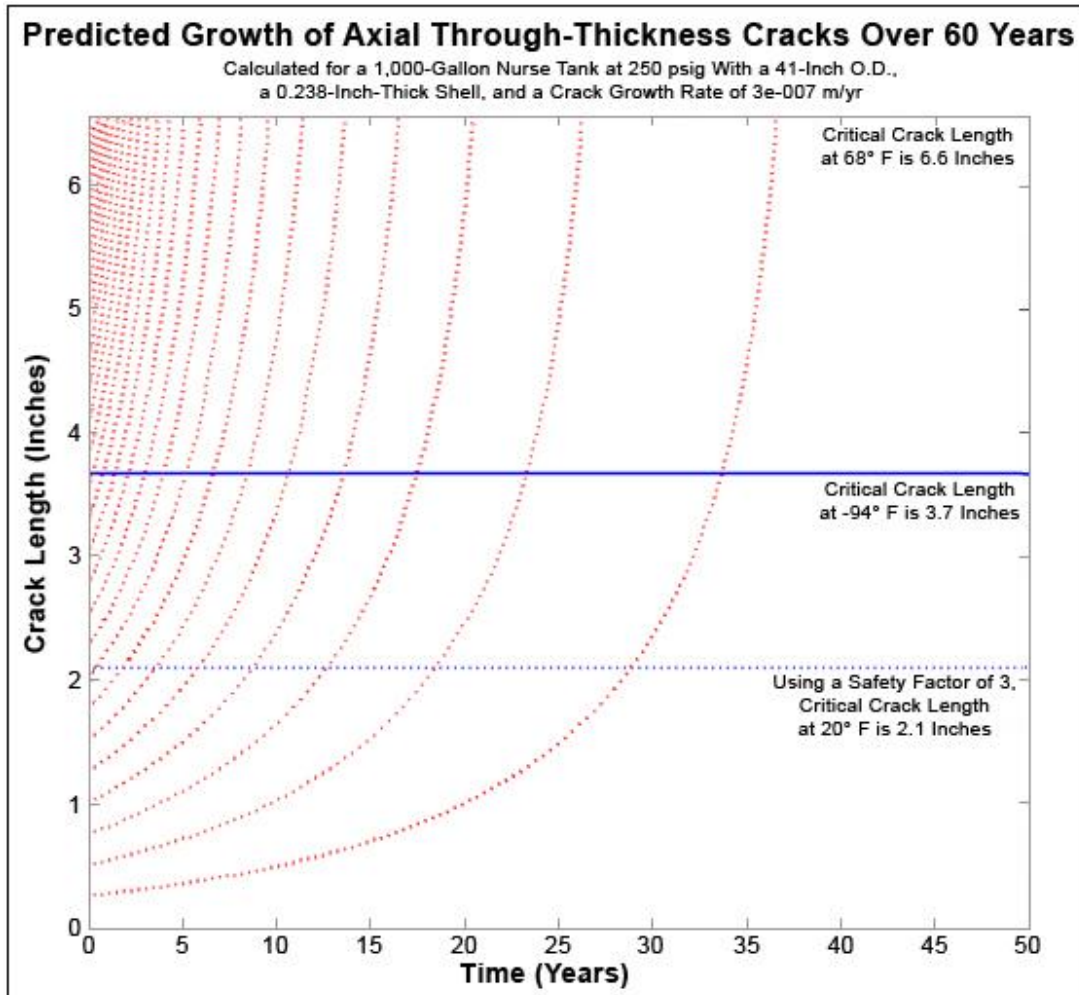


Figure 30. Graph. In this representative 1,000-gallon nurse tank with crack growth based on the highest measured crack growth rate, cracks less than 1.25 inches long will not reach critical length at -94° F for at least 10 years.

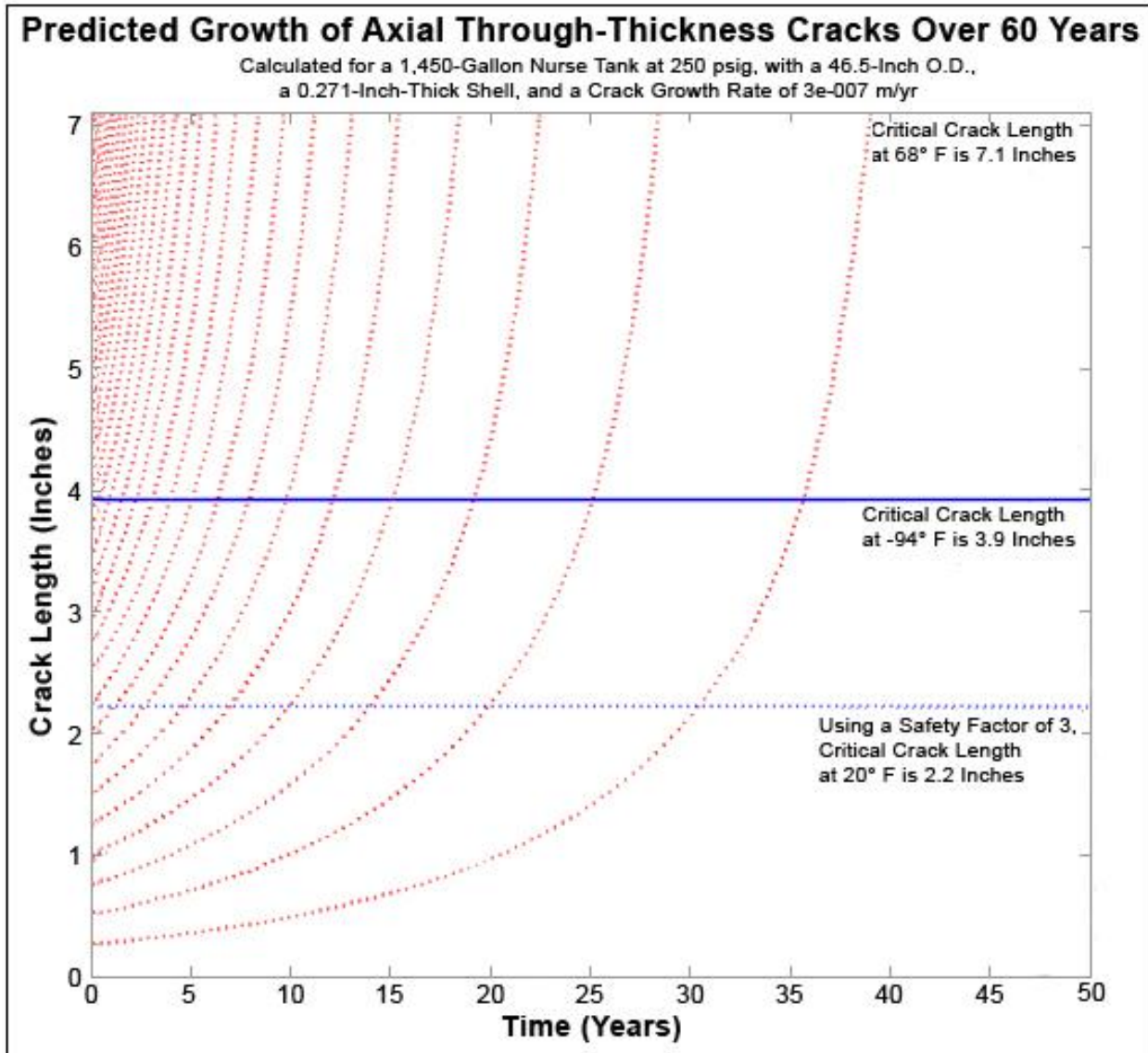


Figure 31. Graph. In this representative 1,450-gallon nurse tank with crack growth based on the highest measured crack growth rate, cracks less than 1.25 inches long will not reach critical length at -94° F for at least 10 years.

Figure 30 and Figure 31 represent calculations for 1,000- and 1,500-gallon tanks respectively. For 1,500-gallon tanks, cracks longer than 1.25 inches will not reach critical length at -70° C (-94° F) for at least 10 years, and 2.25-inch cracks will not reach critical length at -70° C (-94° F) for 5 years. For these two examples, the smaller 1,000-gallon tank fails slightly sooner than the 1,500-gallon tank. These calculations allow safe inspection intervals to be calculated.

In the angle-beam inspections performed on the tanks purchased by this project, cracks less than 0.25 inch long were detected. Even the extreme predictions (Figure 30 and Figure 31) show that cracks of less than an inch will not become critical within 10 years. Thus, if the focus of the angle beam inspections were on determining tanks with cracks of around 1 inch or greater, then a

minimum lifespan of 10 years could be safely predicted. It is also much easier to detect 1 inch or longer cracks, thus speeding up the angle-beam inspection process.

These calculations do not take into account all factors affecting crack growth. Nurse tanks are subjected to cyclical loading, which can lead to faster crack growth as brittle corrosion products break open at the crack tip. That would accelerate crack growth. Transient stresses due to filling the tank and towing tanks across rough terrain would also accelerate crack growth. However, several factors also increase the factor of safety in these crack growth predictions:

- Because many of these axial cracks occur next to the circumferential welds attaching the heads to the shell, they can only grow in one direction, i.e., they cannot cross the weld bead. This would cut the growth rate in half.
- These calculations were figured using a constant pressure of 250 psig. This value represents the vapor pressure of NH_3 at 48.9°C (120°F) and the setting of the pressure relief valve. This is an estimate of how hot a tank might get sitting in direct sunlight in the middle of the summer in a very hot climate. In reality, tanks in most locations in the U.S. are going to operate at lower temperatures, and thus are unlikely to be exposed to constant stress of this intensity.
- These calculations do not incorporate the residual stress due to welding. This is because the region of high residual stress in the heat-affected zones does not extend more than 1 inch (25.4 mm) from the weld as shown in Figure 32. The residual stress in the heat-affected zones is a significant danger for the *initiation* but not for the continued growth of axial cracks.
- These calculations are conservative as they were calculated for *through-the-wall* cracks. Most cracks will not penetrate through the entire thickness of the steel and thus will have lower stress intensities.

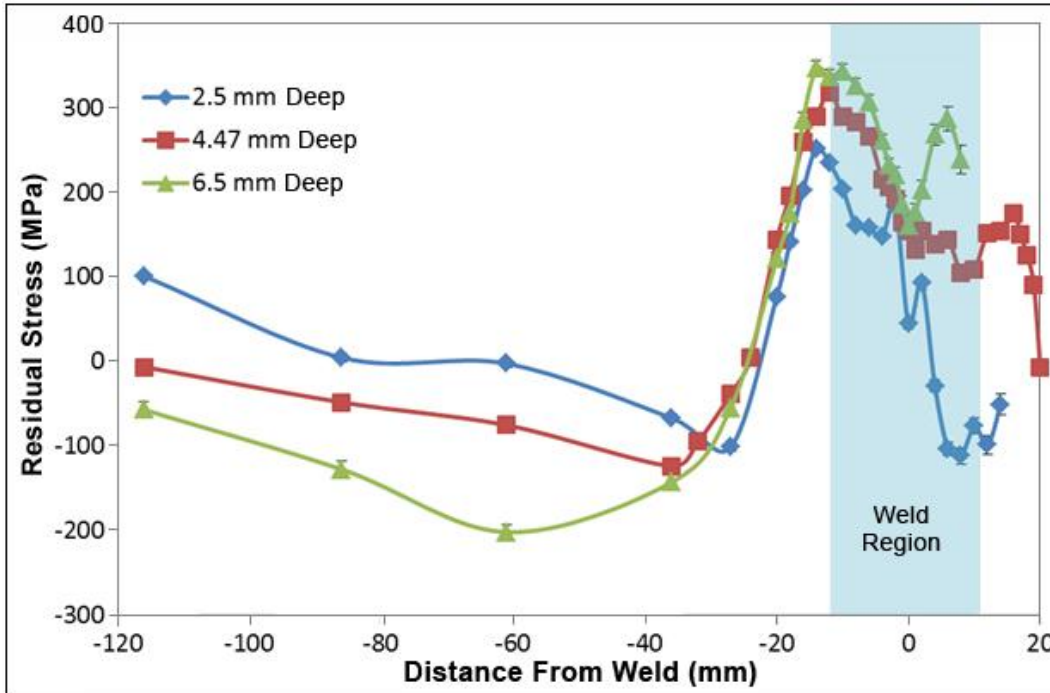


Figure 32. Graph. Hoop stress across the circumferential weld in a 1,000-gallon nurse tank manufactured in 1966. The region of high residual stress extends only 1 inch from the weld.

It should be noted that the vertical band labeled “weld region” on Figure 32 (and on similar residual stress plots that follow) marks the greatest width of the fusion zone of the weld at the surface of the tank (the region where the metal actually melted during welding). However, the fusion zone is tapered (V-shaped). It is widest at the exterior surface of the tank and narrows substantially at greater depths below the exterior surface. All of the neutron diffraction measurement regions were at increasing depths below surface of the tank steel. Thus, although the maximum stress values appear to lie right at the HAZ-weld region boundary, these maximum stress positions actually lie entirely within the HAZ. Although not measured directly by neutron diffraction, the stress right at the interior surface of the nurse tank is probably slightly higher than the highest value shown here. This is because at the surface, residual tensile stress probably equals the steel’s yield strength, meaning that it exceeded the yield strength and caused the metal to plastically deform until the residual stress dropped to the yield strength value. Residual stress equal to the yield strength is often observed in welded structures that have not been given a stress-relief annealing treatment after welding.

The axial residual stress is more dangerous in its effect on cracks that grow in the hoop direction. Axial stress acts directly on these cracks and the cracks continuously grow within the HAZ stress field, i.e., they do not grow out of this stress field. Additionally, circumferential cracks can grow in both directions along the region where stress is the highest. However, as pointed out early in this appendix, the reason for this report’s focus on axial cracks is because the axial stresses that cause perpendicular hoop cracks to initiate were calculated to be half those of the circumferential or hoop stresses that cause axial cracks to initiate. Thus cracks in the hoop direction are much less likely to initiate, but presumably would grow faster if they initiate. This can be easily seen by comparing Figure 32 with Figure 33.

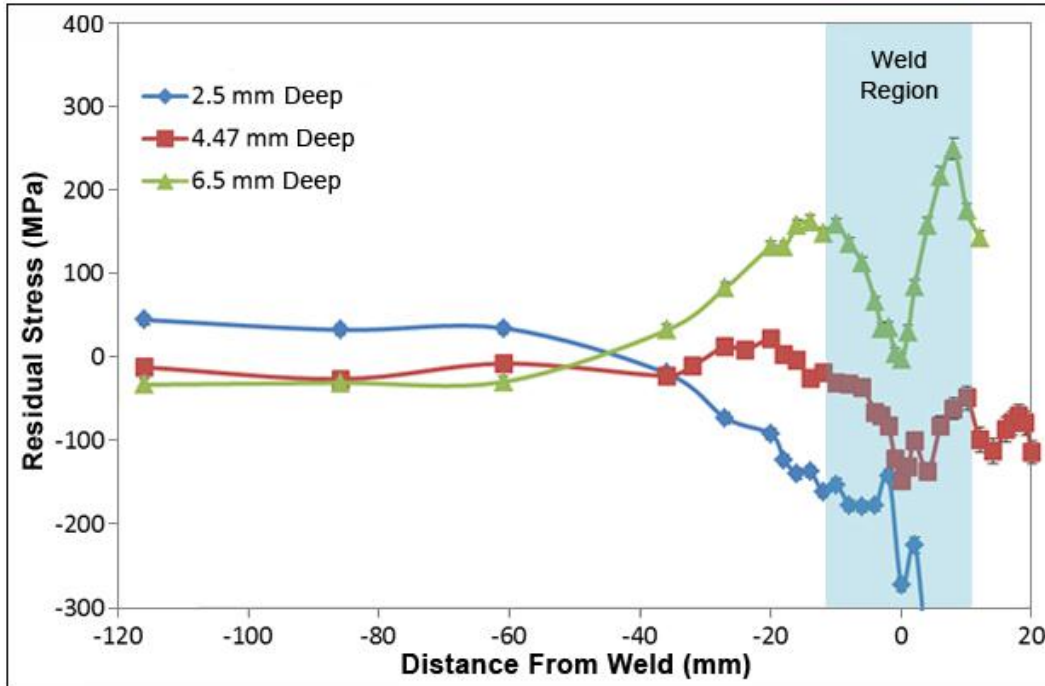


Figure 33. Graph. Axial stress across a circumferential weld in a 1,000-gallon nurse tank manufactured in 1996.

Figure 34 gives an overview perspective of how the stresses in different directions interrelate.

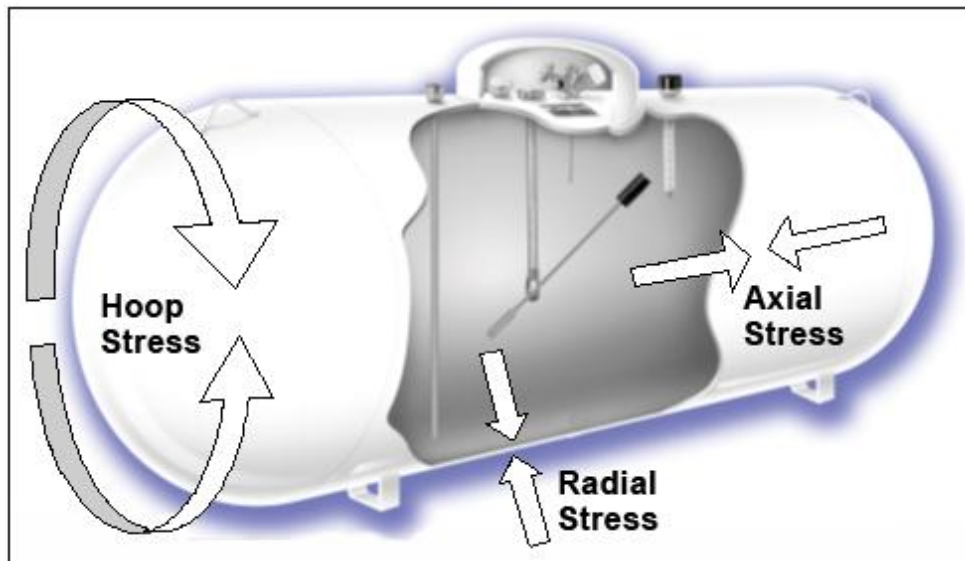


Figure 34. Diagram. Stresses on a pressure tank. Axial-oriented cracks are opened by hoop stress, and circumferential cracks are opened by axial stress.

During the angle-beam investigation of the 20 tanks purchased or donated for this project, cracks growing in the circumferential/hoop direction were found on only two of the tanks. In both of these tanks, the circumferentially-oriented cracks all had Y-shaped regions as shown in Figure 35. The lower photo, in particular, shows that cracks initiated in the axial direction, growing

away from the weld bead. Only after growing to a certain length did they begin to branch. In both cases, these cracks were found in the head of a 1,000-gallon tank of unknown age. The circumferential weld was located where the ruler is placed in the photographs. The cracks originally were hidden from view by the flange attached to the shell of the tank.

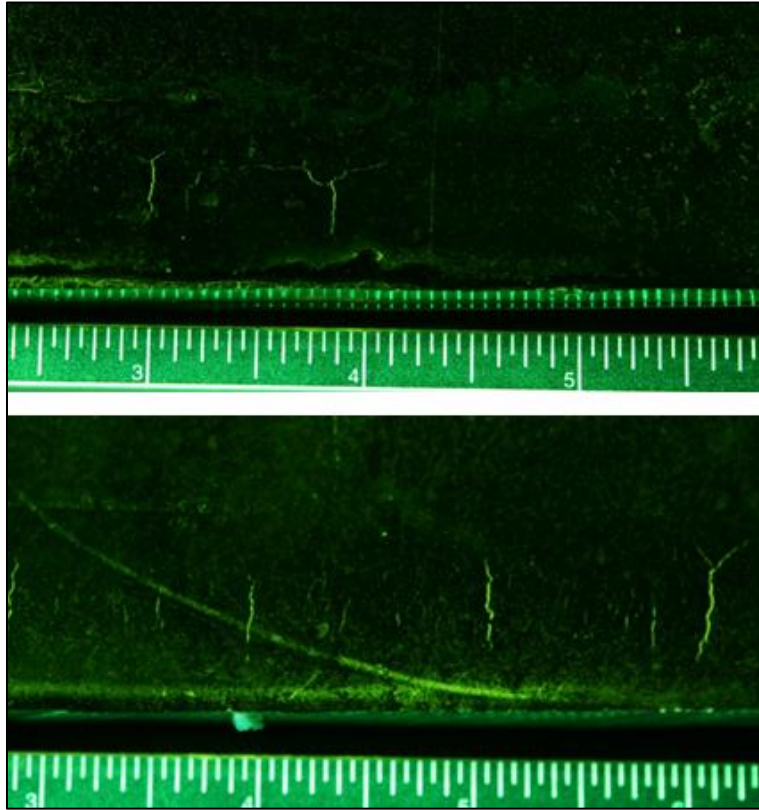


Figure 35. Image. Y-shaped cracks highlighted with florescent magnetic particles found on two tanks.

APPENDIX B—TENSILE TESTS

In Table 2 below, columns 7 to 9 use Engineering stress. In tensile testing, there are two ways to express tensile stress data: true stress-true strain; and engineering stress-engineering strain. True stress is the load on the specimen (newtons or pounds) divided by the cross-sectional area of the specimen (mm^2 or in^2). True stress continually updates the cross sectional area to reflect the fact that the cross-sectional area is steadily decreasing as the test runs. This is because the specimen is being stretched to be longer and thinner. In engineering stress, no attempt is made to adjust for the narrowing of the specimen during the test; the stress is just calculated as the load at a given moment divided by the initial cross sectional area of the specimen before it started deforming. True stress-true strain is used in some scientific reports, but it is more difficult to measure. Engineering stress-engineering strain is much more commonly reported.

Table 2. Data from coupons extracted from used nurse tanks of various ages.

Year Built	Tank Manufacturer	Tank Size, Gals	Sample Number (2 Tensile Samples per Tank)	Upper Yield Point, MPa	Lower Yield Point, MPa	Engineering % UTS, MPa	Engineering % Elongation at UTS	Engineering % Elongation at Fracture
1952	McNamar Boiler & Tank Co., Tulsa, OK	1,000	1	316	306	541	15.7	29.2
1952	McNamar Boiler & Tank Co., Tulsa, OK	1,000	2			542	17.2	29.0
1954	Beaird, Shreveport, LA	1,000	1	354	348	601	16.2	29.1
1954	Beaird, Shreveport, LA	1,000	2	353	353	597	18.0	30.0
1965	Illegible	1,000	1	390	373	584	18.1	29.4
1965	Illegible	1,000	2	391	372	581	15.1	25.6
1965	Illegible	1,000	1	342	339	572	18.1	41.8
1965	Illegible	1,000	2	333	332	580	17.1	40.3
1965	Illegible	1,000	1	283	278	474	14.9	31.9
1965	Illegible	1,000	2	283	279	491	21.7	34.2
1965	Illegible	1,000	1	303	295	510	17.6	38.4
1965	Illegible	1,000	2	320	303	509	17.1	37.3
1966	Illegible	1,000	1	375	364	555	13.5	18.6
1966	Illegible	1,000	2	371	362	563	13.3	25.4
1967	Trinity Steel Co. Inc., Dallas, TX	1,000	1	352	345	582	14.3	21.7
1967	Trinity Steel Co. Inc., Dallas, TX	1,000	2	356	348	568	12.2	21.3
1968	Trinity Steel Co. Inc., Dallas, TX	1,000	1	381	381	617		22.0
1971	Trinity Industries Inc.	1,000	1	333	331	603	14.1	24.4
1971	Trinity Industries Inc.	1,000	2	344	343	598	14.1	29.0
1973	Trinity Industries Inc.	1,000	1	315	306	507	18.3	38.6

1973	Trinity Industries Inc.	1,000	2	318	300	508	20.4	42.1
1977	Chemi-trol Chemical Co.	1,450	1	475	469	615	13.6	20.4
1977	Chemi-trol Chemical Co.	1,450	2	477	473	617	12.7	22.0
1978	Master Welding	1,000	1	459	438	618	16.3	26.3
1978	Master Welding	1,000	2	453	453	618	18.1	38.1
1978	Illegible	1,000	1	313	313	555	12.2	19.9
1978	Illegible	1,000	2	331	326	551	16.8	25.6
1982	Chemi-trol Chemical Co., Freemont, OH	1,000	1	403	390	579	16.4	26.4
1982	Chemi-trol Chemical Co., Freemont, OH	1,000	2	402	391	576	13.6	21.0
1986	American Welding & Tank Co.	1,000	1	352	347	535	15.1	26.7
1986	American Welding & Tank Co.	1,000	2			556	16.3	23.4
2009	ASME SA 455 Sample Plate	N/A	1	525	525	651	8.4	23.5
2009	ASME SA 455 Sample Plate	N/A	2	499	499	637	10.1	27.0
2009	ASME SA 455 Sample Plate	N/A	3	501	501	647	9.6	22.5

[This page intentionally left blank.]

APPENDIX C—INVESTIGATION OF A STRESS CORROSION CRACK IN A 1,450-GALLON NURSE TANK MANUFACTURED BY CHEMI-TROL IN 1977

More than 20 flaw indications were located by angle-beam ultrasound in a 1,450-gallon nurse tank manufactured in 1977. All of these flaws were found in the head. After sectioning the tank for further analysis, several of the cracked regions were further examined by magnetic particle inspection and optical microscopy. The largest crack found was 6 inches in total length. A segment of this crack is shown in Figure 36.

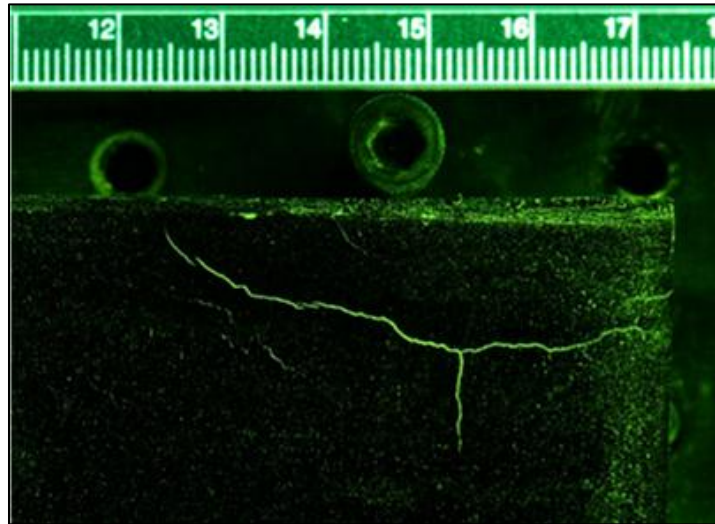


Figure 36. Photograph. Fluorescent wet magnetic particle testing of a segment of a crack in the head of the tank. The scale bar is in cm.

This crack was cut into sections. Two 1-cm sections were then broken open to reveal the crack surface. To open a crack, a notch was cut into the side of the steel opposite the site of the crack, the sample was submerged in liquid nitrogen (LN_2) so that the steel went through its ductile-to-brittle transition, and the section was impact loaded to fracture the sample. The result of this is seen in Figure 37. Below the red line is the SCC region, above the purple line are cut notch regions, and between the two lines is the brittle fracture region from impact loading at liquid nitrogen temperature.

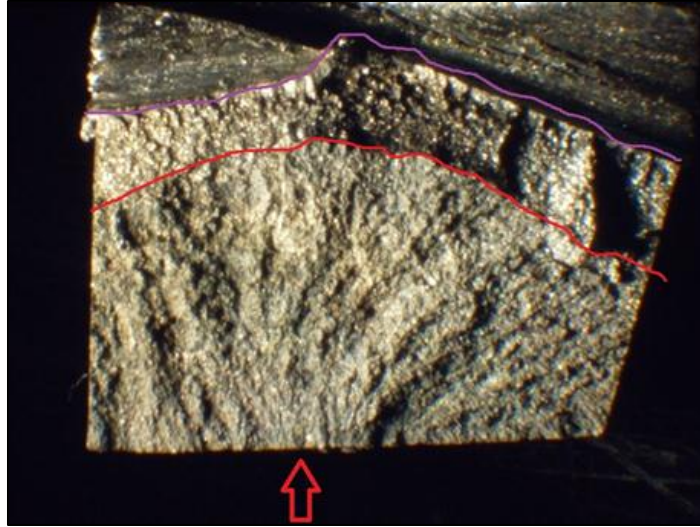


Figure 37. Image. The arrow indicates initiation of a crack on the interior of the tank head.

The arrows in Figure 37 show lines that are caused by preferential crack growth between grains aligned by rolling i.e., intergranular cracks. The bottom line (red) indicates the extent of crack growth. The region between the bottom line (red) and the top line (purple) is more specular due to the brittle fracture after chilling in LN₂. (The term “specular” refers to how shiny or mirror-like the facets of the fracture appear. A highly specular fracture surface suggests a more brittle fracture than does a less specular surface [where some amount of plastic (ductile) flow may have occurred around the crack].)

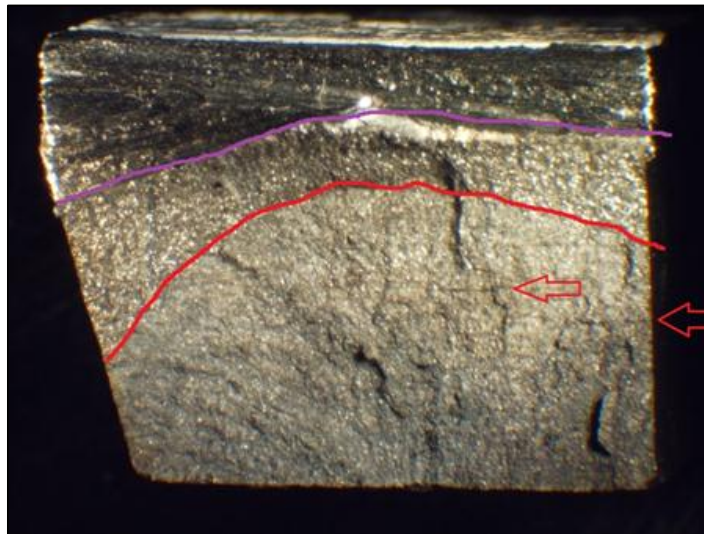


Figure 38. Image. Positioning the light source at a different angle revealed several horizontal lines visible in the cracked region of the sample, two of which are indicated by arrows.

The sections shown in Figure 37 and Figure 38 were then examined with a SEM. Further images of the cracks shown in Figure 38 are in Figure 40. Figure 43 shows that the SCC region is faceted, which indicates that the fracture mode was intergranular.

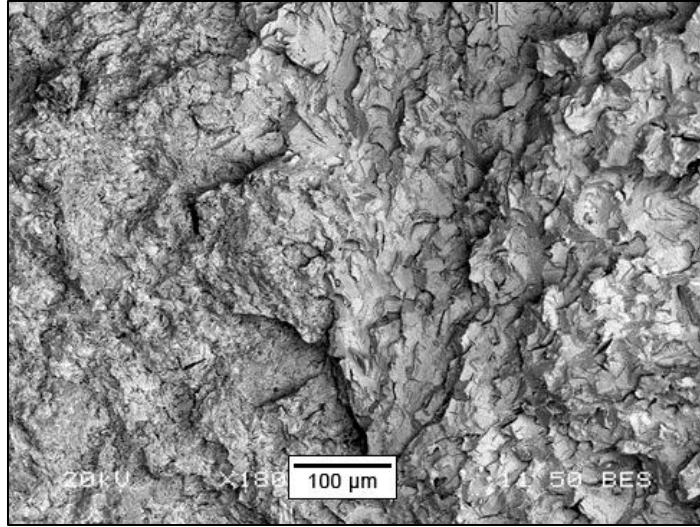


Figure 39. Image. Shadow image of surface before cleaning. The right side has no oxide and is clearly faceted due to cleavage fracture when the sample was subjected to an impact loading after cooling to liquid nitrogen temperatures.

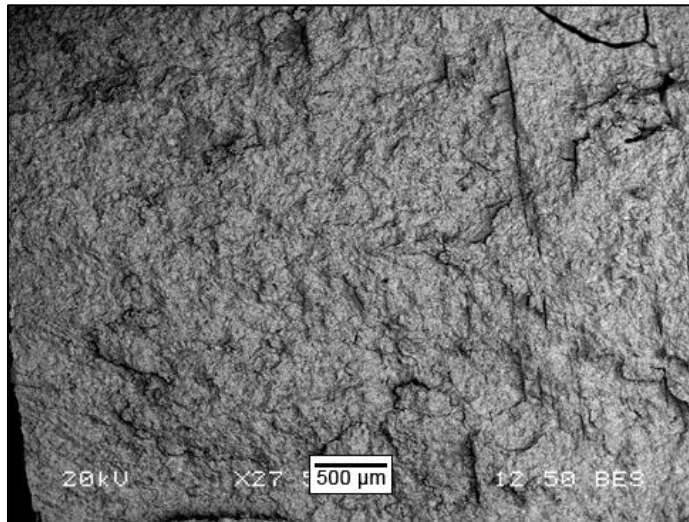


Figure 40. Image. Vertical cracks produced by backscattered electrons.

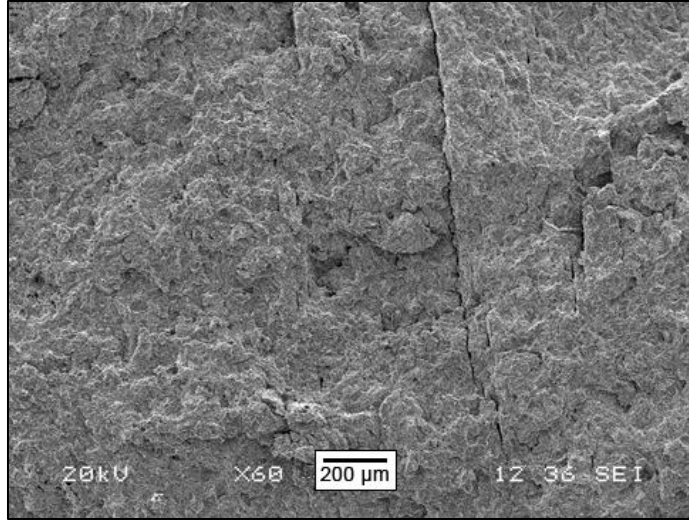


Figure 41. Image. Secondary electron image of vertical cracks.

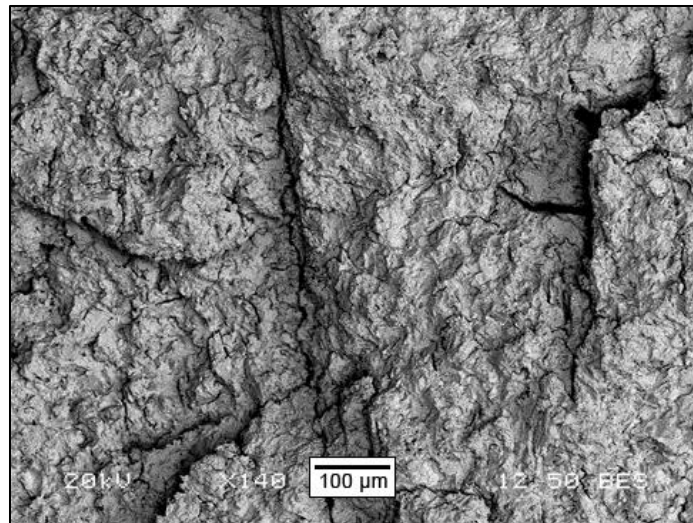


Figure 42. Image. Vertical cracks produced by backscattered electrons.

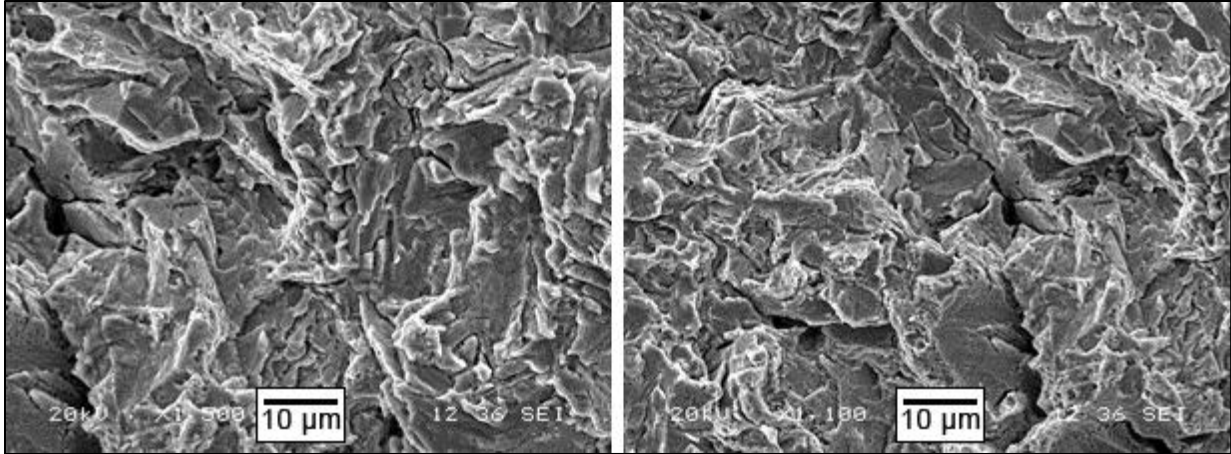


Figure 43. Image. After cleaning, the stress corrosion cracking region shows faceted regions indicating intergranular cracking.

The SCC surface shows faceted regions indicating intergranular cracking. Another section of the crack shown in Figure 36 was cross-sectioned, polished, and then etched with a 2-percent nital etch. Figure 45 and Figure 46 show micrographs of these sections. The crack branches several times, but these micrographs do not clearly distinguish between transgranular and intergranular cracking. (Transgranular is a crack that runs through the grains of a metal and does not follow a path along grain boundaries, which would be intergranular.)

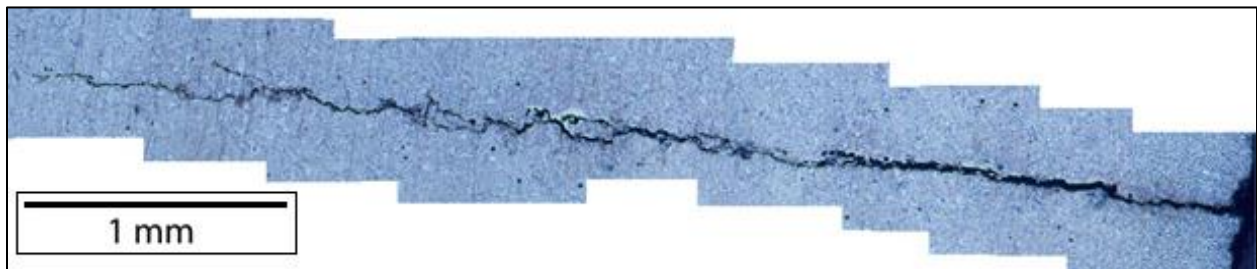


Figure 44. Photograph. Cross-section of a penny-sized crack located in a 1,450-gallon nurse tank head manufactured in 1977. The crack originated near the circumferential weld on the interior.

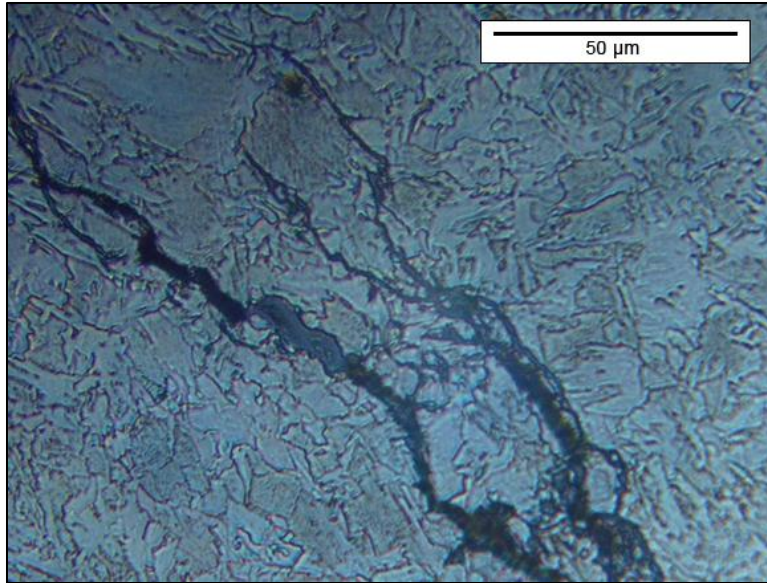


Figure 45. Image. Optical microscopy of the cracks indicates intergranular cracking as the crack path swings around grains.

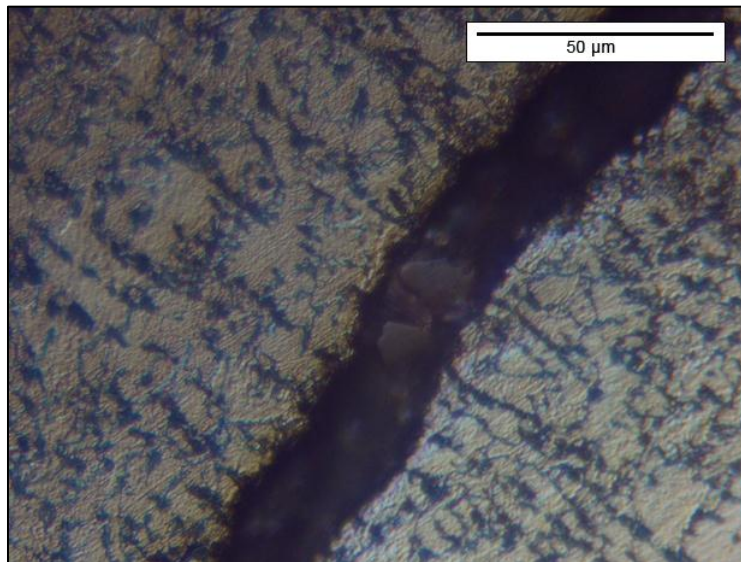


Figure 46. Image. At this point, the crack is larger than the surrounding grains, obscuring whether intergranular or transgranular cracking is occurring.

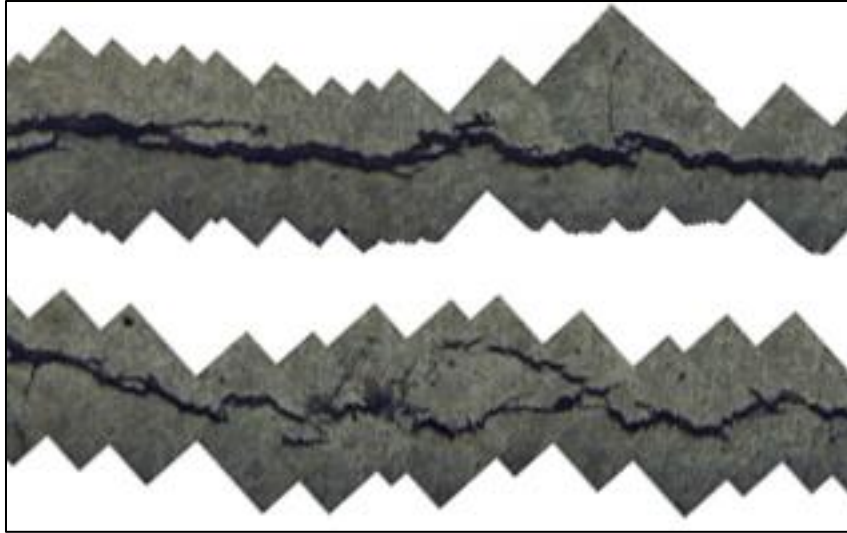


Figure 47. Image. The crack branching is clearly seen in these micrographs.

[This page intentionally left blank.]

APPENDIX D—LATTICE PARAMETER AND STRAIN CALCULATIONS USED TO DEVELOP NEUTRON DIFFRACTION RESIDUAL STRESS DETERMINATIONS

The lattice parameter is data that are taken directly from the neutron diffraction patterns. (Lattice parameter is the length of a crystal unit cell edge dimension. When there is no compressive or tensile stress, the space between atoms in a given crystal is constant. When stress is applied, the lattice parameters increase or decrease slightly depending on whether the material is placed under tensile or compressive stress.) Neutron diffraction data were used to calculate the hoop, axial, and radial strains. The strain is calculated in Figure 49. There was uncertainty in the determination of the lattice parameter due to uncertainty in peak fitting. This uncertainty was recorded for each of the three dimensions, and these are referred to as: delta epsilon sub x, delta epsilon sub y, and delta epsilon sub z.

$$\text{lattice strain} = \frac{(\text{strained lattice parameter}) - (\text{unstrained lattice parameter})}{\text{unstrained lattice parameter}}$$

Figure 48. Formula. Lattice strain is calculated by comparing the lattice parameter of a strained region to the lattice parameter of an unstrained region.

The hoop, axial, and radial stresses are calculated by the three equations in Figure 49.

$$\begin{aligned}\sigma_{hoop} &= \lambda e + 2G\epsilon_{hoop} \\ \sigma_{axial} &= \lambda e + 2G\epsilon_{axial} \\ \sigma_{radial} &= \lambda e + 2G\epsilon_{radial}\end{aligned}$$

Figure 49. Equations. Stress is dependent on strain in three orthogonal directions (hoop, axial, and radial).

Where e is:

$$e = \epsilon_x + \epsilon_y + \epsilon_z$$

Figure 50. Equation. e is the vector sum of the three strains.

And lambda is:

$$\lambda = \frac{\nu E}{(1 + \nu)(1 - 2\nu)}$$

Figure 51. Equation. Lambda is related to Poisson's ratio and the elastic modulus.

And G, the modulus of rigidity is:

$$G = \frac{E}{2(1 + \nu)}$$

Figure 52. Equation. Modulus of rigidity is proportional to the elastic modulus and inversely related to Poisson's ratio.

Where E is Young's modulus (elastic modulus), and ν is Poisson's ratio (the ratio of transverse strain to axial strain). For steel, Young's modulus is 201,000 MPa and Poisson's ratio is 0.3. The error shown in the plots is fitting error bars due to the imprecision in fitting the lattice parameter to the diffraction data. The error in the reported residual stress was calculated by Figure 53.

$$\Delta\sigma_x = \sqrt{\lambda^2(\Delta e)^2 + (2G)^2(\Delta\varepsilon_x)^2}$$

Figure 53. Formula. The error in strain is related to the errors in the strains.

Where delta e is:

$$\Delta e = \sqrt{(\Delta\varepsilon_x)^2 + (\Delta\varepsilon_y)^2 + (\Delta\varepsilon_z)^2}$$

Figure 54. This portion of the error is dependent on the square root of the sum of the squares of the three orthogonal strain errors.

We compared the lattice parameters obtained from neutron diffraction measuring the hoop section taken from the 1,000-gallon nurse tank to an unstressed sample also neutron diffraction measured. The unstressed sample was created by creating a 4-mm-thick slice that was then cut every 4 mm so that the end result resembled a comb. This comb, which contained the regions that had been previously scanned, was rescanned (Figure 55). Because the sample was cut into a comb with 4 mm x 4 mm x 6 mm "teeth," nearly all residual stress was removed, and the reference lattice parameter remains very stable. If the difference in lattice parameter had been caused by a different steel composition due to welding, then the reference lattice parameters would have variations as they crossed the weld; such variations are not seen in Figure 55.

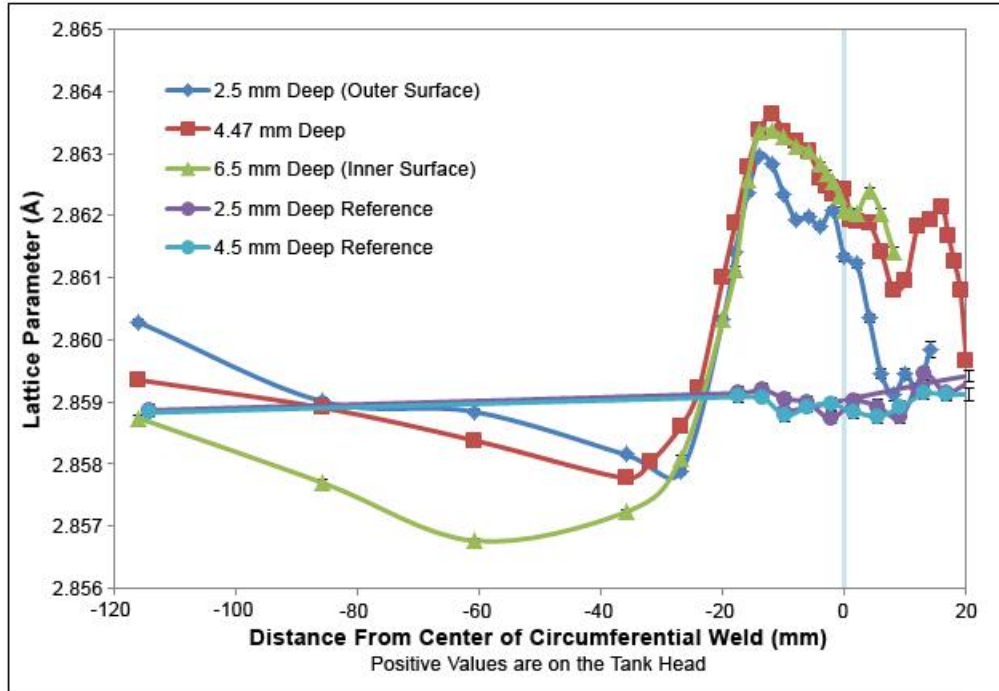


Figure 55. Graph. Hoop lattice parameter across the circumferential weld in a nurse tank manufactured in 1966.

The hoop strain has higher error bars than the radial or axial strain because the beam had to pass through a greater thickness of steel to get these patterns, and there was more attenuation. The highest tensile strain and therefore strongest contributor to SCC is found within 20 mm of each side of the weld (as seen in Figure 57).

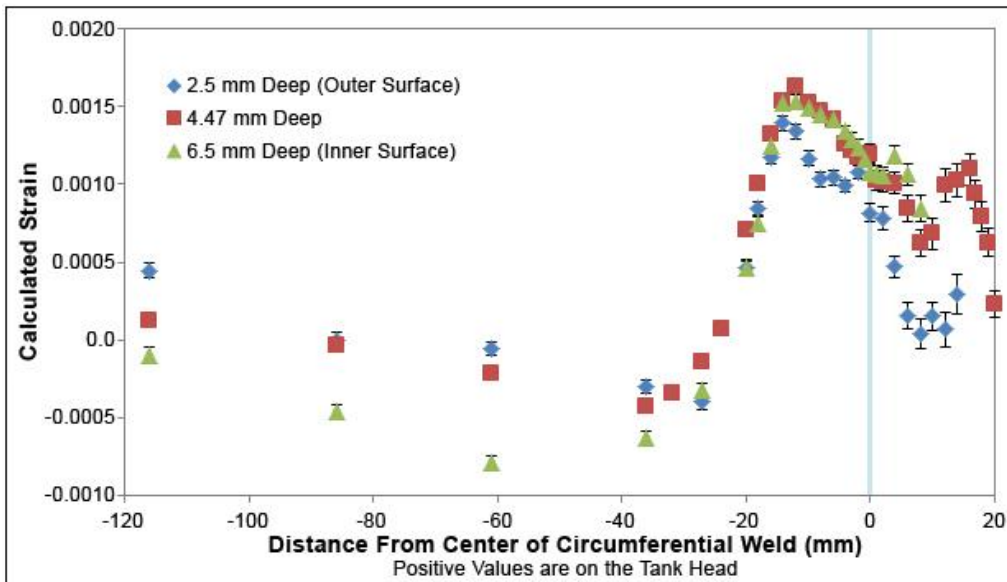


Figure 56. Graph. Hoop strain across the circumferential weld in a 1,000-gallon nurse tank manufactured in 1966.

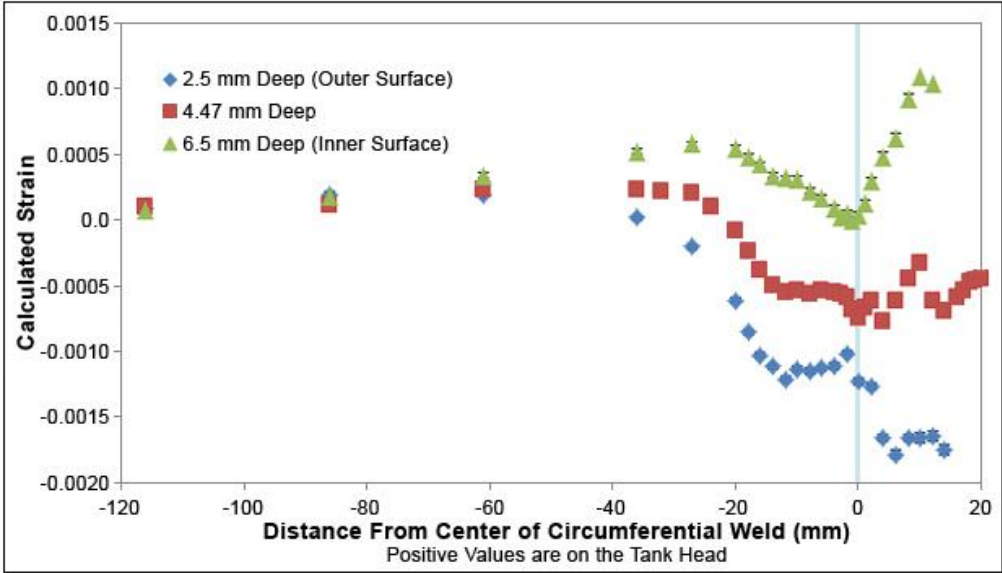


Figure 57. Graph. Axial strain across the circumferential weld in a 1,000-gallon nurse tank manufactured in 1966. The highest strain is on the inner surface of the tank next to the weld.

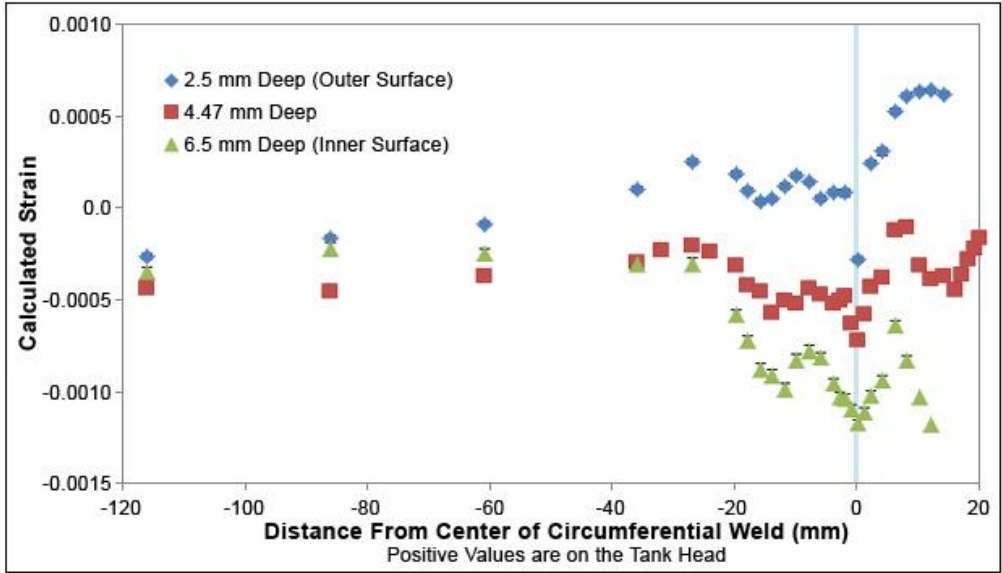


Figure 58. Graph. Radial strain across the circumferential weld in a 1,000-gallon nurse tank manufactured in 1966. The strain is lower for radial than for axial and hoop.

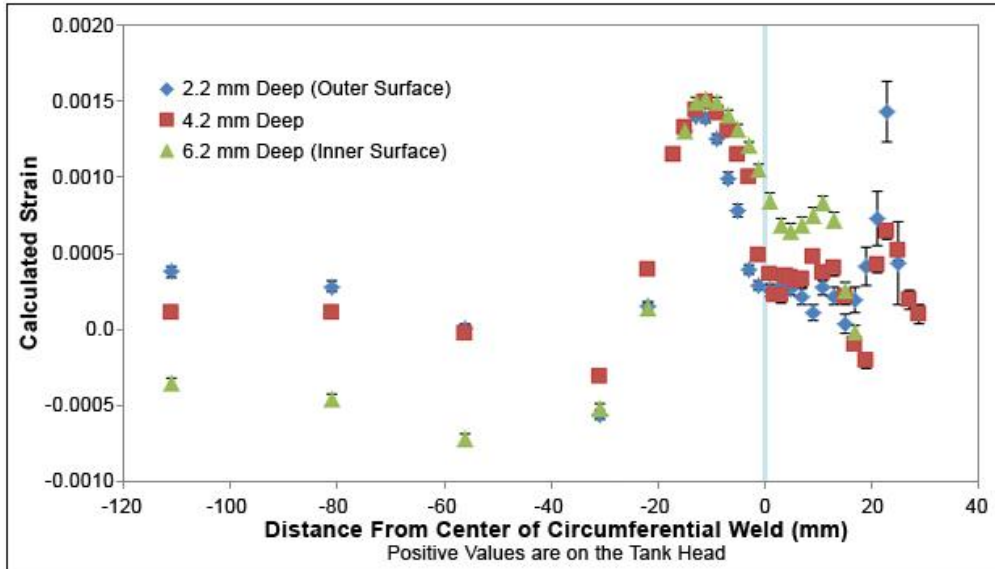


Figure 59. Graph. Hoop strain across the circumferential weld in a 1986 nurse tank.

The error bars grow much larger at 20–30 mm from the weld due to signal attenuation as the beam passed through double thicknesses of steel.

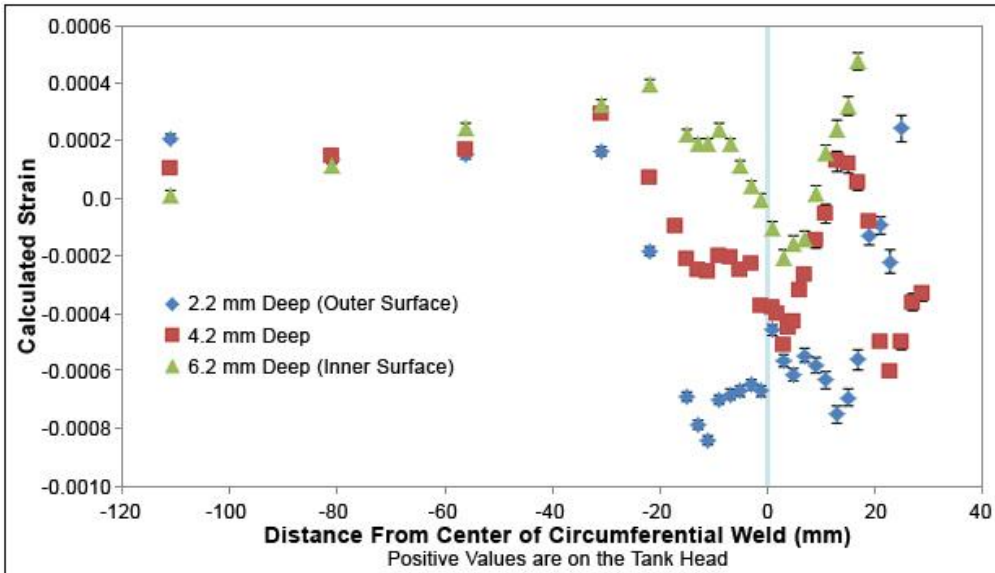


Figure 60. Graph. Axial strain across the circumferential weld in a 1986 nurse tank.

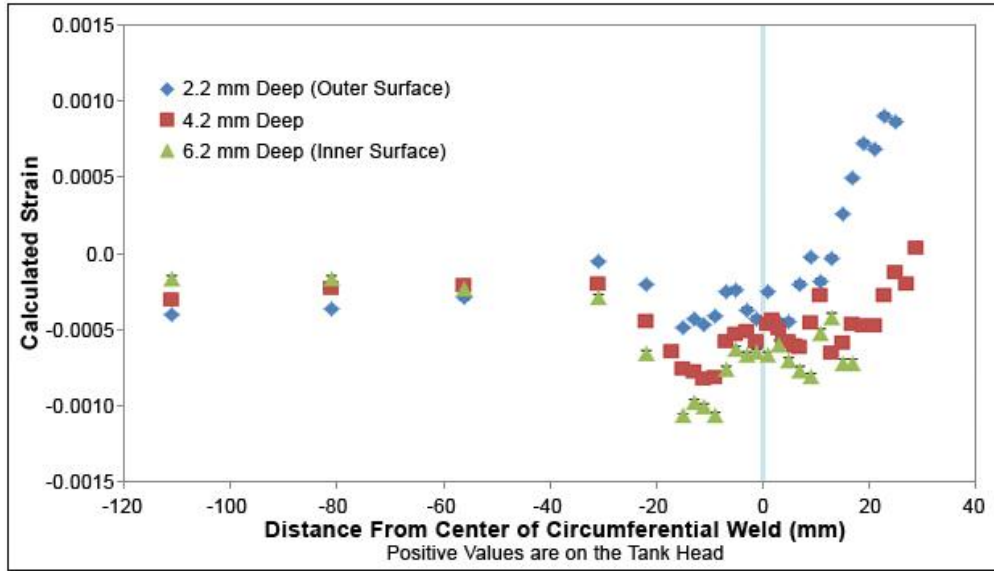


Figure 61. Graph. Radial strain across the circumferential weld in a 1986 nurse tank.

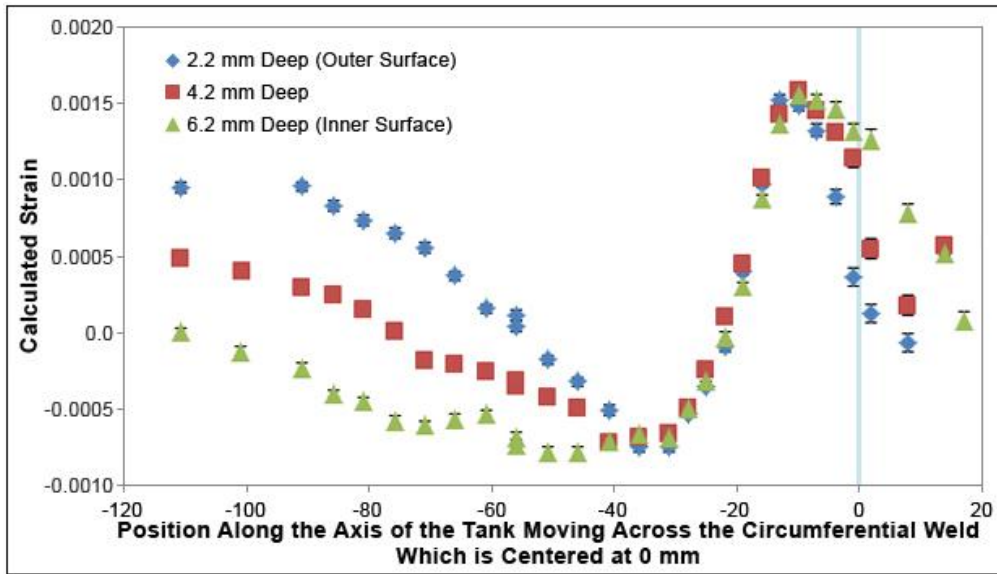


Figure 62. Graph. Hoop strain in the heat-affected zone of the axial weld crossing the circumferential weld in a 1986 nurse tank.

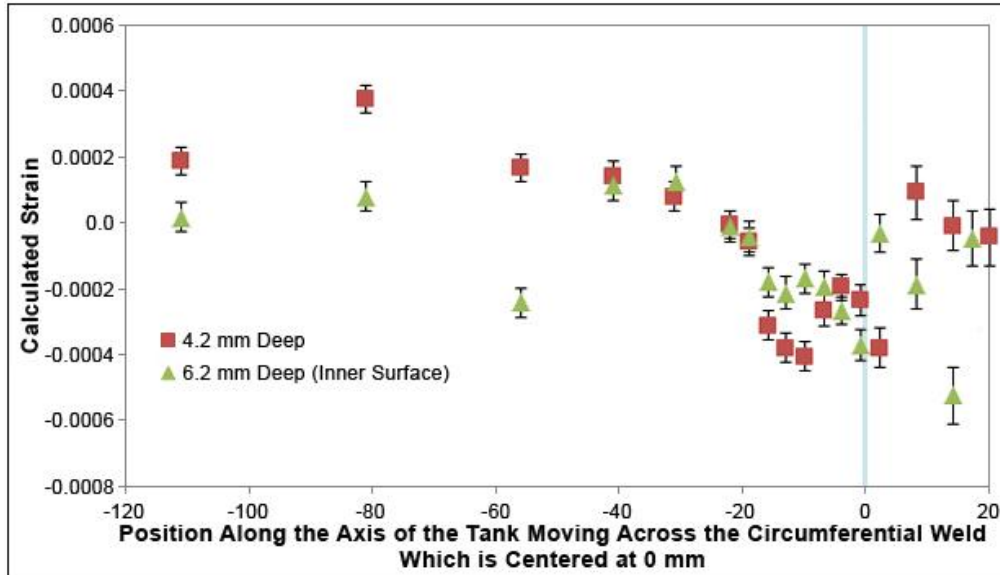


Figure 63. Graph. Radial strain in the heat-affected zone of the axial weld crossing the circumferential weld in a 1986 nurse tank.

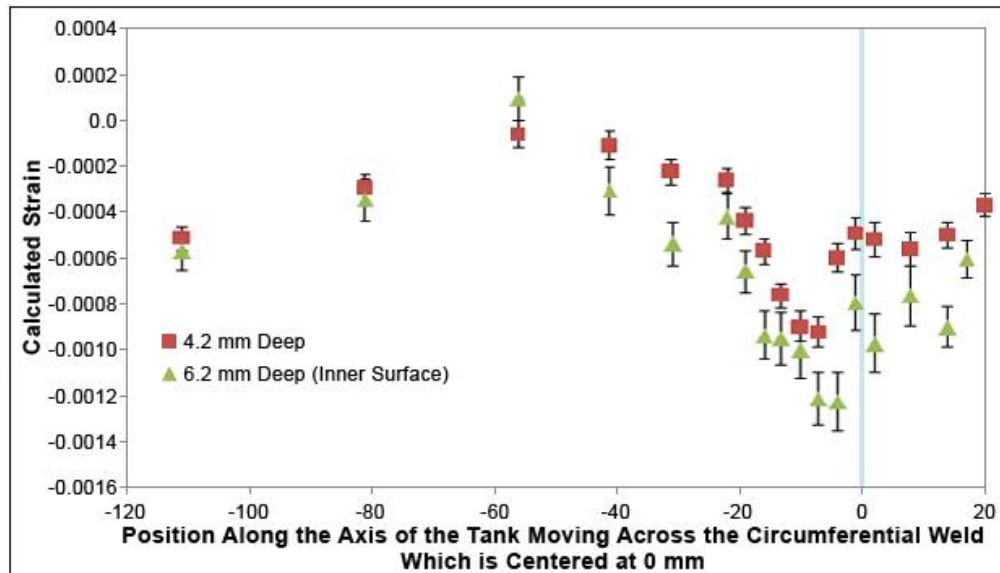


Figure 64. Graph. Radial strain in the heat-affected zone of the axial weld crossing the circumferential weld in a 1986 nurse tank.

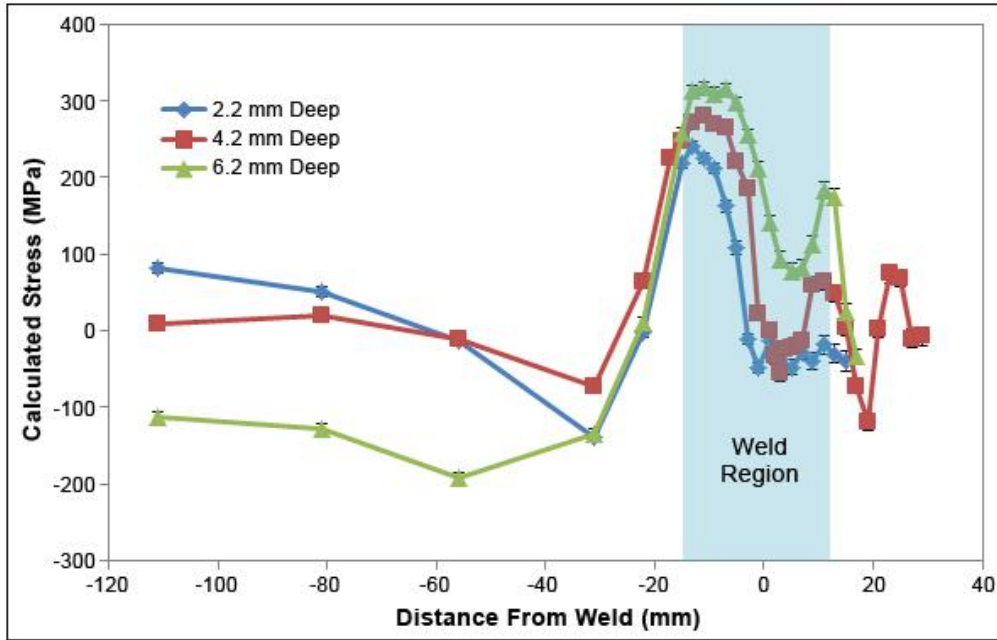


Figure 65. Graph. Hoop stress across the circumferential weld in a 1,000-gallon nurse tank manufactured in 1986.

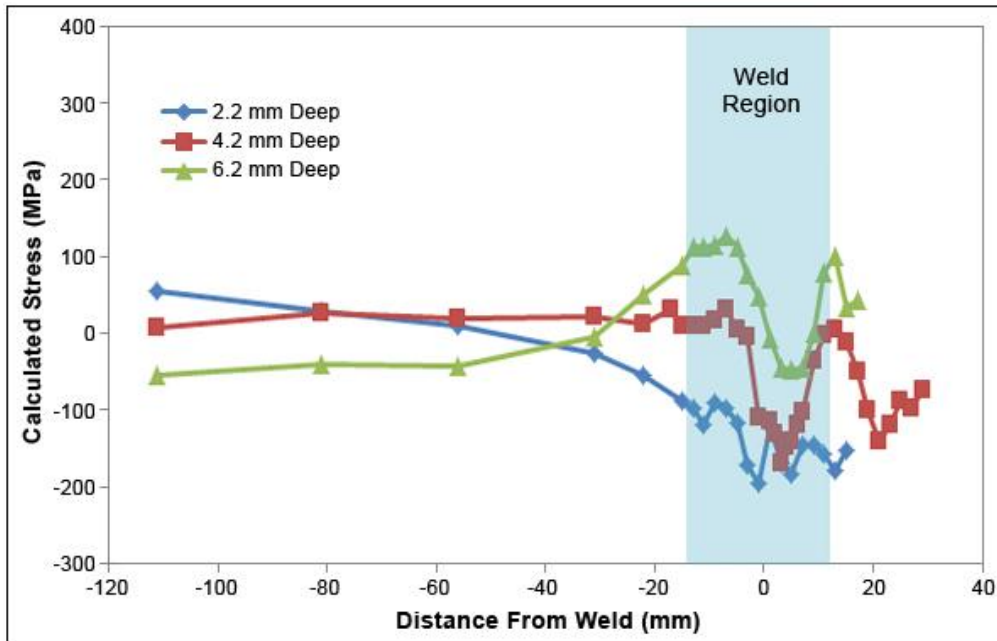


Figure 66. Graph. Axial stress across the circumferential weld in a 1,000-gallon nurse tank manufactured in 1986.

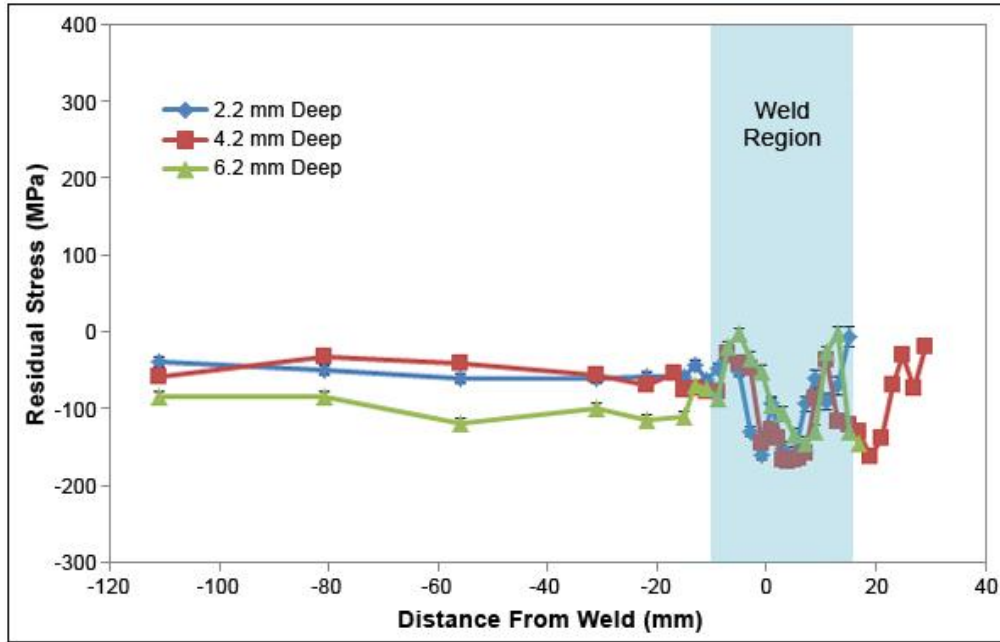


Figure 67. Graph. Radial stress across the circumferential weld in a 1,000-gallon nurse tank manufactured in 1986.

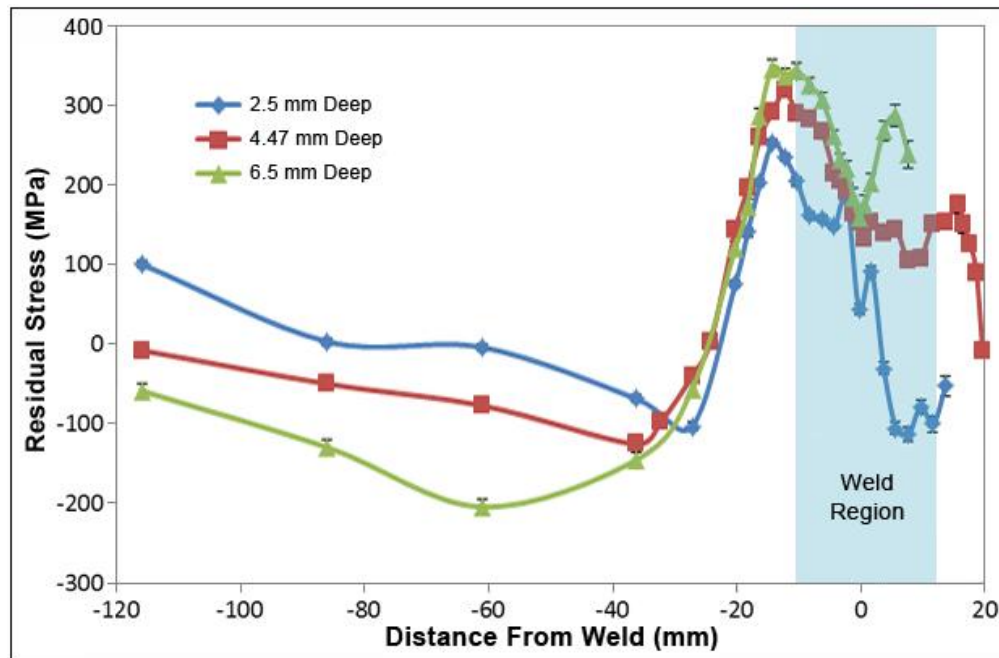


Figure 68. Graph. Hoop stress across the circumferential weld in a 1,000-gallon nurse tank manufactured in 1966.

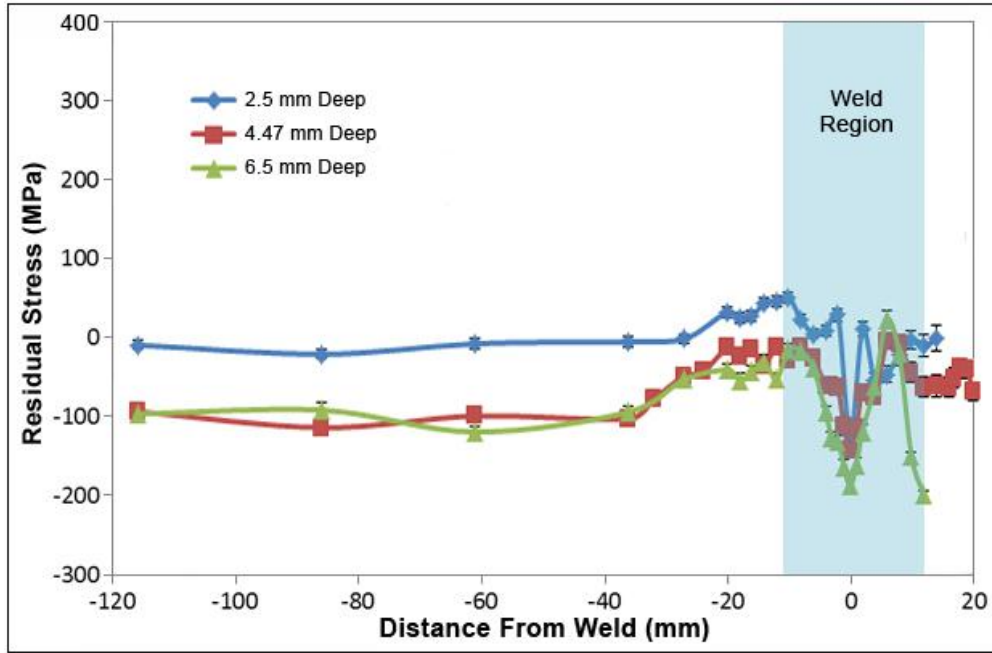


Figure 69. Graph. Radial stress across the circumferential weld in a 1,000-gallon nurse tank manufactured in 1966.

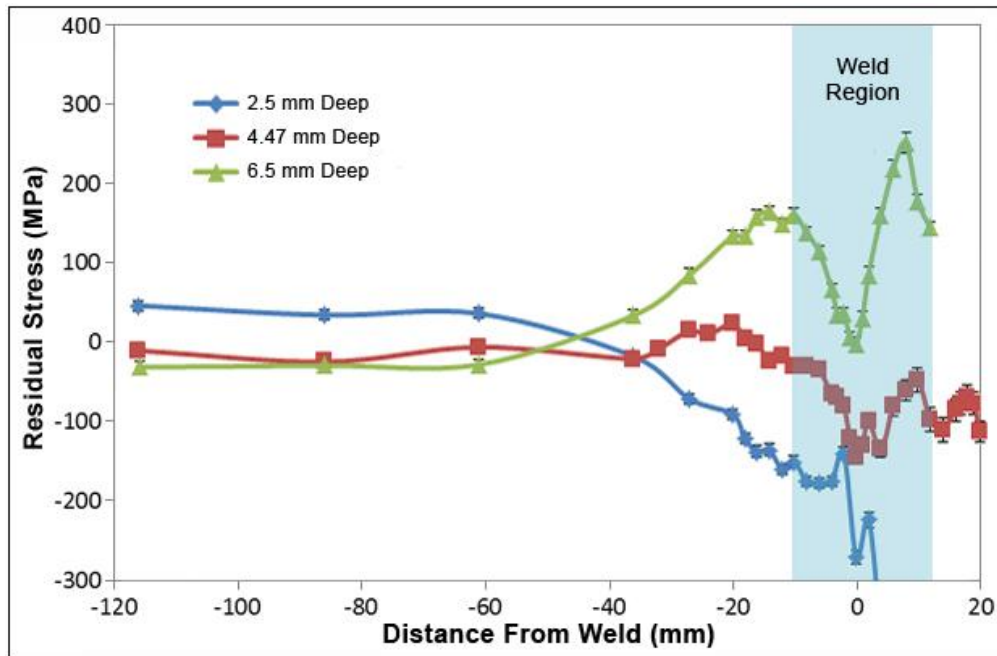


Figure 70. Graph. Axial stress across the circumferential weld in a 1,000-gallon nurse tank manufactured in 1966.

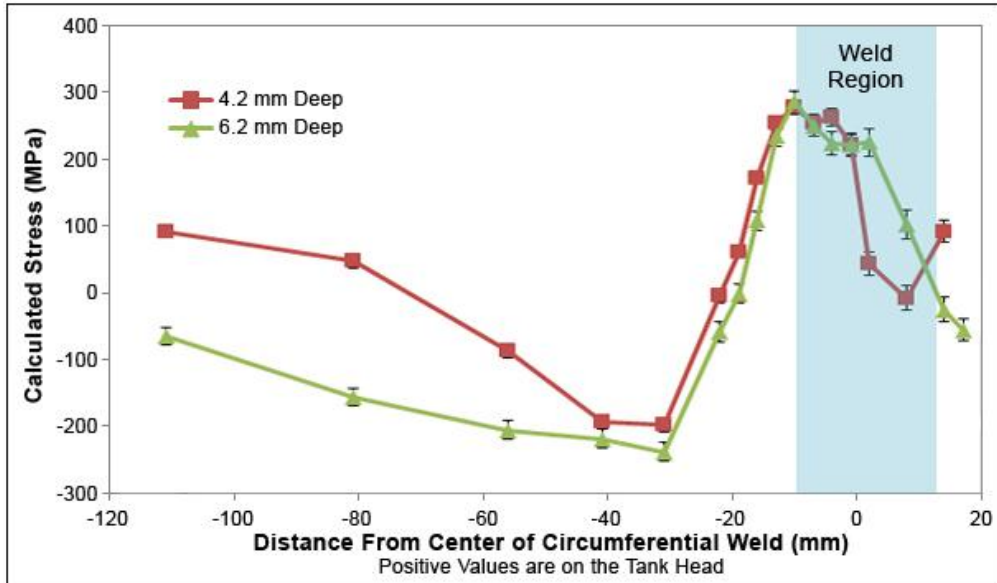


Figure 71. Graph. Hoop stress in the heat-affected zone of the axial weld crossing the circumferential weld in a 1986 nurse tank.

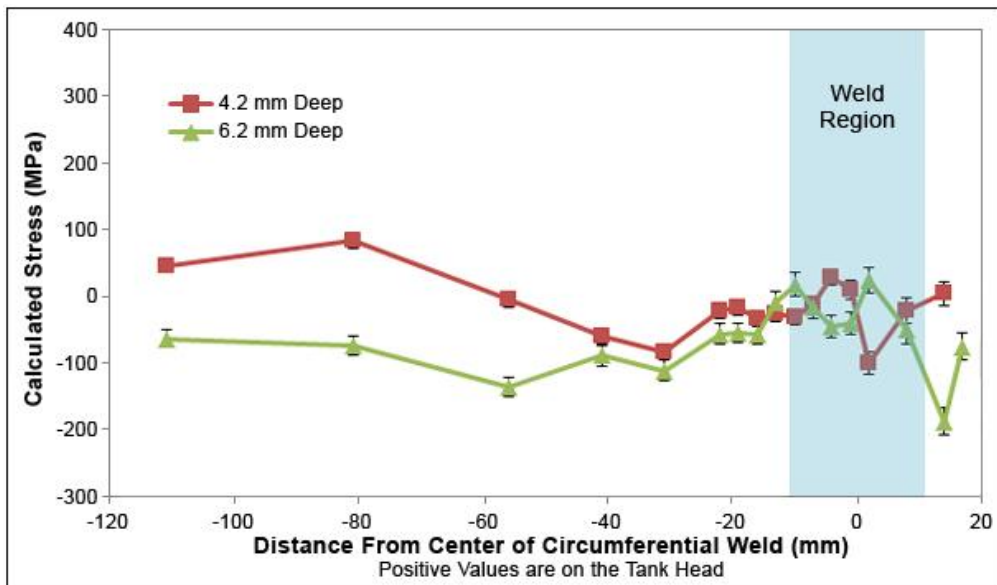


Figure 72. Graph. Axial stress across the circumferential weld in a 1966 nurse tank.

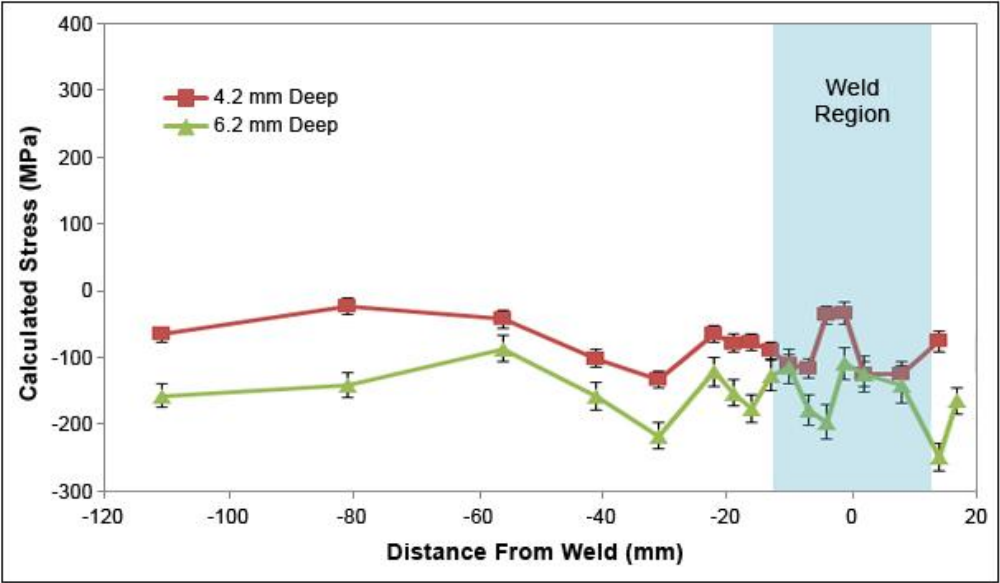


Figure 73. Graph. Radial stress across the circumferential weld in a 1986 nurse tank.

APPENDIX E—LITERATURE REVIEW: ANHYDROUS AMMONIA NURSE TANK STRESS CORROSION CRACKING

INTRODUCTION

This appendix was prepared as the first product of this research. It is included here in its entirety for the interested reader. On a number of subjects, it provides additional background to what is contained in the body of the report. However, some of the material in the body of the report is a full quote of the material from short sections of this appendix.

Anhydrous ammonia (NH_3) is a widely used agricultural nitrogen rich fertilizer locally distributed from regional suppliers like agriculture cooperatives to farm fields via nurse tanks. Nurse tanks are designed to hold NH_3 in liquid form under pressure; they are mounted on running gear and can be towed behind a pickup truck or tractor on highways to reach farm fields. Nurse tanks are cylindrical steel tank shells with hemispherical or elliptical end caps, or “heads.” The Fertilizer Institute (TFI) previously estimated that about 200,000 nurse tanks are in operation across the United States, many of which are 25 to 50 years old.

Typical steels used to construct nurse tanks include ASTM A285, ASTM A455, and ASTM A516 grade 70. These are all low-carbon, low-alloy steels with mixed ferrite and pearlite microstructures. Quenched and tempered high-strength ASTM A517 grade F steel was used to construct nurse tanks in the 1960s and is still used today in NH_3 tanker trucks subject to MC-331 requirements for high pressure vessels. This steel has significantly lower carbon content and higher chromium, molybdenum, and nickel content that could make the SCC behavior differ from that of 455 and 516 steels now used for nurse tanks.

An international survey conducted in 1982 found that more than half of all inspected spherical storage NH_3 tanks were reported to have cracks.⁽¹⁾ NH_3 was reported to be the most frequently released hazardous substance in 1997 by the Hazardous Substances Emergency Events Surveillance branch of the U.S. Department of Health and Human Services.⁽²⁾ Liquefied NH_3 flash vaporizes upon depressurization and causes severe burns if it contacts human tissue. NH_3 most severely affects the high-moisture-bearing eye, skin, gastrointestinal, and respiratory systems. Exposure to greater than 140 ppm NH_3 can cause corneal ulcerations, iritis, cataracts, glaucoma, and retinal atrophy. Exposure to 1,700 ppm NH_3 (1/6 of 1 percent) results in permanent respiratory damage.⁽³⁾ Even short exposure to more than 5,000 ppm NH_3 (1/2 of 1 percent) can be fatal. Therefore, the safe storage of NH_3 is of great concern to persons dealing with its handling or transportation and to the general public.

TECHNICAL LITERATURE

Most studies of NH_3 SCC were performed in the 1960's and 1980's. Current literature on the topic is scarce, suggesting the need for further investigation of the structural integrity of aging nurse tanks.

Stress Corrosion Cracking

SCC is crack formation and growth in metal caused by the combined effects of corrosion at stress fractures caused by straining of the metal from residual or applied tensile stresses. The extent to which SCC damages a material is determined by the material type, environment, and applied mechanical loading. Corrosion can be classified according to three broad categories: active path dissolution, hydrogen embrittlement, and film-induced cleavage.

Active path dissolution occurs in metals having passive protective layers, such as oxide and/or water coatings. Accelerated corrosion occurs along crack tips, grain boundaries, or other paths of high corrosion susceptibility.⁽⁴⁾ When a metal is surrounded by a corrosive solution and a stress is applied, the stress serves to break the protective passive coating layer by opening small cracks. The crack tips act as stress risers and provide a pathway for accelerated corrosion. Thus, the combined effect of corrosive solution and stress serve as an “electrochemical knife” that can slice through the metal.⁽⁵⁾ The speed of active path dissolution is limited by the rate of corrosion at the crack tip; thus, cracks in steel nurse tanks generally grow at rates of less than 1 mm per year.⁽⁴⁾

Hydrogen embrittlement occurs when a source of hydrogen is present in a metal’s environment. Hydrogen can damage nearly all metals by filling interstitial sites (or the gaps between the grains of the steel), which embrittles the metal. Because of its small size, a hydrogen atom can diffuse quickly in metal, even at low temperatures. Moreover, hydrogen diffuses even more readily in regions ahead of crack tips due to local stresses and lattice dilations.⁽⁴⁾

Film-induced cleavage occurs in ductile materials that form brittle films in the presence of a corrosive substance. When stresses crack open the brittle outer layer, the ductile material underneath blunts the crack tip. The film reforms on the freshly exposed metal, and the process repeats, causing the metal to continually corrode away.⁽⁴⁾

Mechanisms of NH₃ Stress Corrosion Cracking in Steel

Wilde has shown that it appears NH₃ SCC in steel occurs by the active path dissolution type rather than a hydrogen embrittlement effect.⁽⁶⁾ In active path dissolution the corrosive attack occurs at a particular weak point on the surface of the material, such as occurs at a grain boundary, or where dislocations or slip steps intersect the surface. Thus, both intergranular and transgranular cracking occurs as the result of NH₃ SCC. Pure NH₃ does not cause SCC, but when mixed with as little as 0.5 ppm oxygen, it does. Note that oxygen at higher levels can actually help to protect the surface by formation of a passivated adsorbed layer of oxygen. It is only in low concentrations (essentially a de-oxidized state) where SCC is of concern. Adding 0.10 percent water by weight to NH₃ has been shown to inhibit NH₃ SCC completely, but only in the liquid phase portion of the tank, not the vapor portion.

Lunde and Nyborg demonstrated that the addition of water to liquid NH₃ does not provide protection against SCC in regions of the tank above the liquid level because vaporized NH₃ (free of the added water) can condense on the upper surfaces of the tank.⁽⁷⁾ Oxygen dissolved in NH₃ increases the corrosion potential of steel, while dissolved nitrogen has little effect on the polarization potential. Though nitrogen has no electrochemical effect, it accelerates SCC in the

presence of oxygen by slowing the repassivation of the metal by oxygen forming an adsorbed layer.⁽⁸⁾

Because quenched and tempered A517 grade F steel was commonly used for nurse tanks in previous years, the following tables summarize test results from a 1981 study on that type of steel in different environments. The finding is that only oxygen and oxygen-nitrogen contaminations of NH₃ caused SCC. Though CO₂ has been shown to be generally corrosive, it does not appear to contribute to NH₃ SCC.⁽⁶⁾

As pointed out in the introduction of the body of the paper, the composition of 517 grade F steel is very different. The research team believes the finding that only oxygen and oxygen-nitrogen contaminations of NH₃ caused SCC also holds up for the other steels now more commonly used in manufacturing nurse tanks. The research conducted at Iowa State University in 2010 for this study on currently used steel types is more representative of SCC rates in the currently used steel types.

Table 3. Corrosion of A517 grade F steel exposed to different components of air.

Environment	Concentration (ppm)	Results of Duplicate Tests
NH ₃ (metallurgical grade)	N/A	no cracking, no corrosion
Air (N ₂ + O ₂ + CO ₂)	200 O ₂ , 338 N ₂ , unknown CO ₂	cracking
O ₂ + CO ₂	200 O ₂ , 1200 CO ₂	general corrosion, no cracking
N ₂ + O ₂	338 N ₂ , 200 O ₂	cracking
N ₂	400	no cracking
O ₂	200	slight cracking observed in heavily cold-worked necked region of specimen
CO ₂	1200	general corrosion, no cracking

Table 4. Summary of SCC test results for A5176 grade F steel in anhydrous ammonia containing various contaminants.

Contaminant	Concentration (ppm unless otherwise indicated)	Results of Duplicate Tests
CO	100	no cracking
CO + O ₂	100 + 200	no cracking
CH ₄	100	no cracking
SO ₂	100	no cracking, severe general corrosion
SO ₂ + O ₂	100 + 200	no cracking, severe general corrosion
NH ₄ HCO ₃	saturated	no cracking
(NH ₄) ₂ CO ₃	saturated	no cracking
NH ₄ NO ₃	0.025 molecules/L	no cracking, severe general corrosion

NaNO ₃	0.05 M molecules/L	no cracking
NO	100	no cracking
NO ₂	100	no cracking
N ₂ O	100	no cracking
NaCl	Saturated	no cracking
NH ₄ Cl	0.019 molecules/L	no cracking, general corrosion
NaNO ₂	0.011 molecules/L	no cracking
NaNH ₂ + air	saturated + 200 ppm O ₂	no cracking

Several theories have been developed to explain the process of NH₃ SCC. A film-rupture model has been proposed by Wilde based upon electrochemical studies. This is: that steel in NH₃ exists in both a film-free active state, and a passive state created by a layer formed by dissolved oxygen molecules (O₂). The oxygen molecules form a noble adsorbed film (oxygen atoms adhering to the surface, but not penetrating beneath the surface) on all steel surfaces. When the steel is stressed and plastic deformation occurs at slip steps, the oxygen film is ruptured. Direct galvanic coupling between the exposed bare steel at the slip step and the still intact portion of the oxygen film causes anodic dissolution of the bare steel until the protective oxygen molecule film reforms locally re-passivizing the steel.

Nitrogen is proposed to compete with oxygen to adsorb to the steel, but without forming a protective film itself, thus hindering repassivation of the exposed steel. When the oxygen film is ruptured by an applied stress, nitrogen adsorbs in place of oxygen and anodic dissolution is allowed to occur for a much longer time (Figure 74 and Figure 75). In the absence of dissolved nitrogen, the oxygen film quickly recovers and crack growth is slow. The nitrogen-oxygen combination allows more rapid dissolution of steel to proceed, thus causing more severe growth of the crack.

Water also has an affinity for adsorption on steel since it is a polar molecule. Thus, it acts to form an additional passive film, thus aiding oxygen in slowing SCC. The following diagram illustrates the principles of the adsorption model.⁽⁸⁾

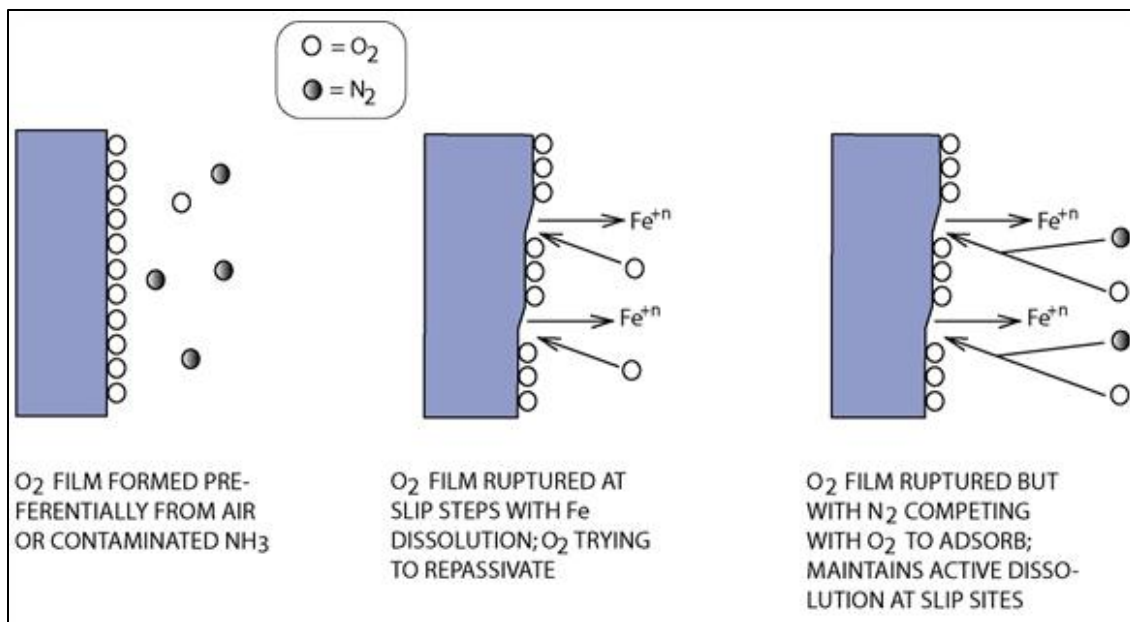


Figure 74. Diagram. Illustration of film-rupture model in which “competitive” adsorption takes place between oxygen and nitrogen molecules.

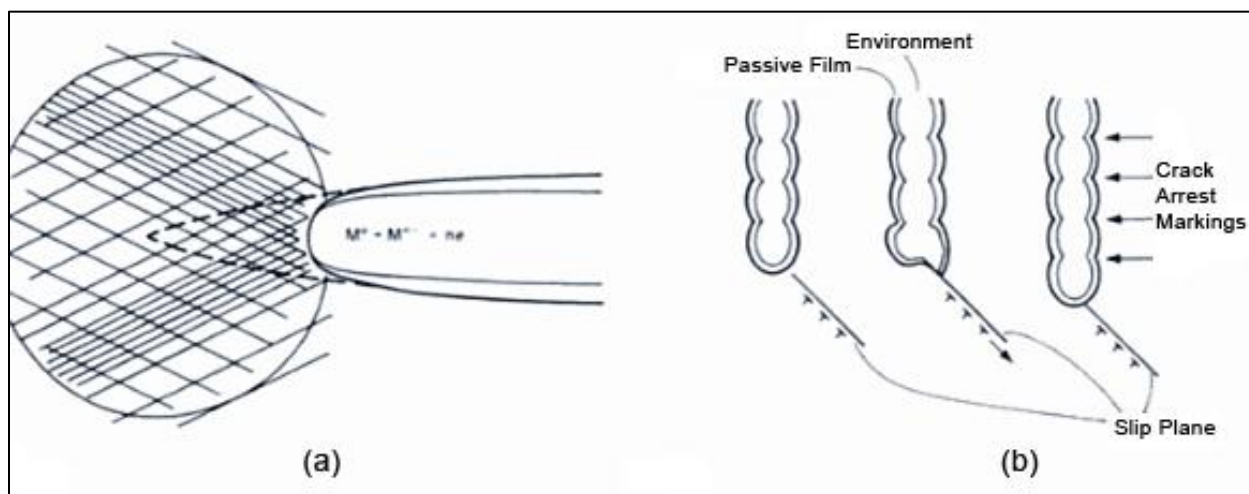


Figure 75. Diagram. Crack propagation according to the general film-rupture model. Continuous deformation causes the crack tip to stay exposed (a), and when a passivating film does form, it is ruptured again (b) ⁽⁹⁾

A chemical mechanism for NH₃–O SCC proposed by Dawson is shown in Figure 76. ⁽¹⁰⁾

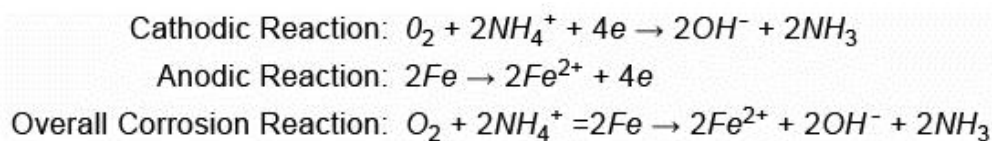


Figure 76. Equations. Three equations for the chemical mechanism for anhydrous ammonia—oxygen stress corrosion cracking (4e = four free electrons).

The presence of oxygen may cause ammonium to form hydroxide ions and oxidize iron in the steel. However, the role of oxygen in NH_3 SCC is controversial, and it may be the case that oxygen simply changes the corrosion potential to within the cracking range, instead of forming a passivating film.⁽¹⁶⁾ Other NH_3 SCC models have been proposed based on the formation of nitrogen-rich and iron oxide protective films.^(17,18)

The free corrosion potential of the carbon steel used to make Figure 77 was in the range of 400-600 mV against an aluminum reference. Cathodic polarization was shown to decrease SCC while anodic polarization accelerated SCC. From Figure 77 it is evident that SCC is ultimately governed by electrochemical potential regardless of environmental conditions.

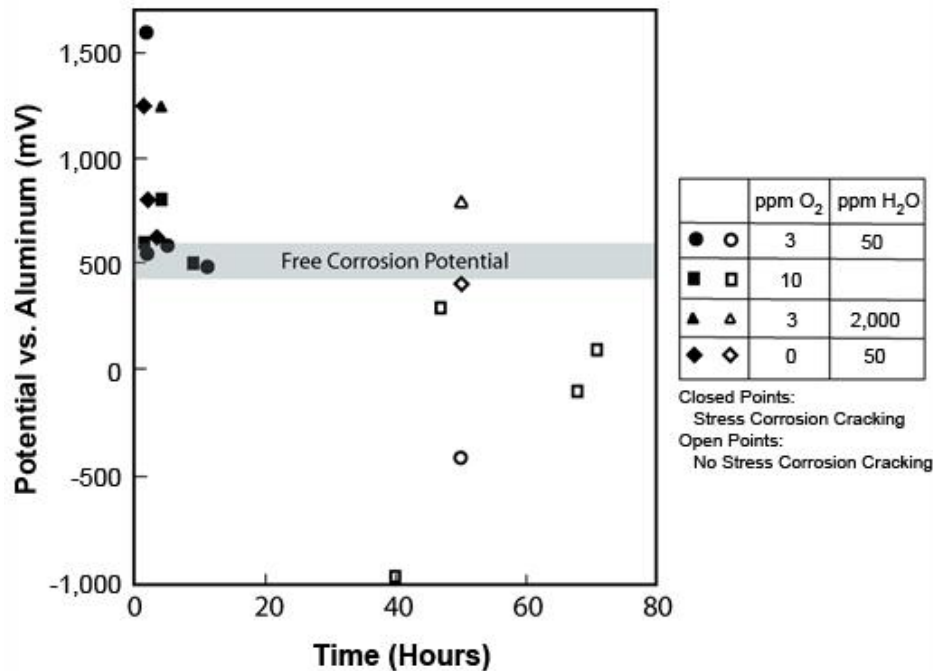


Figure 77. Graph. Corrosion potential of carbon steel as a function of time in different environments.

Effect of Oxygen and Water Concentrations

SCC susceptibility increases as dissolved oxygen content in NH_3 increases and water content decreases. With one exception, no SCC has been observed in environments above and to the left of the dashed borderline in Figure 78 at ambient temperatures (18°C). However, the exception is that SCC has been shown to occur when NH_3 vapor is allowed to condense on steel, even with high concentrations of water present in the liquid solution of NH_3 , as seen in Figure 78.⁽¹⁹⁾

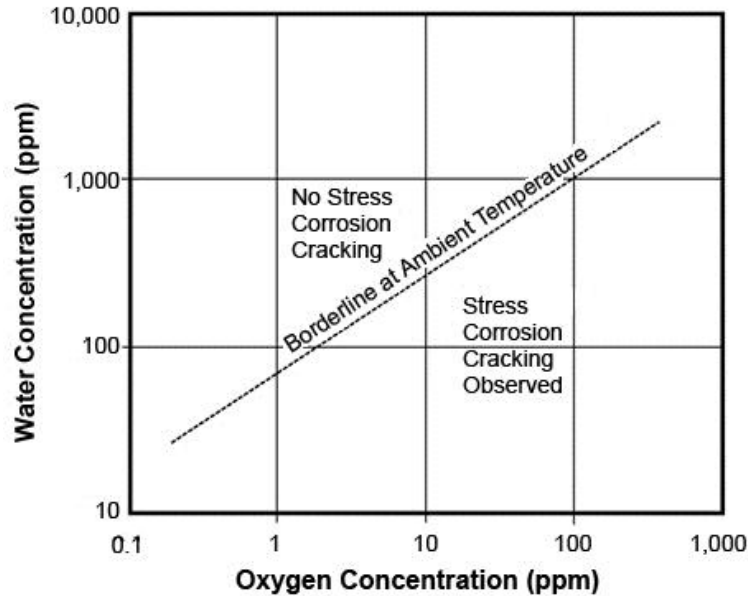


Figure 78. Graph. SSC susceptibility as a function of water and oxygen concentrations in anhydrous ammonia at 18° C (64.4° F). No liquid SCC has been observed above and to the left of the line drawn on the graph.

Effects of Steel Strength

It has been well established experimentally that higher strength steels are more susceptible to NH₃ SCC.^(20,21,22) However, Loginow does not support setting yield strength limit standards, saying *“the formulation of a lower strength limit, below which SCC would not occur, is not practical because it depends on the level and nature of contamination, the degree and nature of inhibition, the magnitude of residual and operating stresses and the operating temperature.”*⁽²¹⁾ Cold-formed tanks have also been shown to be more prone to SCC, presumably because of their higher strength or their higher residual stresses in unannealed steel.⁽¹⁶⁾ In practice, the lowest acceptable yield strength steel should be used to reduce SCC, and tank heads should be hot formed or heat-treated (annealed) to avoid strengthening the steel by the increased dislocation density caused in cold-worked metal. Stronger steel is more susceptible to SCC, so the strengthening that accompanies cold forming is undesirable, while the lack of strengthening that accompanies hot work is benign.

Crack Growth Rates

The crack growth rate of SCC-induced flaws is approximately proportional to the square of K_I, the stress intensity factor. A model for the maximum (worst-case scenario) crack length as a function of time and stress intensity factor is given by Lunde and Nyborg as:

$$a = 3 \times 10^{-4} k^2 \sqrt{t}$$

Figure 79. Formula. Model for the maximum crack depth as a function of time and stress intensity factor.

In this equation, a is crack size in mm, k is the stress intensity factor in MPa times the square root of length in meters *m*, and t is time in years. Typical stress intensities for nurse tanks are

reported to be around $50 \text{ MPa m}^{1/2}$. Thus for a 3-mm crack in an 11-mm wall, the crack will grow 5 mm in 4 years and 6 mm in 8 years according to the model (as shown in Figure 80). The Lunde and Nyborg model above was developed by machining notches into compact tension specimens (as shown in Figure 81) to develop samples with known K_I values. The compact tension specimens were then subjected to different stresses while in an NH_3 -oxygen environment over periods of 200 to 900 hours. The extent of cracking was studied, and crack lengths were compared as a function of stress intensity factor and time (as shown in Figure 82). The maximum observed crack growth rate for 380 MPa yield strength C-Mn steel, an alloy quite similar to the A455 and A516 steels often used in nurse tanks, was 2mm per year for a K_I of $40 \text{ MPa m}^{1/2}$ and 6mm/year for a K_I of $60 \text{ MPa m}^{1/2}$.⁽²²⁾ It was noted that strain rate and amplitude are important factors in determining crack growth rates, and higher values for either led to faster flaw propagation.⁽²³⁾

Welded samples were also tested. Nyborg determined that residual stresses in welds and their heat-affected zones are important factors for SCC, but acknowledged that the geometry of the specimens used in the crack growth rate studies described above do not give a good indication of the residual stresses present in a complete nurse tank. Therefore, he recommended further testing of residual stresses in welds and heat-affected zones to develop a more accurate crack growth model. In all cases, it was observed that crack growth rates decreased with time due to crevice corrosion of the SCC. Crevice corrosion is believed to deplete cracks of oxygen, a local effect that is independent of how much oxygen is present in a nurse tank, thus changing the corrosion potential inside the cracks to a more noble state.⁽²²⁾

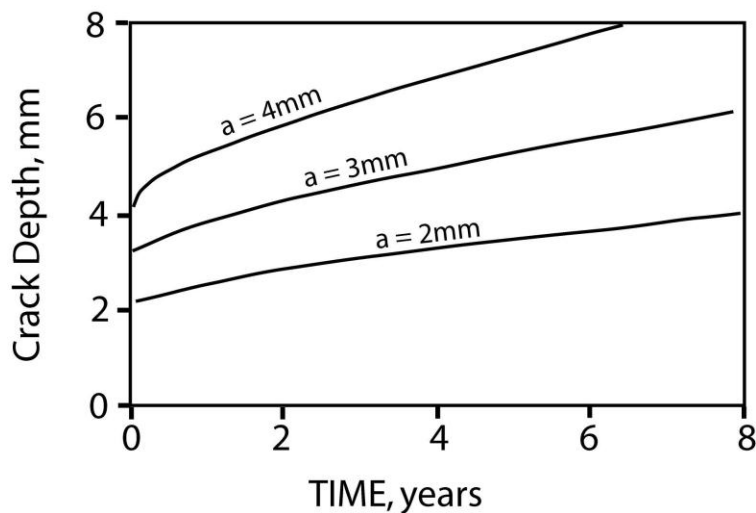


Figure 80. Growth rates predicted by the model above for three possible situations:

<i>Upper line:</i>	<i>a = 4 mm</i>	<i>K = 60 MPam^{1/2} initially</i>
<i>Middle line:</i>	<i>a = 3 mm</i>	<i>K = 50 MPam^{1/2} initially</i>
<i>Lower line:</i>	<i>a = 2 mm</i>	<i>K = 40 MPam^{1/2} initially</i>

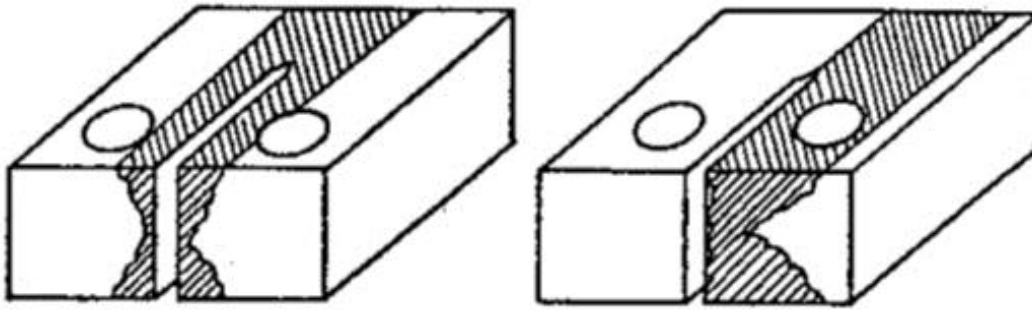


Figure 81. Diagram. Compact tension specimen geometry used for crack growth rate studies. This diagram shows specimens with notches in the weld (left) and in the heat-affected zones (right).

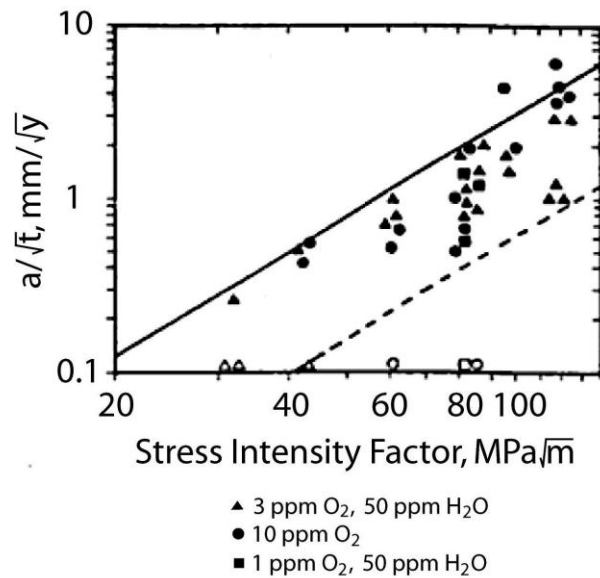


Figure 82. Graph. Crack depth divided by square root of exposure time plotted against stress intensity factor for carbon steel in different oxygen-water environments.

Stress Corrosion Cracking in Welds

Studies at the Norwegian Institute for Energy Research found that most shielded-metal arc-welded carbon steel first develops SCC in the weld metal, and the cracks often propagate into the heat-affected zones. Cracks in weld metal are generally observed to be transgranular, while cracks in the heat-affected zones are usually intergranular (as shown in Figure 83). When a uniform rust layer of 20–30 microns is allowed to form on welded samples, SCC is greatly accelerated. A possible explanation for this occurrence is that galvanic cells develop from scratches in the rust layer and initiate SCC. However, this is not germane to nurse tanks because the outside is painted to prevent rust, and the interior has very little free oxygen to promote rust.

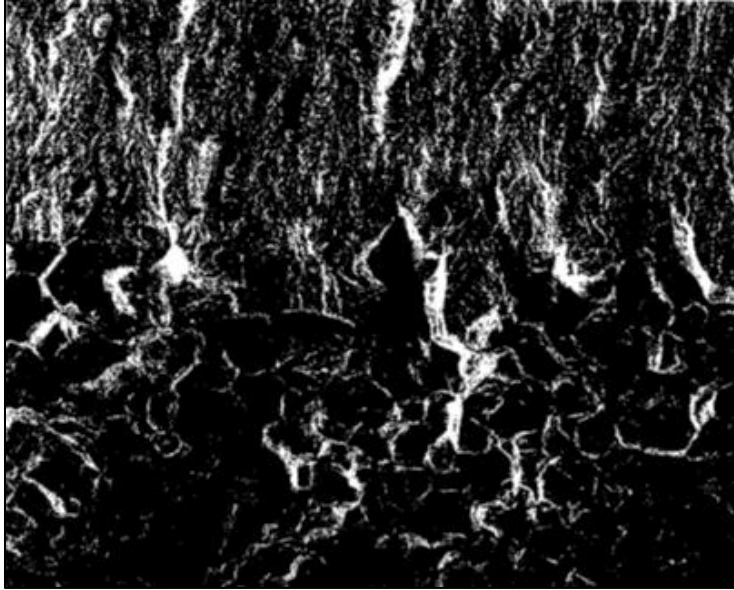


Figure 83. Image. A comparative difference in fracture surface contours between transgranular cracking in the weld metal (top portion of photo) and intergranular cracking in the heat-affected zones (bottom) 125 x magnification.

However, in the research for the Norwegian Institute for Energy Research, the welded specimens examined were cut from larger welded plates. By cutting out those smaller samples, significant residual stresses induced from the welds were released. Measurements of the residual stresses by neutron diffraction for this research project found that for the large plates used in nurse tanks, post-welding, revealed 200 MPa stresses transverse to the weld and 400 MPa stresses longitudinal to the weld. Similarly for this research project, we found that the residual stress measurements of the smaller specimens cut from the nurse tank plates showed that very little stress remained in the small samples comparable to those used in the Norwegian research. Because of this, the crack growth rates experiments did not exactly replicate the operational environmental stress conditions present in nurse tanks.⁽¹⁹⁾

Prevention of Stress Corrosion Cracking

Loginow suggests six ways of managing SCC from NH₃ in nurse tanks:⁽⁴⁾

1. Purge the vessels of air.
2. Add at least 0.2 percent water by weight to the NH₃.
3. Keep the liquid NH₃ temperature lower than the steel temperature to prevent condensation of NH₃ vapor in the vapor space.
4. Heat treat after welding (anneal). This both removes residual stresses from the HAZ, but also reduces the hardness, thus increasing their ductility.
5. Use the lowest strength steel possible to construct the tank.
6. Perform frequent and periodic inspections:

- Magnetic particle inspection should be performed with a magnetic yoke and liquid fluorescent penetrant on the inside of the tank. Of course, such inspections are impossible on tanks without manways for entering the tank.
- Acoustic emission testing should be used to inspect from the outside of the tank. Acoustic emission testing is a detection method based on placing acoustic sensors at various points on the tank to detect sonic pulses associated with crack growth.

Cathodic polarization by flame spraying zinc onto weld surfaces on the tank interior has not been shown to inhibit NH₃ SCC.⁽²⁴⁾ Galvanizing the inner tank surface is ineffective because of NH₃'s large electrical resistance.⁽¹⁶⁾ Galvanizing normally inhibits corrosion of the steel since the coating metal acts as a sacrificial anode in contact with steel. However, such a coating can protect the metal only if the corrosive fluid is an electrical conductor (e.g., water). Conduction of current through the fluid is necessary to complete a path for current to flow through the two metals and the fluid. If the corrosive fluid has very low conductivity (e.g., ammonia), electric current cannot flow through it to complete the circuit, and galvanizing is ineffective at suppressing corrosion.

Keeping oxygen contamination of NH₃ as low as possible is another way to reduce NH₃ SCC. Purging nurse tanks with nitrogen prior to filling them with NH₃ has been observed to be a practical means of reducing oxygen content in NH₃, which deprives the internal tank environment of the oxygen needed for SCC to occur. This method is used in Britain.⁽²⁵⁾

Current Inspection Techniques

Wet fluorescent magnetic particle testing (WFMT) with an electromagnetic yoke has been demonstrated to be highly effective at detecting NH₃-induced SCC. Unfortunately, SCC initiates on the inside surface of nurse tanks, and magnetic particle inspection is limited to detecting surface and near-surface flaws. Therefore, access to the inside of a tank is required to properly perform WFMT testing. Visual and dye-penetrant inspections suffer from the same access limitations.

Radiographic testing of small SCC has been reported to have a mixed record of success. However, ultrasonic testing has been shown to detect SCC, and is even more effective when used in conjunction with acoustic emission testing. Ultrasonic testing and acoustic emission testing can also be performed externally, without the need to access the inside of a tank.⁽¹⁶⁾

Emerging Inspection Techniques

Though magnetic particle and ultrasonic testing have long been used to nondestructively test nurse tanks periodically in countries where nurse tanks have manways that permit interior access, new techniques for monitoring SCC in pressure vessels are being developed that use continuous monitoring systems. Field Signature Method (FSM) is a technique for continuously monitoring corrosion attacks and cracking of pipes, pressurized vessels, and storage tanks, as well as SCC of welds in NH₃ storage tanks.

FSM works by measuring changes in the electric field between pairs of electrodes. Thinning or corrosion causes a change in the potential between electrodes when a direct current is applied. By establishing a reference library containing the effects of different crack depths and types of

corrosion on electrical signals, a computer can interpret electrical signal changes in terms of crack sizes. A network of electrodes is attached to the outside surface of a nurse tank in order to detect cracking anywhere on the vessel (as shown in Figure 84). Next, a pair of reference electrodes is placed in a protected area where SCC cannot occur to account for temperature changes and other background noise. Laboratory tests have shown that FSM can detect single cracks 2–3 mm deep in a 20-mm-thick wall and cracks 1–2 mm deep in a 13-mm-thick wall.⁽²⁶⁾ However, in-service detection reliability has not been established.

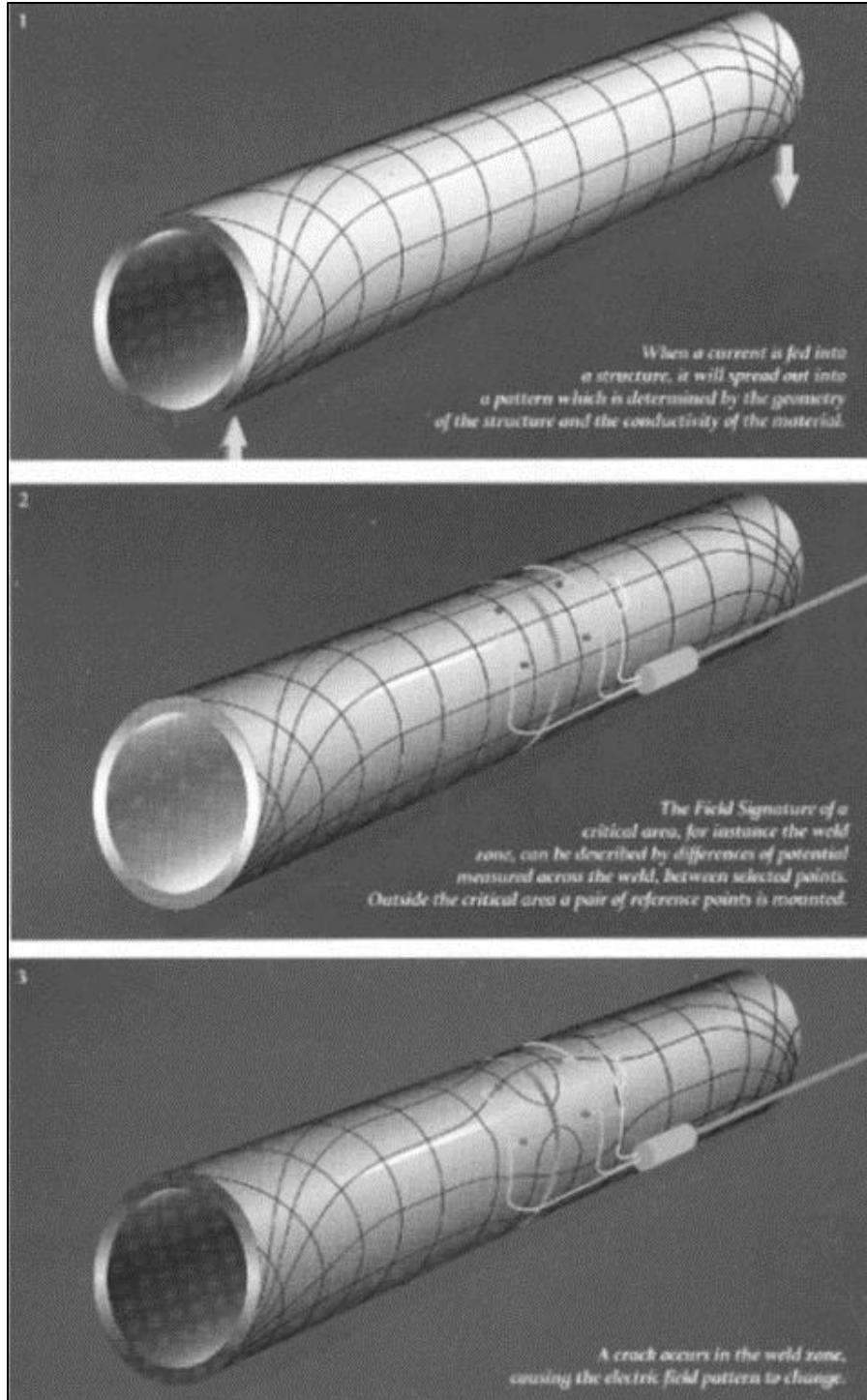


Figure 84. Diagram. Schematic of FSM principles. The top image shows the ideal electric field pattern of an unflawed vessel and the bottom depicts the distorted electric field lines of a flawed vessel.

EXAMPLES OF CATASTROPHIC FAILURE BY STRESS CORROSION CRACKING

In 1956, Dawson reported that 3 percent of anhydrous nurse tanks failed within 3 years of service in a southern State with a large number of vessels.⁽¹⁰⁾ Recommended industry-agreed-upon best practices were put forward by ASME and have been cooperatively modified over the years, but failures continue to occur in tanks both old and new.

Calamus, Iowa Incident

In the spring of 2003, a cooperative worker in Calamus, Iowa, was killed when the nurse tank he and another man were filling ruptured. The forcefulness of the NH₃ gas rupture threw one man against a truck, knocking him unconscious. When his coworker came to his aid and pulled him to safety, that coworker inhaled sufficient NH₃ gas that he eventually died of pneumonia due to inhalation burns.

After the accident, a detailed investigation was performed by the NTSB.⁽¹²⁾ The tank was constructed of 3/8-inch SA-455 steel in 1976 and was designed to withstand 250 psig as recommended by the ASME *Boiler and Pressure Vessel Code: Section VIII, "Rules for Construction of Pressure Vessels."* Furthermore, the tank was hydrostatically pressure tested by the manufacturer at 375 psig after manufacture. Twenty-seven years after construction, the nurse tank ruptured along a longitudinal weld seam that ran along the bottom of the tank. The 53.5-inch-long split is shown in Figure 85 and Figure 86.⁽¹¹⁾



Figure 85. Photograph. Calamus nurse tank post-accident. The white oval indicates the location of the ruptured seam.



Figure 86. Photograph. Close-up picture of the ruptured seam circled in Figure 128.

The NTSB determined that the probable cause of the sudden failure of the nurse tank was inadequate welding and insufficient radiographic inspection during the tank's manufacture as well as lack of periodic testing during the tank's service life. The NTSB recommended that the use of radiosopic inspection of 100 percent of longitudinal welds be made mandatory in place of spot radiography. Current industry-approved ASME specifications still allow spot checks. However, they also provide an incentive for a 100-percent radiosopic check. Namely, they allow for the use of slightly thinner steel if there is a 100-percent radiographic check.⁽¹²⁾ The two surviving U.S. manufacturers of nurse tanks are performing a 100-percent radiographic check of the longitudinal seam in the shell of nurse tanks, and thus taking advantage of using slightly thinner steel for the shell.

Morris, Minnesota Incident

On June 6, 2005, at approximately 6 p.m., a 1,000-gallon NH₃ tank explosively ruptured in Morris, Minnesota, at the Cenex Cooperative. The tank, which was still sitting at the filling station dock, had been filled to 85 percent capacity 3 hours before it ruptured. When the tank ruptured, a portion of the rear head was blown off, releasing 841 gallons of NH₃. The bulk of the tank tore free of the running gear and shot 100 yards across the lot, split a utility tractor in half, and hit a parked automobile before coming to rest (Figure 87, Figure 88, Figure 89, and Figure 90). The tank's path narrowly missed other filled nurse tanks by 25 yards. Since the explosion occurred after hours, no employees were in the area, and no workers were injured or killed. However, a farmer living three-tenths of a mile to the west was hospitalized for NH₃ inhalation treatment. The tank was coined the "Morris Missile" because of its destructive nature.⁽¹³⁾

Table 5. Morris nurse tank manufacturing data.

National Board Number	NB 175175
Manufacturer	Chemi-Trol Chemical Company
Year Manufactured	1973
Capacity	1,000 gallons
MAWP	250 psi
Width	40.5''
Length	192''
Minimum Head Thickness	0.2306''
Minimum Shell Thickness	0.321''



Figure 87. Photograph. Front end of Cenex vessel showing impact damage.



Figure 88. Photograph. Severed tractor and automobile damage caused by the propelled nurse tank.



Figure 89. Photograph. Blown-out rear end of nurse tank.



Figure 90. Photograph. Point of vessel where the fracture meets the circumferential weld.

Silver Lake, Minnesota Explosion

On December 21, 2007, a 1,000-gallon nurse tank being towed by a farmer in his pickup truck explosively ruptured. Just like in the Morris incident above, the tank tore away from its running gear. It then slammed into the back of the truck, and shot across the farmer's front yard (Figure 91, Figure 92, Figure 93, and Figure 94). All of the NH_3 in the tank vaporized, and the farmer was hospitalized for NH_3 exposure. Packer Engineering performed an investigation of the accident for the USDOT.

The tank was constructed in 1973 by Chemi-Trol Chemical Co. in Ohio. (Chemi-Trol may now be part of American Welding and Tank.) The nameplate information indicated that upon manufacture, the tank was partially inspected by radiography, and the heads had been stress relieved before they were welded onto the tank body. Visual examination revealed that the crack originated on the inside diameter of the rear head at a region that had previously been dented by an impact with something, thus establishing stresses in the steel of the head. Metallographic examination of the crack initiation site revealed that severe crack branching as well as intergranular and transgranular brittle fracture had occurred (Figure 95 and Figure 96). The cause of the accident was reported as rupture due to SCC, accelerated by likely significant stresses induced from the dent.⁽¹⁴⁾



Figure 91. Photograph. Silver Lake nurse tank post-accident.



Figure 92. Photograph. Ruptured tank head.

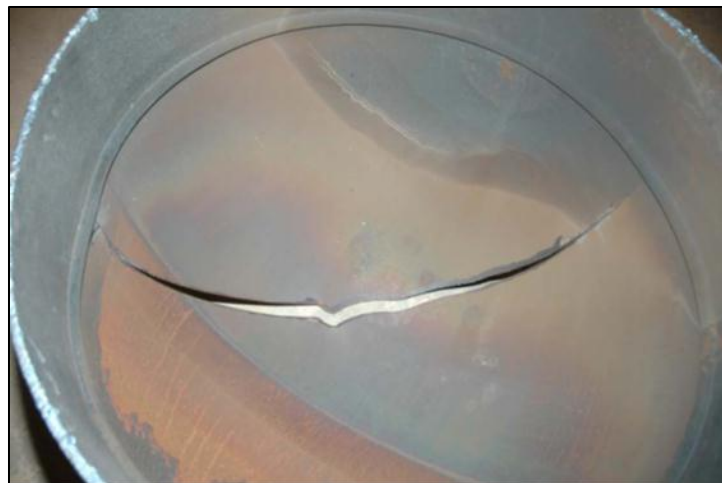


Figure 93. Photograph. Inside view of the ruptured tank head.



Figure 94. Photograph. Crack initiation site.

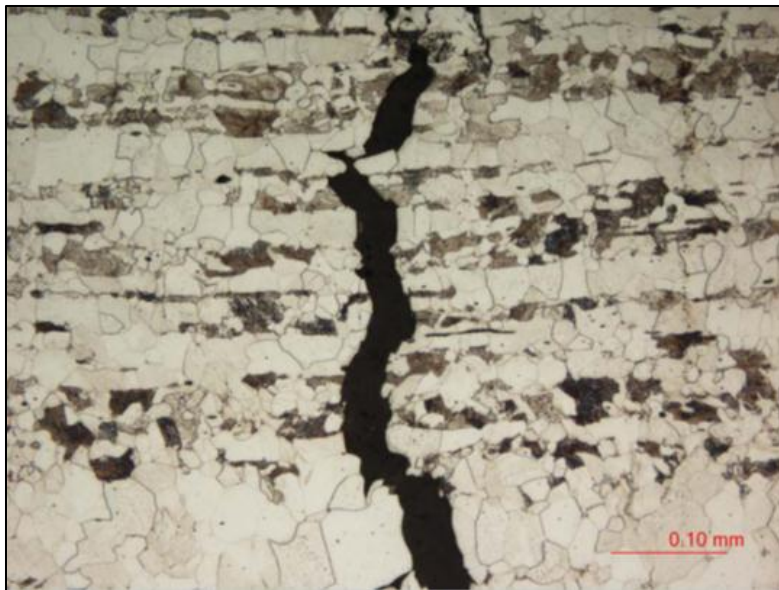


Figure 95. Image. Ferrite/pearlite microstructure at crack initiation site, 200 x magnification. Both transgranular and intergranular fractures are observed.

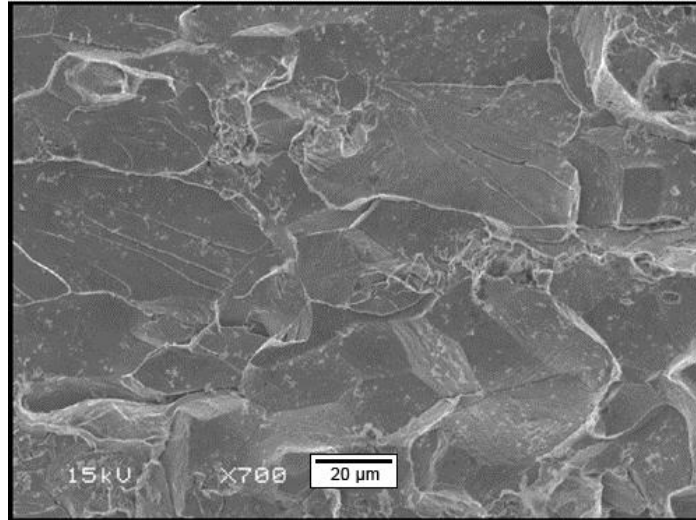


Figure 96. Image. SEM image of fracture surface showing transgranular and intergranular fractures.

Middleton, Ohio, Tanker Accident

On August 22, 2003, the head of a USDOT MC 331 cargo tank ruptured while the tank was being filled with NH_3 in Middleton, Ohio. Unlike nurse tanks, cargo tanks are larger containers used for highway transport of NH_3 over longer distances. The tank was manufactured in 1977 of ASTM A516 grade 70 quenched and tempered steel. It had a nominal shell thickness of 0.399 inch, minimum head thickness of 0.250 inch, and maximum allowable working pressure of 265 psig at 150° F. The tank's capacity was 10,600 gallons. The head failure occurred when the tanker was about half full of NH_3 at 26.7° C (80° F) with an internal pressure of 170 psig. The release of NH_3 caused 100 employees to be evacuated from buildings downwind of the tank. Five people were given medical treatment for inhalation injuries, but no one was seriously hurt. The damage from the tank rupture caused an estimated \$25,000 in damages to equipment.

Before the accident, the tank had been inspected with magnetic particle and hydrostatic testing in March 2002 and with a visual inspection in 2003 in accordance with USDOT mandates. Unlike nurse tanks, which have single piece heads, the head on this cargo tank was made up of multiple pieces which have radial welds joining them together into a single head.

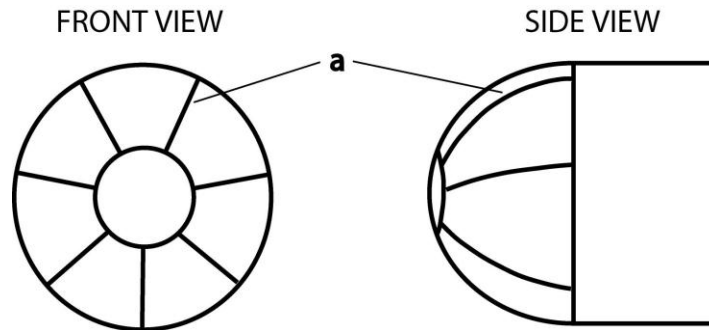


Figure 97. Diagram. Schematic of observed crack locations. The letter “a” denotes the location of a through-wall crack. Lines represent weld seams.

An NTSB investigation into the accident revealed that a 16-inch through-wall crack next to a radial weld had developed on the head. Post-mortem magnetic particle inspection revealed cracks along other radial head welds that had not yet penetrated completely through the wall. When investigators opened the 16-inch through-wall crack to examine it with a SEM, a previously undetected 3-inch through-wall crack opened up as well. Both through-wall cracks exhibited intergranular corrosion and separation (Figure 98).



Figure 98. Photograph. Through-wall crack in head.

Investigation into the NH_3 filling process revealed that water was not being added to the liquid NH_3 , even though the tanker company handbook stated that 0.2 percent water by weight was to be added to NH_3 when it was carried in its LPG tanks. The NH_3 being pumped into the tanker when it ruptured contained less than 0.1 percent water. The reported cause of the failure was SCC, which developed because company practices were not established to explicitly prohibit

quenched and tempered steel tankers from carrying NH₃ with less than 0.2 percent water.⁽¹⁵⁾ FMCSA has subsequently found other manufacturers not adding 0.2 percent water, against which it conducted enforcement cases during 2011–12.

STATIONARY TANK FAILURES

Cases of NH₃ SCC failures have also been observed in stationary NH₃ storage tanks.

Liquefied Anhydrous Ammonia Gas Cylinder, Egypt

In 2003, a 20-year-old industrial liquefied ammonia gas (LAG) cylinder filled with NH₃ ruptured into four pieces. The tank was designed to hold 46 kg of NH₃ at a maximum pressure of 33 times average sea level atmospheric pressure. This is approximately twice the working pressure of nurse tanks. Their maximum is 250 psig or approximately 17 atmospheres. Thus, the maximum operating pressure for this Egyptian tank must have been around 485 psig.

The tank had been annually inspected using a 30 kg/cm² hydrostatic pressure test. Post-mortem tests of the tank showed that the fracture sites were of the same ferritic-pearlitic structure as the rest of the tank. However, significant intergranular SCC was observed at the fracture site, which occurred right beside a girth weld as shown in Figure 99, Figure 100, Figure 101, and Figure 102. Furthermore, the ruptured tank was shown to have a higher tensile strength (46.0 kg/mm²) than that of a similar unruptured tank of the same age (32 kg/mm²). The higher tensile strength presumably resulted from use of an alloy different from that of the unruptured tank or from a greater amount of cold-forming work in the ruptured steel. Investigators of the accident concluded that the cause of catastrophic failure was SCC induced by high-tensile stresses in the fractured weld coupled with a corrosive environment of NH₃.⁽²⁷⁾



Figure 99. Photograph. Pieces of LAG cylinder post-explosion.

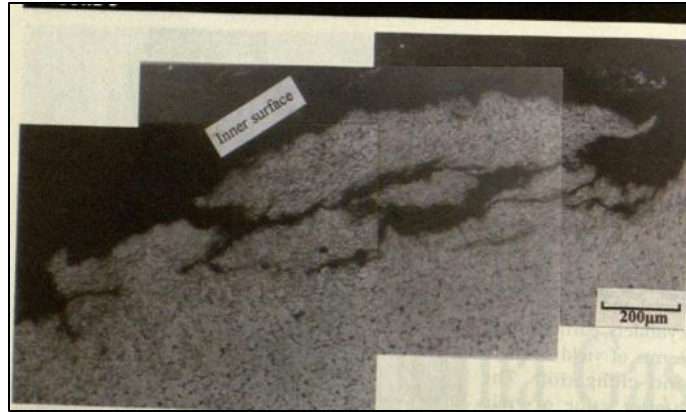


Figure 100. Photograph. Rupture initiation site showing severe cracking.

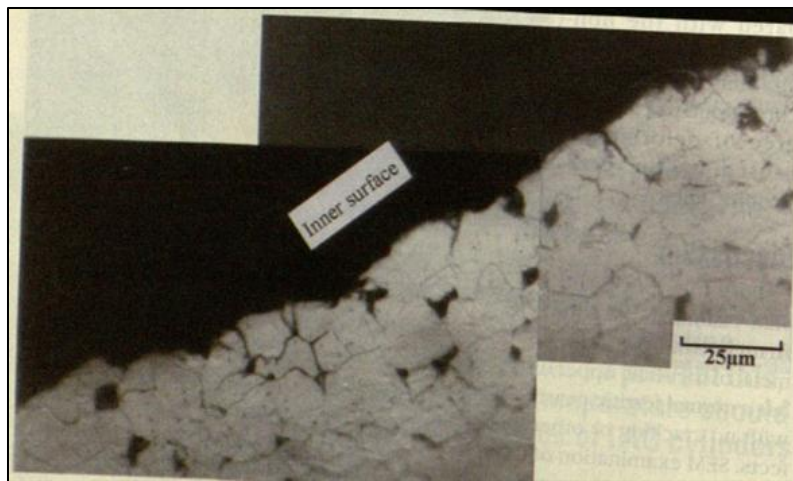


Figure 101. Photograph. Grain boundary microcracks at the crack initiation site.

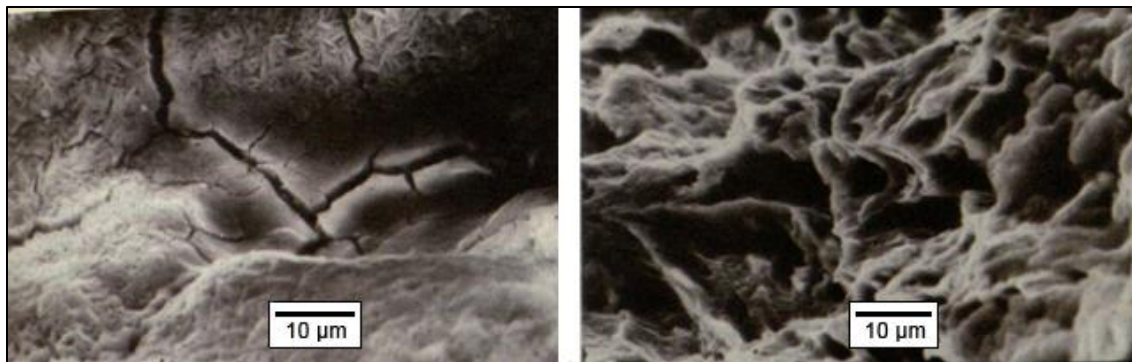


Figure 102. Grouped Image. SEM of fracture site showing grain boundary microcracks (left) and SEM showing the dimpled morphology of the fracture region (right).

LAG STORAGE TANK, LITHUANIA (USSR)

An NH_3 cryogenic storage tank ruptured in Lithuania (then the USSR) in 1989, reportedly killing 7 people and wounding 57. However, because of limits on Soviet reporting, the actual casualty

numbers from the released cloud of NH_3 may have been much higher. The disaster took place at a military controlled fertilizer plant in Jenova, a town with about 40,000 residents. The tank was a simple cryogenic storage tank (not a pressure vessel). It was 30 meters in diameter and 20 meters tall. It was designed to hold ammonia at very low pressure (0.1 bar, which is 1.5 p.s.i.) by maintaining the ammonia temperature below its boiling temperature. The tank was built in 1978 and was designed to hold 10,000 tons of NH_3 at temperatures between -34°C and -32°C .⁽²⁸⁾ At the time of the accident, the tank was filled with 7,000 tons of (NH_3).

Because of the fertilizer plant's military significance, little information was released about the cause of the failure except that a joint near the base of the tank shell failed, causing a jet of NH_3 to stream into a nearby store of 15,000 tons of NPK. "NPK" is a fertilizer comprised of a mixture of compounds. The "N" stands for nitrogen, "P" for phosphorus, and "K" for potassium.

NPK has many different possible percentage compositions and is usually sold as dry, granulated powder. It is widely custom-blended for the particular crop in question, and to match the soil needs of a local area. Tobacco needs one ratio, potatoes another, etc. Most of the compounds present in NPK are non-flammable, but one common ingredient, ammonium nitrate, is both flammable and explosive, so blended powders containing a substantial amount of ammonium nitrate will burn.

The NPK caught fire and burned for 3 days.⁽²⁹⁾ Liquid NH_3 rapidly flowed from the tank and was 70 cm deep in some areas. The 7,000 tons of NH_3 evaporated in less than 12 hours under a light breeze. The resulting cloud of toxic vapor spread over 400 square kilometers and reached a height of 800 meters.^(28,29) It has been theorized that an operating error allowed warm NH_3 to flow into the tank, which caused an overpressure that resulted in failure. SCC has not been reported in this case, but no analysis was done on the fracture site, so it is uncertain if SCC contributed to the accident.

AMMONIA REFRIGERATION INDUSTRY FAILURES

Cases of SCC in steel vessels using NH_3 have also been reported by members of the ammonia refrigeration industry. When NH_3 is used as a refrigerant, it is kept at -33°C . While it was once believed that NH_3 SCC could not occur at such low temperatures, both practical experience and experimental studies have shown otherwise. The Industrial Refrigeration Consortium (IRC) has developed classes and issued technical bulletins for its members to address the causes and prevention of NH_3 SCC.

The IRC has identified non-stress-relieved (non-annealed) welds and areas exposed to condensing NH_3 vapor as "hot spots" for SCC. In one incident, a SCC attack formed a hole through a high-pressure receiver line from an NH_3 refrigeration system. The hole initiated on the inside of the vessel and grew completely through the weld and heat-affected zones to the exterior surface. After the leak occurred, the interior surface of that pressure vessel was examined with a liquid penetrant, and this showed that several SCC 5- to 10-cm long cracks were present, all oriented perpendicular to the weld line.^(30,31)

Other cases of failure have been reported by the International Institute of Ammonia Refrigeration:

High Pressure Receiver, England

In the 1980's a high-pressure NH₃ receiver made of 10-mm-thick steel failed after just 3 months of service. The vessel had been constructed according to BS5500, the relevant British standard, which like U.S. nurse tanks does not require post-weld heat treatment for stress relief. NH₃ was discovered leaking out of a crack oriented perpendicular to a weld seam. Upon further examination, several cracks transverse to the weld seam were found, and the yield strength of the BS1501-151-430 steel was determined to be 332 MPa. No injuries were reported in the incident, but high-pressure vaporous NH₃ was released to the atmosphere.

Shell Condenser, France

An ice cream shell and tube condenser was made of A48CP steel (European standard NF A 36-205) instead of the recommended lower strength A42CP steel and failed by SCC within a few months of service. (There are many steel classification systems. A reader who is interested in converting a designation to another system can obtain "translations" on the Internet.) A48CP steel has a yield strength of 285 MPa. However, the condenser was not stress-relieved and thus had a measured yield strength of about 365 MPa.

High Pressure Receiver, Holland

A cold-formed pressure receiver began leaking shortly after it was put into service due to the formation of transverse weld cracks near the end cap of the vessel. The vessel had not been post-weld stress-relieved.

Low Pressure Shell and Tube Evaporator, England

A low-pressure evaporator vessel experienced SCC along a weld at the normal liquid level where liquid and vaporous NH₃ coexist. The evaporator was constructed of steel with a yield strength of 370 MPa and was not post-weld heat-treated. Unlike the previous cases, this failure occurred in an environment of low pressure. Thus, the tension stress contributing to the SCC was dominantly from residual stress, not for stress induced by working at high pressure.

Suction Pipe on Freezer, U.S.

A freezer suction pipe failed due to thermal shock, which was aided by SCC of welds. The cracks caused a section of the pipe to weaken to the point that it failed. Contributing factors included NH₃ condensate (comparable to the vapor area of nurse tanks) coupled with the presence of residual stresses due to pipe fabrication welding.⁽³²⁾

CURRENT CODES AND STANDARDS

International Standards—IACS No. 33

The International Association of Classification Societies (IACS) is a London-based society that establishes standards for marine-related structures and pressure vessels. IACS standard No. 33 pertains to all cargo tankers used for the transport of NH₃ at ambient temperatures. It states that fine-grained carbon-manganese steels with nominal yield strengths below 355 MPa and actual yield strengths below 440 MPa should be used for the construction of plates, and hot-formed

dished ends (i.e., “heads” on nurse tanks). Furthermore, the composition of the steel should be within the limits given in Table 6.

Table 6. Required chemical composition of steels used for anhydrous ammonia containment (percent maximum unless otherwise noted).

C	Si	Mn	P	S	Al	Cr	Cu	Mo	Ni [†]	V
0.18	0.10 to 0.50	1.65	0.030	0.025	0.020‡	0.20	0.35	0.08	0.40	0.10

†If Nickel will intentionally be alloyed, the maximum may be 0.85%.

‡Minimum.

Cold-formed, dished ends (heads) are to be heat-treated for stress relief. Impact energy requirements are as follows:

Table 7. ISO-V-notch impact energy requirements for carbon steels.

Type of Product	Test Temp. (° C)	Impact Energy [†] Joule min. Longitude/Transverse
Plates	-20°	-/27
Pipes	-20°	41/-
Forgings	-20°	41/27

†Average value. One value may be below the average value, but not lower than 70 percent of this value.

All welds are to be made using low-hydrogen consumables, and preheating temperatures are not to exceed 100° C in order to minimize weld hardness and residual stresses. Weld and heat-affected zone hardness values should be less than 230 HV, as verified by a workmanship test.

“HV” stands for “Hardness, Vickers.” The Vickers hardness scale is a micro-hardness measurement unit widely used in metallurgical analysis. A small, pyramid-shaped diamond is pressed into the surface of a test specimen with a calibrated load (a few grams for soft materials up to several kg for very hard materials), and the width of the resulting indentation in the specimen surface is measured and assigned an HV value. The above observed 230 HV is a fairly high hardness for steel. Generally, as hardness increases, crack resistance and toughness decrease, so it is common to specify a maximum allowable hardness value in applications where toughness is an important safety consideration. HV testing is fast and non-destructive, so it is often used instead of tensile testing, which is slow, costly, and damages or destroys the part being tested.

Stress relieving treatments (annealing) should be conducted at temperatures of 570° C ± 20° C (1058° F) and held for 60 minutes for a 25-mm wall thickness. No welding is allowed after stress relieving.

After manufacture, 100-percent longitudinal and transverse inspection of butt welds and full penetration welds are to be carried out using an ultrasonic non-destructive examination. All butt welds and fillet welds are to be tested using magnetic particle inspections on the inside surface of the tank. Magnetic particle inspection of the outside of the tank should be done everywhere

welds cross (500 mm in each direction). Fillet welds (connecting steel plates at right angles) are to be 100-percent inspected with magnetic particle inspection on the outside surface as well. At least 10 percent of the non-destructive examinations must be repeated in the presence of an official IACS surveyor after a hydrostatic pressure test. The 10-percent repeat inspection must include all weld crossings and dome welds.

Periodic non-destructive inspections are to be performed at intervals set by IACS and should include ultrasonic testing of all weld crossings, dome welds, and sump welds. Magnetic particle inspection should also be performed on at least 10 percent of the inside butt and fillet welds. Upon detection of flaws, more tests are required, the extent of which are at the discretion of the IACS surveyor overseeing the testing procedure. All inspections must be reported to IACS by certified non-destructive testing personnel for approval.⁽³³⁾

United Kingdom Code of Practice

A standard code of practice was jointly developed by the British Health and Safety Executive, Chemical Industries Association, and the Imperial Chemical Industries PLC. This code of practice provides guidance on storage and handling of NH₃ and has been updated to address SCC. The code calls for all newly constructed nurse tanks to undergo hydrostatic pressure testing, 100-percent radiographic inspection of butt welds, and ultrasonic or magnetic particle inspection of all other welds.

In addition, the tanks should be thermally stress-relieved and made to withstand at least 15.5 bar pressure (227.85 psig). Any welds made after stress relieving should be thermally stress-relieved, as well. In-service tanks are to be inspected after the first 3 years of use and at least every 6 years after that. These inspections should include a complete visual examination, magnetic particle inspection of all butt welds, and ultrasonic thickness measurements of any areas with observed or suspected corrosion. If any defects are found, 100-percent magnetic particle inspection of internal welds should be done, and a hydrostatic test should be issued at the discretion of the inspector.⁽²⁵⁾ (The U.K. inspection protocol requires access to the tank interior, and U.K. nurse tanks are built with manways for this purpose. Such inspections are not possible with U.S. nurse tanks, since they are built without manways.)

Australian/New Zealand Standards

Nurse tank construction and inspection requirements are given by three standards and a law called the Australian Code for the Transport of Dangerous Goods by Road and Rail, commonly referred to as the Australian Dangerous Goods (ADG) Code. The ADG Code refers to AS/NZS 2,022 for NH₃ storage and handling requirements, AS/NZS 1210 for nurse tank construction specifications, and AS/NZS 3,788 for in-service inspection procedures. Special care is given to address SCC, and the following storage and handling practices are required:

- Procedures should be exercised to eliminate oxygen from NH₃ tanks.
- Whenever a tank is opened to the outside atmosphere, it shall be thoroughly purged with NH₃ or an inert gas, excluding CO₂.
- NH₃ tanks that will sit out-of-service for long periods of time shall be kept under positive pressure with either NH₃ gas or an inert gas.

- NH₃ shall not be transported in a quenched and tempered steel tank unless 0.2 percent water has been added to the NH₃. Shipping papers must be marked with “0.2 percent water” to indicate that water has been added.

Risk control methods for the construction and design of NH₃ nurse tanks are also given. Steels with yield strengths below 300 MPa are recommended for use in nurse tank construction. However, this figure is only a recommendation, as the standard states that “a strength threshold below which SCC does not occur has not yet been identified.” Nurse tanks must be constructed to withstand at least 1.73 MPa.

If the tank is expected to be used in areas where temperatures exceed 46° C (115° F), the minimum design pressure must be greater than the maximum vapor pressure at the expected maximum temperature. Low-strength electrodes are specified for welding, and all tanks are to be post-weld stress-relieved. Welds are to be dressed to reduce surface stress and hardness, and soft grinding wheels are to be used on welds so that metal smearing does not occur. Repair welds must be stress-relieved. When thermal stress relief is not possible, shot peening should be considered.

Peening is the process of working a metal's surface to improve its material properties, usually by mechanical means such as hammer blows or by blasting with shot (shot peening). Peening is normally a cold work process. Peening a surface spreads it plastically, causing changes in the mechanical properties of the surface.

Inspections should be performed in accordance with AS/NZS 3788, which classifies NH₃ as “very harmful” cargo—a rating second only to “lethal.” Under this standard, nurse tanks must be visually inspected internally and externally upon manufacture and after the first year of service. (As noted above, this implies the Australian/New Zealand Standards, apparently like the British, must require a manway in the nurse tanks to afford such access for internal testing.) Following those inspections, the nurse tank must be externally inspected every year and internally inspected every 5 years. If the visual examination shows corroded or cracked areas, thickness testing must be performed. If the thinning is significant, the tank must be decommissioned until it is repaired and inspected again.

Furthermore, welds subjected to cyclic bending stresses must be inspected every 3 years with a suitable surface non-destructive method such as magnetic particle inspection or liquid penetrant inspection. Welds experiencing bending stresses include baffle mounting brackets and vessel-mounting attachments to running gear. (Note: This code requires even more frequent testing of running gear attachment points than it does for the rest of the tank. Based on U.S. experiences with running gear failures, this may be important to consider.) All other welds are to be non-destructively inspected every 6 years. All non-destructive inspections are to cover the weld bead as well as 30 mm in each direction to include the heat-affected zones around the weld.^(34,35,36)

Drive-away protection measures are also mandated. Road tanks must have one of the following two options to prevent movement of nurse tanks while filling hoses are attached:

- An air brake interlock system that prevents brakes from being released while hoses or a loading arm are attached.

- The static storage tank must be fitted with breakaway couplings that shut off upon release.

Incitec Pivot, Australia's only producer of NH₃, provides its customers with an inspection program in order to keep all of its nurse tanks in code. Maintenance and auditing checklists from this program are given in reference.⁽³⁷⁾

Canadian Standards

Nurse tanks are regulated by CSA B620, CSA B621, CSA B622, and ASME Boiler and Pressure Vessel Code under the Transportation of Dangerous Goods Act. Tanks should be designed to withstand 250 psig. The minimum tank thickness shall be 5 mm throughout. Steel used in construction of nurse tanks shall have a minimum Charpy V-Notch impact energy of 27 J (20 ft-lb).

Post-weld heat treatment is also required of all NH₃ nurse tanks, and it should be performed at no less than 565° C metal temperature. Quenched and tempered steel may be used, but 0.2 percent water must be added to any NH₃ put in the tank. Tests of water content must be performed and documented every time NH₃ is added to a tank. NH₃ nurse tanks are classified as TC 51 portable tanks and must be inspected accordingly.

Every 3 years an external inspection is required and includes checking for dents, scratches, and corrosion; examining hoses for cracking and wear; checking the function of valves; and ensuring that all required markings are visible. All areas showing dents or corrosion are to be thickness tested. If the tank wall is 10 percent less than the nominal thickness listed on the data plate, the tank must be taken out of service. A tank will also be decommissioned if it has any dents greater than 12.7mm (0.5 in) deep, has a dent with depth greater than 10 percent of the dent length, or has visible weld defects.

Every 5 years a hydrostatic test is required. The hydrostatic test is to be performed at 1.5 times the design pressure of the tank. Inspection and repair of nurse tanks can only be performed by qualified persons who have received a "Certificate of Registration" from the Canadian government. Repair welds greater than 60 linear cm should be post-weld heat-treated and followed by a magnetic particle inspection and hydrostatic test.^(38,39,40,41)

The Fertilizer Safety and Security Council, an organization composed of fertilizer manufacturers, distributors, and agri-retailers, has issued a code of practice and implementation guide for users of NH₃ in Canada. The guide provides auditing checklists for owners of nurse tanks to help ensure that the vessel, hoses, inspections, and markings are all within code. It also contains practical advice for the implementation of practices mandated by the code.⁽⁴²⁾

GOVERNMENT-FUNDED INVESTIGATIONS

United States Government

The NTSB investigated the Calamus, Iowa and Middleton, Ohio incidents discussed earlier. The USDOT sponsored the investigation of the Silver Lake, Minnesota accident.

Foreign Governments/Corporations

The Norwegian Government's Institute for Energy Technology sponsored a research program to:

- Investigate the effect of oxygen and water content on SCC of carbon steel in liquid and vaporous NH₃.
- Perform crack growth studies and develop crack growth models as well as cathodic protection measures.
- Examine SCC of welds in NH₃ at ambient temperatures.
- Study SCC of steels in NH₃ at -33° C.

The investigation was also sponsored by Norwegian and international companies, NH₃ producers, and international safety regulators. The sponsor list includes BASF, Germany; DSM, The Netherlands; DuPont, United States; Kemira, Finland; Norsk Hydro, Norway; Health & Safety Executive, UK; ICI, UK; and Agricultural Minerals Corporation. United States.

Papers from this series of experiments have been referenced in this report and are primarily written by Lunde and Nborg. (See references 7, 14, 22, 23, and 24.)

[This page intentionally left blank.]

ACKNOWLEDGEMENTS

We gratefully acknowledge the assistance of the West Central Coop of Jordan, Iowa, and particularly the assistance of Tom Mowrer, formerly of the West Central staff, for providing facilities, storage space, ammonia for testing, and helpful guidance for our research on more than 20 used anhydrous ammonia (NH₃) nurse tanks and a test tank specially fabricated with a manway for this research project to internally access the tank for placing and retrieving specimens.

We gratefully acknowledge the contribution that Trinity Containers made to this project in the form of a specially fabricated 500 gallon tank with a manway to allow internal access for conducting the stress corrosion tests on the 56 test specimen coupons.

We gratefully acknowledge the contributions that Jordan Tank, an R-Stamp repair facility, made to this project.

We gratefully acknowledge the following persons from various aspects of the community for participating as members of the voluntary peer review group who provided periodic review and suggestions for ways to achieve the most effective research to identify how to non-destructively evaluate the safety condition of nurse tanks.

Francis Brown, The National Board of Boiler and Pressure Vessel Inspectors, OH
Kevin Danner, West Central Coop, IA
Scott Drey, Crop Production Services, IA
Pam Guffain, The Fertilizer Institute, VA
Mark Kane, Judson Tank, MN
Terry Jensen, Department of Agriculture, IA
Kevin Klomnhaus, Department of Agriculture, IA
Greg McRae, Trinity Containers, TX
Thomas Mowrer, Thompson Environmental Consulting, Inc., IA
Dave Powers, RCI Safety, KS
Terry Ross, American Welding and Tank, PA (initial)
Tom Vandini, American Welding and Tank, PA (replacement)

The following Federal Government personnel also participated in the peer review group:

Andrea Carpenter, FMCSA, OH
Arthur Fleener, FMCSA, IA - We especially thank Mr. Fleener for his effective advocacy to initiate this research project and his continuing assistance in recruiting knowledgeable interested personnel to serve on the technical review group.
David Goettee, FMCSA, HQ (Project Manager)
Charles Hochman, PHMSA, HQ (retired)
Shirley McGuire, FMCSA, IA
Kris Phillips, FMCSA, Midwest Service Center
Terry Pollard, PHMSA, Field
Suzanne Rach, FMCSA, HQ
James Simmons, PHMSA, HQ

We gratefully acknowledge the following individuals for agreeing to have their organizations review the draft final report and provide helpful comments and advice:

Kevin Garrity, NACE International, The Corrosion Society, President 2012-13

Ian Friedland, Bridge & Structures R&D, FHWA, HRD F-219, HQ

Robert Smith, PHP-80 Engineering & Research, PHMSA, HQ

REFERENCES

1. Blanken, J.M., et al., *Plant/Operations Progress*, Vol. 2, No. 4, p. 247, 1983.
2. HSEES 1997 Annual Report, U.S. Department of Health and Human Services.
3. Welch, Ann, "Exposing the Dangers of Anhydrous Ammonia," *The Nurse Practitioner*, Vol 31, No 11, p. 40-45, Nov. 2006.
4. Cottis, R.A., "Stress Corrosion Cracking: Guide to Good Practice in Corrosion Control," National Physical Laboratory. Teddington, UK. 2000.
5. Woodtli, J. and Kieselbach, R. "Damage Due to Hydrogen Embrittlement and Stress Corrosion Cracking," *Engineering Failure Analysis*, 7: 427-450, 2000.
6. Wilde, B.E., "Stress Corrosion Cracking of ASTM A517 Steel in Liquid Ammonia: Environmental Factors," *Corrosion*, Vol 37, No 3, p. 131-142, March 1981.
7. Lunde, L. and Nyborg, R., "Stress Corrosion Cracking of Different Steels in Liquid and Vaporous Ammonia," *Corrosion*, Vol 43, No 11, p. 680-686, Nov. 1987.
8. Jones, D., Kim, C., Wilde, B., "The Electrochemistry and Mechanism of Stress Corrosion Cracking of Constructional Steel in Liquid Ammonia," *Corrosion*, Vol 33, No 2, p. 50-55, 1977.
9. Jones, Russell. "Stress-Corrosion Cracking," Materials Park: ASM International, 1992.
10. Dawson, T.J., "Behavior of Welded Pressure Vessels in Agricultural Ammonia Service," *Welding Journal*, Vol 35, p. 568-574, 1956.
11. "Anhydrous Ammonia Nurse Tank Rupture Kills Agricultural Cooperative Worker," University of Iowa College of Public Health. National Institute for Occupational Safety and Health. Jun 2005.
12. "Nurse Tank Failure With Release of Hazardous Materials," *Hazardous Materials Accident Report* NTSB/HZM-04/01, PB2004-917001. NTSB. Apr 2003. Washington, D.C.
13. <http://dli.mn.gov/CCLD/BoilerIncidentsPressure.asp>. Minnesota Dept. of Labor and Industry.
14. "Metallurgical Evaluation of a Cracked Head. Final Report," Packer Engineering. Office of Hazardous Materials Technology, U.S. Department of Transportation. DAS-438, April, 2008.
15. Hazardous Materials Accident Report NTSB/HZM, Accident No: DCA03MZ002. NTSB. Jul 2004. Washington, D.C.
16. NACE International, "Integrity of Equipment in Anhydrous Ammonia Storage and Handling," Publication 5A192 (2004 Edition).
17. R.C. Newman, W. Zheng, C.R. Tilley, R.P.M. Proctor, "Exploration of a Nitrogen-Induced Cleavage Model for Anhydrous Ammonia Cracking of Steel," CORROSION/89, paper no. 568 (Houston, TX: NACE, 1989).

18. D.A. Jones, B.E. Wilde, "Corrosion Performance of Some Metals and Alloys in Liquid Ammonia," *Corrosion* 33, 2 (1977): p. 46.
19. Nyborg, R. and Lunde, L, "Control of Stress Corrosion Cracking in Liquid Ammonia Storage Tanks," Presented before the Fertilizer Society in London Oct. 10, 1996.
20. J. Hutchings, G. Sanderson, D.G.S. Davies, M.A.P. Dewey, "Stress Corrosion of Steels in Anhydrous Ammonia," Safety in Ammonia Plants Symposium, (New York, NY: AIChE, 1971)
21. Loginow, A.W., "A Review of Stress Corrosion Cracking in Liquefied Ammonia Service," *Material Performance*, Vol 25, p. 18, 1986.
22. Lunde, L. and Nyborg, R. "Stress Corrosion Crack Growth Rate of Carbon-Manganese Steels in Liquid Ammonia." in Corrosion Prevention in the Process Industries: Proceedings of the First NACE International Symposium, November 8-11, 1988, Amsterdam, The Netherlands. Houston, Tex: National Association of Corrosion Engineers, 1990.
23. Lunde and Nyborg, "Stress Corrosion Cracking of Carbon Steel in Ammonia," *Corrosion*, Vol 28, p. 28-32, Dec. 1989.
24. Lunde, L. and Nyborg, R. "Stress Corrosion Cracking of Carbon-Manganese Steel in Ammonia Efficiently Prevented by Metal Flame Spraying." in Corrosion Prevention in the Process Industries: Proceedings of the First NACE International Symposium, November 8-11, 1988, Amsterdam, The Netherlands. Houston, Tex: National Association of Corrosion Engineers, 1990.
25. Great Britain. "Storage of Anhydrous Ammonia Under Pressure in the United Kingdom: Spherical and Cylindrical Vessels," Health and safety booklet, HS(G)30. London: H.M.S.O., 1986.
26. Hallan, Tom. "FSM - Developments for monitoring of stress corrosion cracking in storage tanks," *Process Safety Progress*, Vol 13, No 2, p. 101-104, 1994.
27. "Anhydrous Ammonia Nurse Tank Rupture Kills Agricultural Cooperative Worker," University of Iowa College of Public Health. National Institute for Occupational Safety and Health. Jun 2005.
28. *Nurse Tank Failure With Release of Hazardous Materials*, Hazardous Materials Accident Report NTSB/HZM-04/01, PB2004-917001. NTSB. Apr 2003. Washington, D.C.
29. <http://dli.mn.gov/CCLD/BoilerIncidentsPressure.asp>. Minnesota Dept. of Labor and Industry. Visited June 1, 2009.
30. "Stress Corrosion Cracking: Defining and Diagnosing," *The Cold Front*, Vol 5, No 1, 2005.
31. "Stress Corrosion Cracking: Prevention," *The Cold Front*, Vol 5, No 2, 2005.
32. Pearson, Andy. "Stress Corrosion Cracking in Refrigeration Systems," *International Journal of Refrigeration*, Vol 31, p. 742-747, 2008.

33. IACS, 1992. *Guidelines for the Construction of Pressure Vessel Type Tanks Intended for the Transportation of Anhydrous Ammonia at Ambient Temperatures*. International Association of Classification Societies. Guideline No. 33.
34. AS/NZS 1210:1997, "Pressure vessels," *Standards Australia*. 1997.
35. AS/NZS 2022:2003, "Anhydrous ammonia - Storage and handling," *Standards Australia*. 2003.
36. AS/NZS 3788:2006 "Pressure equipment—in service inspection," *Standards Australia*. 2006.
37. "Pressure Vessel Certification for Anhydrous Ammonia tanks," *Invitec Pivot*, BigN customer service bulletin.
38. CSA B620:2009, "Highway Tanks and Tc Portable Tanks For The Transportation Of Dangerous Goods," *Canadian Standards Association*, 2009.
39. B621:2009, "Selection and Use of Highway Tanks, TC Portable Tanks, and Other Large Containers for the Transportation of Dangerous Goods, Classes 3, 4, 5, 6.1, 8, and 9," *Canadian Standards Association*, 2009.
40. CSA B622:2009, "Selection and Use of Highway Tanks, Multi-Unit Tank Car Tanks, and Portable Tanks for the Transportation of Dangerous Goods, Class 2," *Canadian Standards Association*, 2009.
41. Boiler and Pressure Vessel Code: Section VIII, "Rules for Construction of Pressure Vessels," *American Society of Mechanical Engineer (ASME)*, 1998.
42. "Ammonia Code of Practice and Implementation," *Fertilizer Safety and Security Council*, <http://www.fssc.ca/Home/Farmer.html>, June 2008.

[This page intentionally left blank.]